AMERICAN UNIVERSITY OF BEIRUT

EFFECT OF CORTICAL BONE QUALITY AND QUANTITY ON
FIVE MAXILLARY POSTERIOR INTRUSION MECHANICS
USING MINISCREWS:
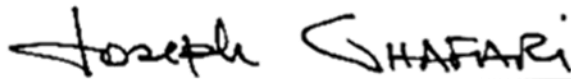A FINITE ELEMENT ANALYSIS STUDY

by
CHRISTOPHE CAMIL ZGHEIB

A thesis
submitted in partial fulfillment of the requirements
for the degree of Master of Science in Orthodontics
to the Department of Otolaryngology- Head and Neck Surgery
of the Faculty of Medicine
at the American University of Beirut

Beirut, Lebanon
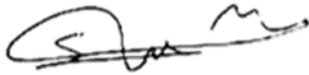June 2020

AMERICAN UNIVERSITY OF BEIRUT

EFFECT OF CORTICAL BONE QUALITY AND QUANTITY ON
FIVE MAXILLARY POSTERIOR INTRUSION MECHANICS
USING MINISCREWS:
A FINITE ELEMENT ANALYSIS STUDY
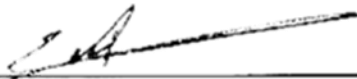

by
CHRISTOPHE CAMIL ZGHEIB

Dr. Joseph Ghafari, Professor and Head   Primary Advisor
Orthodontics and Dentofacial Orthopedics
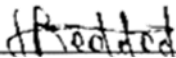
Dr. Samir Mustapha, Assistant Professor   Co-primary Advisor
Department of Mechanical Engineering

Dr. Elie Shammas, Assistant Professor   Member of Committee
Department of Mechanical Engineering

Dr. Ramzi Haddad, Associate Professor   Member of Committee
Orthodontics and Dentofacial Orthopedics

Date of thesis defense: June 12, 2020

AMERICAN UNIVERSITY OF BEIRUT

THESIS, DISSERTATION, PROJECT RELEASE FORM

Student Name: _____ Zgheib _____Christophe _____Camil_____

| | Last | First | Middle |

● Master's Thesis   ○ Master's Project   ○ Doctoral Dissertation

☐ I authorize the American University of Beirut to: (a) reproduce hard or electronic copies of my thesis, dissertation, or project; (b) include such copies in the archives and digital repositories of the University; and (c) make freely available such copies to third parties for research or educational purposes.

☒ I authorize the American University of Beirut, to: (a) reproduce hard or electronic copies of it; (b) include such copies in the archives and digital repositories of the University; and (c) make freely available such copies to third parties for research or educational purposes after:

One ---- year from the date of submission of my thesis, dissertation, or project.
Two ---- years from the date of submission of my thesis, dissertation, or project.
Three -X- years from the date of submission of my thesis, dissertation, or project.

_____ July 7, 2020_____

Signature   Date

ACKNOWLEDGMENTS

"Talent wins games, but teamwork and intelligence win championships."
Michael Jordan

I thank all who in one way or another contributed to the achievement of this dissertation.

Foremost, my sincere gratitude to my advisor *Doctor Joseph Ghafari* to whom I would look up to as a role model and honored to work with. Thank you for the continuous support of my research project, your patience, enthusiasm, and immense knowledge.

I would like to express my gratitude to *Doctor Samir Mustapha* for the useful comments, remarks, and engagement through the learning process of this master thesis.

Doctor Ramzi Haddad, your advice on both research as well as on my career has been invaluable. I am extremely thankful and indebted to you for sharing your experience and time.

Doctor Elie Shammas, for sharing his intellectual and engineering knowledge and for being part of the committee.

Furthermore, *Doctor Makram Amouri* thank you for introducing me to the topic as well for the support on the way.

Doctor Ingrid Karam, without you and your precious time, no statistical computation would have been possible,

Words cannot express how grateful I am to *my mother, and father* for all of the sacrifices that you have made on my behalf. Your prayer for me was what sustained me thus far. And my siblings for their moral and emotional support.

I thank my God, my good Father, for letting me through all the difficulties.

Sara, you made this journey enjoyable and smooth.

Very special gratitude goes out to *all the residents* for helping and providing the best working atmosphere.

I am also grateful to the following department staff: *Michella Semaan, Jessica Chaaya and Nourhane Nasser* for their unfailing support and assistance.

Christian, thank you for never getting tired of helping, listening, motivating me, and, for accompanying me from the beginning till the last second.

Thanks for all your encouragement!

AN ABSTRACT OF THE THESIS OF
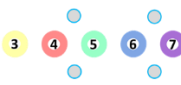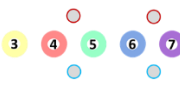
Christophe Camil Zgheib   for   Master of Science
                                               Major: Orthodontics

Title: effect of cortical bone quality and quantity on five maxillary posterior intrusion mechanics using miniscrews: A FINITE ELEMENT ANALYSIS STUDY

Introduction: Orthodontic mini-implants (MI) have been used as an alternative modality to correct posteriorly extruded maxillary molars notably in anterior open bite cases, which constitute a challenging clinical situation for Orthodontists. The influence of cortical bone on the rate of tooth movement in intrusion has not been studied. Moreover, the definite mechanics involved in predictable outcomes should be explored.

Aims: Compare in a finite element analysis (FEA) the stresses and displacements generated on maxillary teeth through five intrusion modalities, accounting for individual variation.
Our hypothesis was that cortical bone quality and quantity influence the rate of tooth movement in all modalities.

Methods: A 3D simulation model of a maxilla containing the different components (teeth, PDL, trabecular and cortical bones) was developed with 5 intrusion modalities:

Model	1	2	3	4	5
MIs	1B, 2 P	2 B, 2 P	2 B, 1 P	2 B, 2 P	2 B, 2 P
Buccal MIs position between	2nd PM and 1st M	- 2nd PM and 1st M - Ms	-PMs - Ms	-PMs - Ms	-PMs - Ms
Palatal MIs position between	-PMs - Ms	-PMs - Ms	2nd PM and 1st M	-PMs - Ms	-PMs - Ms
Force applied on	archwire	archwire	brackets	brackets	archwire

Bone stiffness/thickness measurements of 11 subjects utilizing the data generated by Peterson et al. (2006), in human cadavers. The specimens were meshed through using the software ScanIP™ 7.0 (Simpleware, Synopsys, Mountain view, CA, USA) according to data from measurements made on the CT scans of 11 patients. FEA was ran using ABAQUS 6.13 (Dassault Systèmes, Tokyo Japan) software by simulation of five intrusion modalities: intrusion was replicated with a force equivalent to 400gms.

Stress levels and displacement were measured at the molar and adjacent teeth. Outcome measures included stress distribution and displacement of the following permanent teeth: canine, first and second premolars, first and second molars.

Potential clinical implications that may be illustrated are the determination of the modality causing the least stress. In parallel, evaluating different mechanical assemblies used will help determine the difference in efficacy among these assemblies about extruded teeth.

Results: The highest stress was concentrated on the root surface of the second premolar in the first modality, mostly on its buccal and palatal aspects, in all the other modalities, the first premolar withstood the highest stresses. The least on the extremity teeth, the canine and the second molars. Similar displacement patterns were registered in all modalities especially on the premolars with the highest rate of stress/displacement in the fourth and the fifth model. The second molar intruded the most in the second modality where the force is concentrated posteriorly. Secondary effects varied between models. Upon stiffness and thickness variation, stress configurations in the PDL and initial displacement on the mesial, distal, buccal, and lingual sides of each tooth differed significantly ($p<0.05$) between modalities. Bone stiffness configuration correlated negatively with the stress on the molars and positively with the displacement, the opposite applied to bone thickness.

Conclusion: Generalizing on best intrusive modality is not suitable, as anatomical, and biologic individual traits may influence one or the other in individualized treatment. Further investigations must untangle anatomy conditions on which one protocol is better than the other. This pure numerical method is unable to precisely predict long-term orthodontic tooth movement and may not provide definitive formula for the whole mechanotherapy planning. But at the same time, the capacity for FEA in combination with clinical data input and time-dependent protocol in the analysis can help determining the specificity of the movement in a patient for a better planning of the treatment.

CONTENTS

ILLUSTRATIONS

TABLES

ABREVIATIONS

FEM	Finite Element Method	**FEA**	Finite Element Analysis
FE	Finite Element	**HU**	Hounsfield Unit
3D	Three Dimensional	**2D**	Two Dimensional
CT	Computed Tomography	**CBCT**	Cone beam computed tomography
DICOM	Digital Imaging and Communications in Medicine	**CAD/ CAM**	Computer Aided Design/ Computer Aided Manufacturing
MSCT	Multi-Slice Spiral CT	**BMD**	Bone Mineral Density
MI	Mini-implant	**TAD**	Temporary Anchorage Device
TP	Transpalatal Bar	**SS**	Stainless Steel
RMI	Rapid molar intrusion device	**VHA**	Vertical holding appliance
HG	Headgear	**TMJ**	Temporomandibular joint
g	grams	**N**	Newton
mm	millimeter	**kPa**	Kilopascal
GPa	Gigapascals	**PDL**	Periodontal ligament
B	Buccal	**P**	Palatal
D	Distal	**M**	Mesial
PM	Premolar	**BC**	Boundary condition
S1	stiffness in the cortical bone cross section	**S2**	stiffness parallel to the cortical bone plane
S3	stiffness perpendicular to the cortical bone plane (perpendicular to the occlusal plane)	**S/T S3**	Stiffness/thickness comparison for the stress on the canine
S/T S4	Stiffness/thickness comparison for the stress on the first premolar	**S/T S5**	Stiffness/thickness comparison for the stress on the second premolar
S/T S6	Stiffness/thickness comparison for the stress on the first molar	**S/T S7**	Stiffness/thickness comparison for the stress on the second molar
S/T U3	Stiffness/thickness comparison for the displacement on the canine	**S/T U4**	Stiffness/thickness comparison for the displacement on the first premolar
S/T U5	Stiffness/thickness comparison for the displacement on the second premolar	**S/T U6**	Stiffness/thickness comparison for the displacement on the first molar
S/T U7	Stiffness/thickness comparison for the displacement on the second molar	**U1**	Displacement on axis 1 (x) Bucco-lingual direction
U2	Displacement on axis 2 (y) Antero-posterior direction	**U3**	Displacement on axis 3 (z) vertical direction

CHAPTER 1

LITERATURE REVIEW

1.1. Definitions

1.1.1. Intrusion

Intrusion was given many definitions in the literature but all basically concordant with each other's, Burstone et. al (1977) defined it as the "apical movement of the geometric center of the root in respect to the occlusal plane or a plane based on the long axis of the tooth.". According to Marcotte (1976), it is the "tooth movement that occurs in an axial (apical) direction and whose center of rotation lies at infinity. It is an axial type of translation". Nikolai (1985) defined it as "a translational form of the tooth movement directed apically and parallel to the long axis" Intrusion can be either a true intrusion within the bone or a relative intrusion if the teeth are maintained in the same position relative to their adjacent.

For many years, the dental intrusion was supposed impossible or problematic and was associated with many side-effects on the periodontium and cementum (root resorption (Table 1)) (Fig.1-2) (Proffit et al. 2000).

More recently, effective orthodontic intrusion was clinically documented and considered a safe procedure, provided that the magnitude and direction of forces are cautiously scrutinized (Topkara et al. 2012). Treatment differs when dealing with growing patients or adults; in growing patients, the vertical forces applied against the molars serve to intrude the molars and control their vertical eruption. In non-growing patients, the vertical compensation of ramus growth is absent; consequently, true intrusion of molar teeth is needed for the mandible to

autorotate and close an open bite anteriorly (Nanda, 2005). Moreover, true intrusion of an over erupted tooth is challenging, and controlled mechanics must avoid the undesirable extrusion of adjacent teeth. (Moon et al., 2007).

Table 1.1. Comparison of root resorption after mini-screw intrusion on first molar (Mean±SD) (mm3) (Li et al., 2013)

	n	root resorption amount	P
mesiobuccal root	12	22.48±2.58	<0.05[a]
distobuccal root	12	16.22±1.11	<0.05[b]
palatal root	12	19.68±1.49	<0.05[c]

[a]$P<0.05$,compared to distobuccal root.
[b]$P<0.05$, compared to palatal root.
[c]$P<0.05$, compared to mesiobuccal root.
doi:10.1371/journal.pone.0060962.t001

1.1.1.1. Etiology and skeletal features of openbite malocclusion

Open bite is one of the major challenging malocclusions needing the intrusion of posterior teeth. The malocclusion results from the interaction of numerous etiological factors, (genetic, dental, skeletal, functional, soft tissue, and habits) [1]. Patients with skeletal open bites often exhibit vertical skeletal-growth discrepancies, including increased lower face height, short posterior face height with hyperdivergency, [2] increased gonial and mandibular plane angles, [3] and increased maxillary molar dentoalveolar height [4] (Fig.1), abnormal muscular and soft-tissue development, or habits that cause unfavorable tongue and orofacial muscle activity (Fig.2) (Ghafari, Macari, 2013).
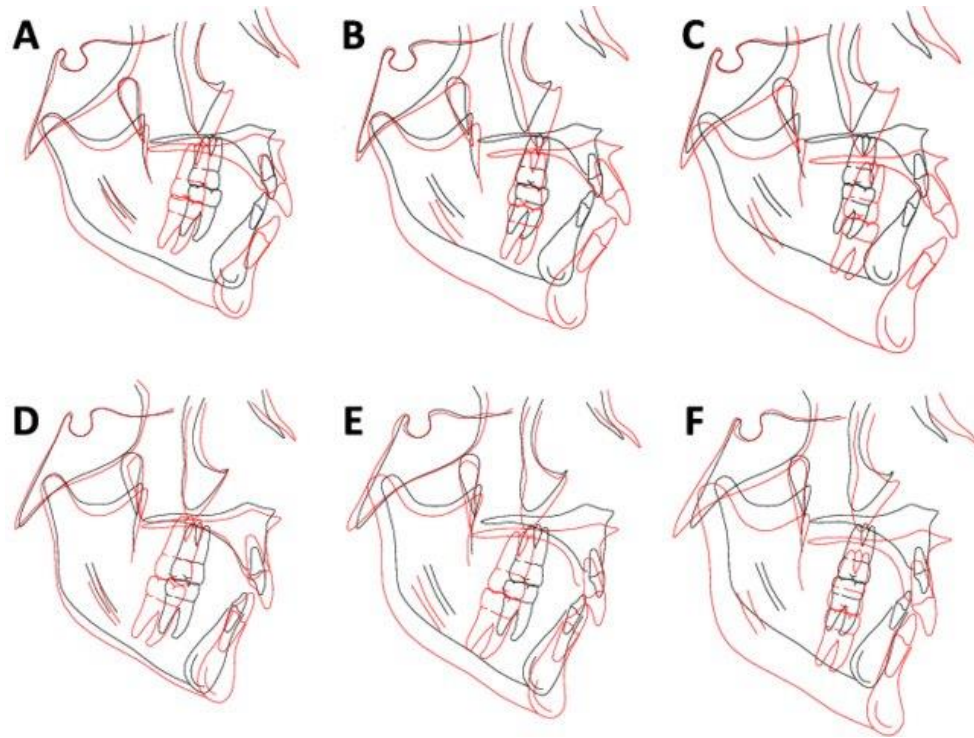
Fig.1.1. Growth of hyperdivergent (top row) and normal (bottom row) children, with cranial base superimpositions showing the growth changes between 6 and 9 years of age (A and D), 6 and 12 years of age (B and E), and 6 and 15 years of age (C and F) (Buschang et al., 2013)
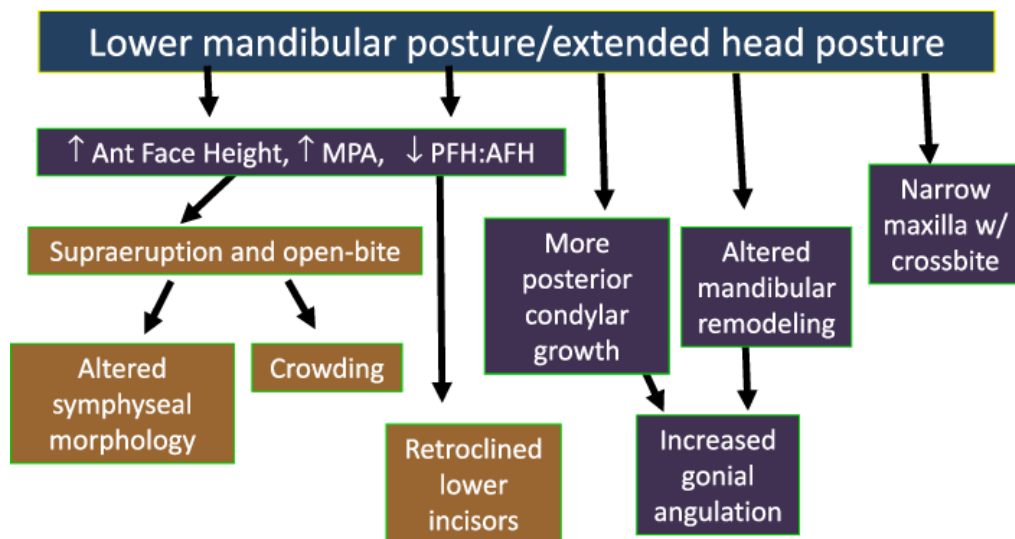
Fig.1.2. The development of the hyperdivergent retrognathic phenotype from lowered mandibular posture produced by weak muscles or airway compromise (Buschang et al., 2013)

An open bite can be unilateral or bilateral in the buccal segments, but it is predominantly seen in the anterior teeth. Researchers have reported a relationship between orofacial muscle activity and vertical facial morphology, mostly positive correlations between the anterior open bite and weak musculature. (Abdullah, et al, 2015; Alsafadi, et al. 2016).

Dental open bite is principally caused by over erupted molars and has been associated with intruded anterior teeth. The causes of the open bite include habitual thumb sucking, tongue thrust, and, mouth breathing.

High relapse tendencies of anterior open bite treatment have been associated with the underlying skeletal components, the difficulty in closing the bite, and the ensuing challenge of retaining bite closure (Wajid et. al, 2018). Appropriate diagnosis is essential to develop a successful treatment plan with appropriate retention of the corrected overbite (Seo, et al. 2014).

1.1.1.2. Open Bite treatment options

Treatment options for open-bite malocclusions include the elimination of the etiology, extrusion of the anterior teeth, intrusion of the molars, surgical impaction of the maxilla, inhibition of molar eruption in growing patients, and a combination of these (Gurton, et al, 2004).

The various surgical and nonsurgical approaches proposed for treatment of open-bite include miniplates, multiloop edgewise archwire therapy, passive posterior bite blocks, functional appliances, active vertical correctors, vertical-pull chin cups, and glossectomy. However, most are unable to achieve significant bite closure (Beane et. al, 1999; Kim et. al 2000; Cambiano et

al, 2018). The stability of anterior tooth extrusion is questionable, and it is subtle because the anterior open bite is often associated with shorter roots and less facial bone support of the anterior teeth (Harris, et al.1992); therefore, posterior tooth intrusion is desirable in most instances (Tasanapanont et al. 2017) especially in patients who usually have increased molar height (Ucera et. al, 2011), but it is difficult to accomplish because of the anatomy of the molars which are multirooted teeth (Tao et al., 2015).

1.1.1.3. Conventional treatment of over-erupted molars

Before the advent of mini-screws and mini-plates, the intrusion mechanotherapy depended heavily on patient compliance including high pull headgear, high pull headgear to a splint, vertical pull chincap, posterior bite-block, magnetic bite-blocks, and, spring-loaded bite-block (Hakami, 2015). Compliance-free appliances include: the rapid molar intrusion device (RMI) and the vertical holding appliance (VHA) (Cinsar et al. 2007) (Fig.3-4).

Table 1.2. Molar intrusion techniques (Hakami, 2016)

Patients compliance dependent	Compliance-free	Surgical approach
high pull headgear (Fig.3)	Rapid molar intrusion device (RMI) (Fig.4.E)	Corticotomy-enhanced molar intrusion
high pull headgear to a splint (Fig.4.A)	Vertical holding appliance (VHA) (Fig.4.F)	Osteotomy-assisted molar intrusion
vertical pull chincap (Fig.3)		(Oliveira et al., 2010).
posterior bite-block (Fig.4.B)		
magnetic bite-block (Fig.4.C)		
spring-loaded bite-block (Fig.4.D)		
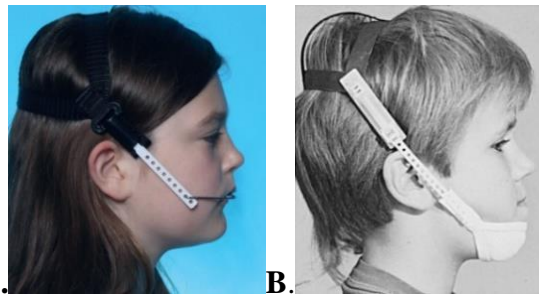
Fig.1.3 A. High pull Headgear **B.** Vertical pull chincup
(Christensen et al., 2019)
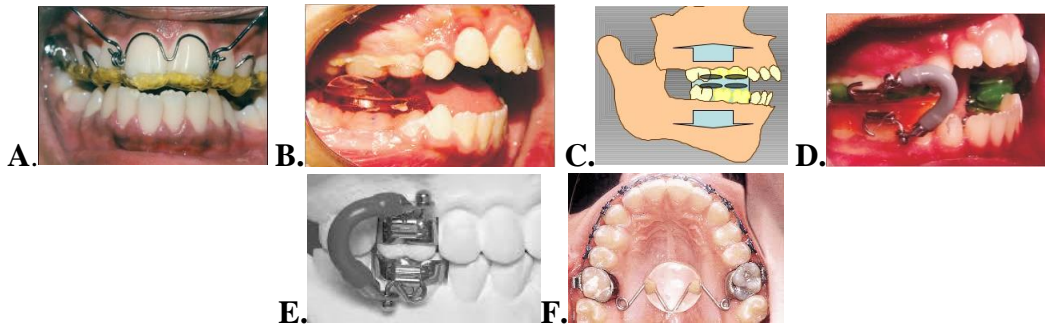
Fig.1.4 A. High pull headgear to a splint **B**. Posterior bite-block **C.** Magnetic bite-block
(Al-Zubair et al., 2014) **D.** Spring-loaded bite-block (Albogha et al. 2015) **E.** RMI **F.** VHA
(AAO) (DeBerardinis et al., 2000)

Separate from open-bite treatment dental intrusion often is a fundamental part of

orthodontic treatment to correct sagittal and vertical incisor relationships, to optimize interincisal

angle and thus, the gingival line and reinstate the esthetics of smiling (Sarver et. al, 2001).

The nature of intrusion may be orthopedic, surgical (superior maxillary displacement), or

orthodontic (a single tooth or groups of teeth) (Zubair, 2014).

Depending on its etiological factors, different approaches are described:

The most stable treatment of dento-alveolar/ habit-related open bites is the modification strategy

at an early age to stop the habit. If left untreated and skeletal discrepancies have developed, other

treatment modalities are considered (Ngan et al., 1997):

- Thumb sucking and tongue thrust treatment for behavior modification

- Control molar extrusion to prevent further vertical growth

- Attempts at growth modification which affects the mandible rotation to compensate for the vertical growth

- Extrusion of anterior teeth to close the open bite if molars have a normal vertical position

- Molar intrusion with or without anterior teeth extrusion whether the etiology is posteriorly or antero-posteriorly combined. (Beane et al., 1999)

Behavior modification techniques for the thumb sucking and the tongue thrust

Patient compliance is essential, to stop the habit before starting treatment by realizing the benefit and the consequences of their cooperation. When the habit ceases, most of open bites improve spontaneously. The most commonly utilized appliances include:

Tongue crib appliance (Fig 1.5), the myofunctional tongue bead which keep the tongue away from the anterior teeth, spurs on a tongue crib, tongue tamers, transpalatal bar and Goshgarian bars (Fig.1.6), all these appliances aimed to encourage a normal tongue position at rest, allowing the eruption of incisors to close anterior open bite, inhibiting the eruption of maxillary molars, and creating a new neuro-muscular equilibrium (with time) thus decrease in the potential of relapse. The appliances should be kept at least for 6 months after open bite closure for stable results and retention.

Fig.1.5. Open bite caused by habit treated with tongue crib appliance (DiBiase et al. 2017).

A. **B.** **C.**

Fig.1.6 A. Tongue bead **B.** Tongue tamers bonded on palatal aspect of maxillary central incisors **C.** Transpalatal bar *(Goshgarian bar is a transpalatal bar 3-4mm away from the palate and by the upward vertical tongue pressure the molars will intrude until the bar hits the palate)* **(Five-star orthodontics, 2019)**

The effects of mouth breathing also alters the position of the tongue and requires a multidisciplinary approach including the otorhinolaryngologist to monitor and if necessary clear the patient's airways. Early intervention is favorable for patient growth (Macari et. al, 2012; Tanaka et al., 2016).

Techniques to control molar extrusion and prevent further vertical growth include:

a. The high-pull HG, prevents the extrusion of the maxillary molars or further vertical eruption to minimize the clockwise rotation and enhance more forward than downward growth of the mandible (Van Steenbergen et al., 2004) (Fig.9).

b. Posterior bite blocks, that counteract the posterior teeth eruption and counterclockwise rotation of the mandible and may be combined with the high-pull HG.

c. Extraction of posterior teeth, that allows bite closure by reducing the dento-alveolar posterior height.

1.1.2 Intrusion and bite closure

It is assessed that every 1mm of intrusive vertical movement of the posterior teeth would result in bite closure of 3mm by dint of counterclockwise mandibular rotation. However, the actual amount of closure may be less than 3mm in some clinical individuals. This pattern is exemplified by what is commonly referred to as a "wedge effect" (Paik et. al, 2016).

Fig.1.7. Open bite patient.

1.1.2.1. Posterior intrusion on mini-implants

1.1.2.1.1. Orthodontic treatment vs orthognathic surgery

Skeletal openbite configuration is often associated with excessive vertical development of both maxillary and dentoalveolar components, especially in the posterior tooth region.

In growing patients, treatment modalities for an anterior open bite are aimed at reducing, redirecting, impeding, or modifying the patient's vertical growth (Lin et. al, 2013). In nongrowing adult patients, the absolute intrusion of the posterior part of the dentition (both maxillary and mandibular) might be required to improve the malocclusion. However, the severity of anterior open bite and underlying skeletal discrepancy are best treated with orthognathic surgery is the most credible treatment plan suggested (Alsafadi et al, 2016).

Less-invasive treatment options are possible orthodontically with mini-implants or plates anchoring the posterior teeth. The resulting changes in occlusal plane, mandibular plane, lower anterior face height, and anterior dental overbite would close the patient's open bite (Sherwood et al, 2002).

Reportedly, extrusion of the anterior teeth modifies the occlusal plane when associated with uprighting and intruding the posterior teeth to seal the anterior open bite (Baek et. al, 2010). To assess the outcome of molar intrusion, it is essential to know the consequence of the posterior teeth intrusion on the mandibular rotation and facial morphology (Alsafadi et. al, 2016).

Intrusion of the posterior teeth is difficult. Many factors are to be scrutinized, such as the magnitude and direction of the forces and orientation of the anchorage units, to prevent undesirable movement and root resorption (Park et al, 2005; Kravitz et. al, 2007).

1.1.2.1.2. Optimal intrusion force

Numerous researches have tried to quantify the optimal force needed for orthodontic maxillary posterior tooth intrusion (Carillo 2007; Akan 2013). The force varies between 100 g to

200 g for a single tooth intrusion and from 200 g to 400 g for a segmental maxillary posterior tooth intrusion. Melsen and Fiorelli (1996) suggested 50 g of force for single molar intrusion in adults. S. Kato and M. Kato (2006) postulated that 100 g of force was not enough for segmental posterior tooth intrusion, but progressive intrusion was achieved when the force levels were augmented to 300 g per side. The different intrusion techniques justify variation between the values. There is an accord that the magnitude of force, acting upon the tooth and causing tooth movement, must be meticulously controlled. The weighty intrusive force has been reported to expose pulpal blood flow and risk of pulp necrosis (Erhasan et. al, 2015). Thus, the need for careful, perhaps progressive monitoring of the orthodontic force magnitude required to intrude the maxillary posterior teeth.

Intrusion with conventional posterior intrusion mechanics such as bite-blocks and fixed appliances with vertical elastics and multi-loop archwire therapy is limited and accompanied by collateral effects from insufficient anchorage (Kiliaridis 1990; Küçükkeles 1999). Once temporary anchorage devices in orthodontic treatments were introduced, patient cooperation was nearly eliminated, and side effects on the surrounding tissues were reduced significantly. The posterior intrusion methodology with temporary anchorage devices has also reduced the need for orthognathic surgery for some borderline open-bite patients (Sherwood 2002; Xun 2007).

1.1.3. Mini-implants

1.1.3.1. History

Patients' compliance was significantly improved with the advent of temporary anchorage devices (TADs) (Krafitz et al., 2007). After Branemark introduced the concept of osseointegrated pure titanium threaded implants to treat edentulous patient, the same implants have been used as skeletal anchorage for the correction of open bite by molar intrusion (Posterman et al., 1995).

Creekmore and Eklund (1983) introduced skeletal anchorage with surgical vitallium bone screws insertion just below the anterior nasal spine for deep bite patients. New sites for implant placement were then proposed such as endosseous implants in the retromolar pad area (Roberts et al. 1989) and the midpalatal implant (Block et al., 1995). Till Kanomi (1997) and Costa (1998) advocated the concept of miniscrew for orthodontic anchorage.

TADs have gained extensive popularity in orthodontics, mainly for their provision of "absolute" anchorage (Cope et al, 2005) allowing for a controlled and predictable tooth movements with negligible requirements for patient compliance (Yao et al., 2004-2005).

A wide range of anchorage devices including miniscrews and on-plants has been used in research and clinical settings. The most regularly used TADs offer numerous advantages, such as the absence of complex surgical procedures and easiness of insertion, low cost, great patient acceptance, and more secure under optimal force loads when compared to other orthodontic anchorage devices with the possibility for loading directly after insertion (Geng et. al, 2004; Huang et. al, 2007)
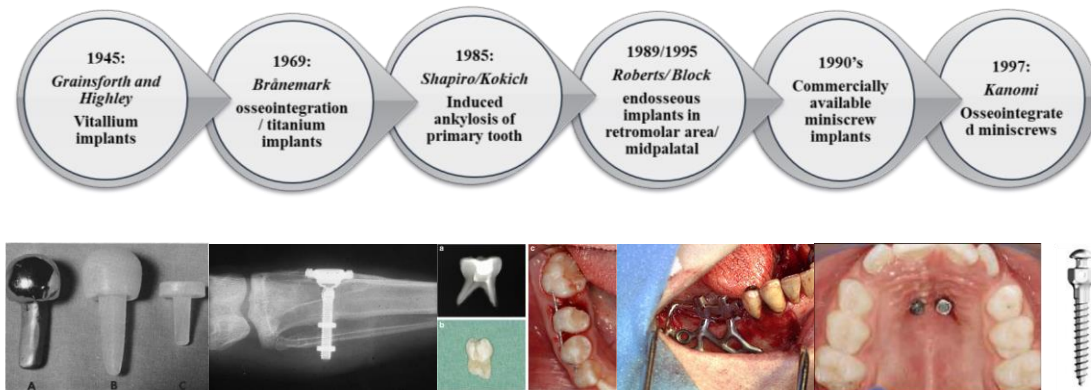
Fig.1.8. Summary of history of mini-implants evolution.

1.1.3.2. Safe zones and success rate

The success rate of mini-implants, ranges between 70.7 and 95.2% (Garfinkle 2008; Shigeeda 2014). MI failure has been linked to factors related to the patient, the screw design, and the placement technique. Haddad and Saadeh (2019) reported that implant stability is associated with the distance from the MI to the alveolar crestal bone. Root proximity was not associated with the MI as suggested by previous studies. The clinical corollary to placing the MI within the attached gingiva but away from the alveolar crest would be to angulate the MI apically to position it in a thicker bucco-lingual/palatal level of bone. On the palatal side, the miniscrew should be embedded for up to 8 mm, to avoid damaging the facial roots. Accordingly, the guidelines for MI include:

a. Screws should be inserted in the maxillary molar region up to 11 mm above the bone crest to avoid impinging on the sinus.

b. Insert the MI at an oblique angle: if inserted perpendicular to the dental axis, it may touch the roots of the teeth particularly in a narrow interradicular space.

c. Because of the reduced tip diameter, a conic screw insertion has a lower risk of damaging roots.

d. The ideal miniscrew for orthodontic skeletal anchorage in the interradicular spaces should be 1.2- to 1.5-mm maximum diameter, with 6–8 mm cutting thread and a conic shape.
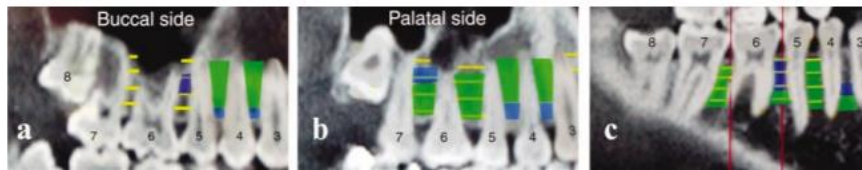
Fig.1.9. (a) Maxillary buccal and (b) palatal side, and (c) mandible images. In green are the zones with a mesiodistal measure over 3.1mm. In blue are the zones with a mesiodistal measure between 2.9 and 3.1mm (Poggio et al., 2006).

1.1.3.3. Intrusion of molars against mini-implants

Umemori and his group (1999) were the first to use miniplates as temporary skeletal anchorage for molar intrusion in managing the open bite malocclusion. Because mini-implants did not require the surgical intervention needed with mini-plates, they became widely used allowing for effective anchorage with easy insertion and removal (Crismani et. al. 2010; Kuroda et. al 2004; Lee et. al.2004).

Molars were intruded approximately 2-4 mm using skeletal anchorage, with better results in the maxilla than mandible because of the resistance from the thicker cortical bone in the mandible. (Degushi 2011; Sugawara 2002). The mechanics involved in intrusion against the buccally positioned TADs include of a vertical intrusive force applied directly to the molar tube or archwire. When necessary, palatal support helps control the three-dimension moments generated by the force system and prevent transverse buccal tipping of the posterior teeth during

force application principally. The palatal support is provided by through the use of a TPA in the maxilla or a lingual arch in the mandible (Ng et al., 2006) but more efficiently with the placement of palatal TADs.

For faster and more predictable results some authors have shown in case reports the integration of surgical interventions such as corticotomy-enhanced molar intrusion and osteotomy-assisted molar intrusion (Moon et al.2007; Grenga et. al, 2013).

Even though MIs design differs between manufacturers, TADs are generally 1–2 mm in width, 6–12 mm in length (thread area) and have a head that serves as a point of force application for the desired forces (Pollei et. al, 2009).

Several protocols have been advocated for the intrusive mechanics of the maxillary molars against TADs, but the comparisons are not available among them, including the determination of the optimal ideal number of TADs to be used for the intrusion (Paccini et. al, 2016; Chen et. al, 2006; Lee et. al. 2013) Listing of specific protocols is displayed in table 3 corresponding to the illustrations 10.

Table 1.3. Summary of pertinent intrusion researches

	Number of cases	Amount of intrusion (mm)	Force applied (gm)	Technique of comparison
Melsen et al. 1996 (Fig 10.A)	3	3-4.5	25	Lateral cephalometrics superimposition
Sherwood et al, 2002 (Fig 10.B)	4	1.99	Not mentioned	Panoramic and lateral cephalometrics
Yao et al, 2005 (Fig 10.C)	22	3-4	150-200	Mechanical 3D digitizer
Lin et al, 2006 (Fig 10.D)	30	3.1-3.4	150-200	Clinical/radiographic evaluation
Lin et al, 2006 (Fig 10.D)	10	Not mentioned	100-150	Radiographic evaluation
Erverdi et al, 2007 (Fig 10.B)	11	1.99	B= 200 L= 200	Lateral cephalometrics superimposition
Heravi et al, 2011 (Fig 10.F)	10	1.7 ± 0.6	50g/miniscrew	Clinical/radiographic evaluation
Akan et al, 2011 (Fig 10.D)	19	3.37	400	EMG/ Lateral cephalometrics
Xun et al, 2013 (Fig 10.F)	56	1.8	100	Radiographic evaluation
Lin et al, 2013 (Fig 10.E)	36	3.4	150-200	Radiographic evaluation
Paccini et al. 2016 (Fig 10.G)	G1: 2 MIs (15M) G2: 3MIs (10M)	G1: 2.18 ± 1.14 G2: 1.86 ± 1.07		Radiographic evaluation
Paik et al, 2016 (Fig 10.H)	3	Not mentioned	Not mentioned	Clinical evaluation

Fig.1.10 A. Mechanics used in Melsen's group in 2 patients (Conventional intrusion method including palatal bas, with or without splints and intrusive archwire bucally)
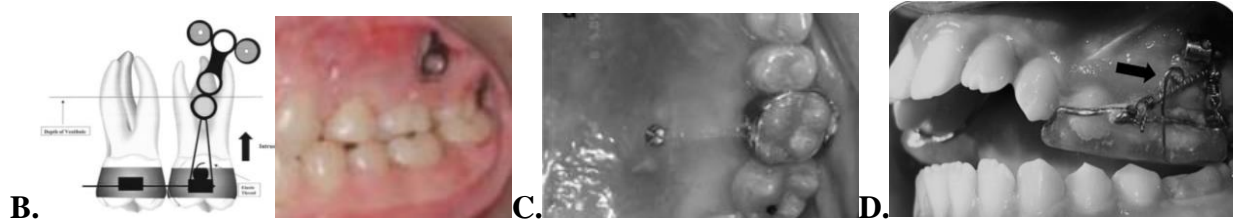
Fig.1.10 B. Zygomatic anchorage used for intrusion in Sherwood and Everdi's studies **C.** associated with one palatal miniscrew used for intrusion in Yao's study **D.** Zygomatic anchorage to a splint to simulate intrusion (Akan et al, 2011)

Fig.1.10 E. Buccal and palatal miniscrews used in Lin's study in 2006 and 2013 for single tooth intrusion and modified transpalatal arch bar with loops placed 5mm away from palate in their second study.

Fig.1.10 F. TMA spring (0.017x0.25-in) with one-point application, intrusion supported by miniscrews (Heravi 2011; Xun 2013)
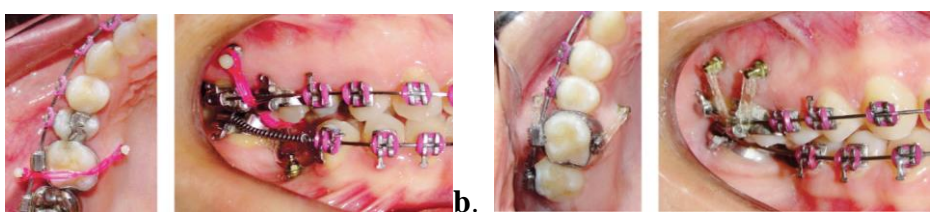
Fig.1.10 G. G1 (a): 2 miniscrews: 1 buccal and 1 palatal compared to G2 (b): 2 buccal miniscrews (Paccini et al. 2016)

Fig.1.10 H. Intrusion protocol adopted by Paik et al. in 2016 including a mid-palatal mini-implant associated with a TP bar.

1.1.4. Finite Element Analysis (FEA)

Although clinical reports and studies have been published on posterior intrusion mechanics; on the biomechanical properties involved with this treatment such as strain, stress, and displacements on the teeth and the surrounding tissues are limited (Rudolph et al, 2001). The oral cavity is a compound biomechanical system with limited access, therefore, most biomechanical research of the oral environment such as in orthodontics, implantology, restorative dentistry, endodontics, and prosthodontics have been executed in vitro (Soares et al, 2012).

Finite element analysis (FEA), a prevailing method in engineering, became a valued choice for the evaluation of biomechanical factors in orthodontics aiming to determine stresses in the dental structures and improve their mechanical strength by modification of load magnitude and application (Çifter et al, 2011; Shetty et al. 2010).

<u>1.1.4.1. FEA in engineering</u>

FEA is a modern tool for numerical stress analysis that approximates physical models into numerical mathematical equations (Tanne, Sakuda, & Burstone, 1987). The analysis involves, first discretization of the structure into its components called "finite elements" connected to each other by nodes with well-defined physical properties (e.g. stiffness, elasticity). Then, a quantitative analysis is conducted to approximate the reactions and interactions within each element (Vasudeva, 2009). Equations from all the elements need to be solved simultaneously, a task that can only be performed by computers. Engineering phenomena such as deflection, stress, strains, vibration, energy storage and many other can be calculated (Fig 14.).

The finite element method (FEM), which has been successfully applied to the mechanical study of stresses and strains in the field of engineering, makes it practicable to elucidate stresses in the biological structures caused by various internal and external forces (Kazuo 1987; Geng 2001).

According to Cook et al, individual finite elements can be visualized as small pieces of a structure. In each finite element, a field quantity can have only a simple spatial variation. The structure is discretized into so-called "elements" connected through points called nodes. The specific organization of elements is called a mesh. Numerically, an FE mesh is symbolized by a system of algebraic equations to be solved for unknowns at nodes. Field quantity over the entire structure is approximated element by element, in pieces (Cook et al. 2002). It includes sequences of computational measures to compute the stress and strain in each element making it possible to adequately model the tooth and periodontal structure by dividing the problem domain into a collection of much smaller and simpler domains, helping in the validation of the clinical assumptions (Salmon et al, 1980).
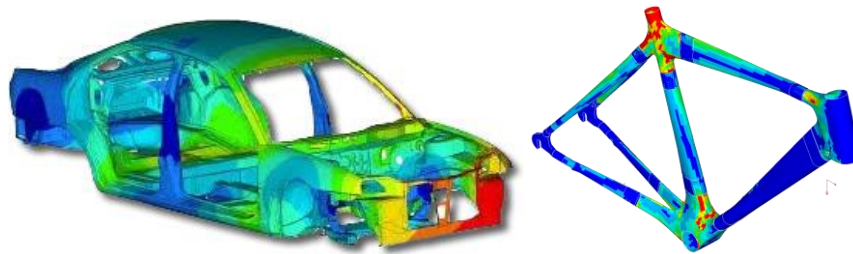
Fig.1.11. FEA applied before the construction to verify the design and detect any critical locations (www.katcon.com/advancedmaterials/design-engineering/)

1.1.4.2. FEA in Orthodontics

The FE method was introduced into dental biomechanical research in 1973 (Farah *et al.*, 1973) and since then has been broadly pragmatic to study the stress and strain fields in the alveolar support structures (Tanne et al., 1987, 1998; Middleton et al., 1990, 1996; Cobo et al., 1993; Bourauel et al., 1999; van Driel et al., 2000; Provatidis, 2000; Qian et al., 2001; Toms and Eberhardt, 2003). The study of orthodontic biomechanics was structured in the 1960s with the works of Burstone and later Nikolai (Bourauel et al. 2007). In previous studies stress levels were assessed in a single tooth system constructed on the basis of average anatomic morphology. The introduction of 3D radiography in dentistry permitted the generation of more complex models to study stresses in a group of teeth (Cobo 1993; Kaipatur 2014).

Through FEM, the analysis of any material or dento-maxillofacial structure was possible (Lotti et al. 2006) by breaking a complex structure down into the smaller "elements" (Shaw et al. 2004) to which corresponding physical properties, such as the modulus of elasticity, are assigned. The great advantage of the method lies in the control of the degree of simplification

(Jones et al. 2001). With FEM, it became possible to anticipate the tissue responses to the specific orthodontic mechanics applied.

Alternative experimental models used to analyze the biomechanics of tooth movement include photo-elastic models (Caputo et al. 1974); however, they have the shortcoming of exploring only the surface of the model without analyzing the internal structures, such as the periodontal ligament.

The study of stresses on teeth is complex because of the non-homogeneous character of tooth material and corresponding material properties (pulp, cementum, periodontal ligament, and surrounding bone), as well as the irregularity of tooth contours (Senka et al., 2003), and the complex external and internal morphology (Hussein et al., 2012). In addition, chewing forces lead to furthermore complications (Rubin et al., 1983).

All the salient factors (forces, deformation, stress, and movements) are reciprocally linked. Thus, by determining any one of them the extent, amount, interval, and intensity of the remaining physical factors can be figured out (Rudolph et al., 2001).

FEA simulates the load transfer from the tooth through the PDL to the alveolar bone accounting for the physical properties and morphology of the periodontium. Although PDL is a nonlinear viscoelastic material, most of the preceding FE models integrate homogeneous, linear elastic, isotropic, and continuous PDL properties (Cattaneo et al. 2005).
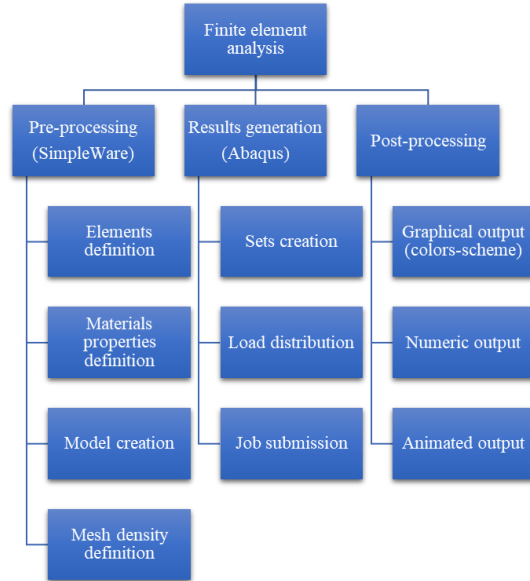
Fig.1.12. Summary representing phases of finite element analysis. (Adapted from: Mohammed et al., 2014)
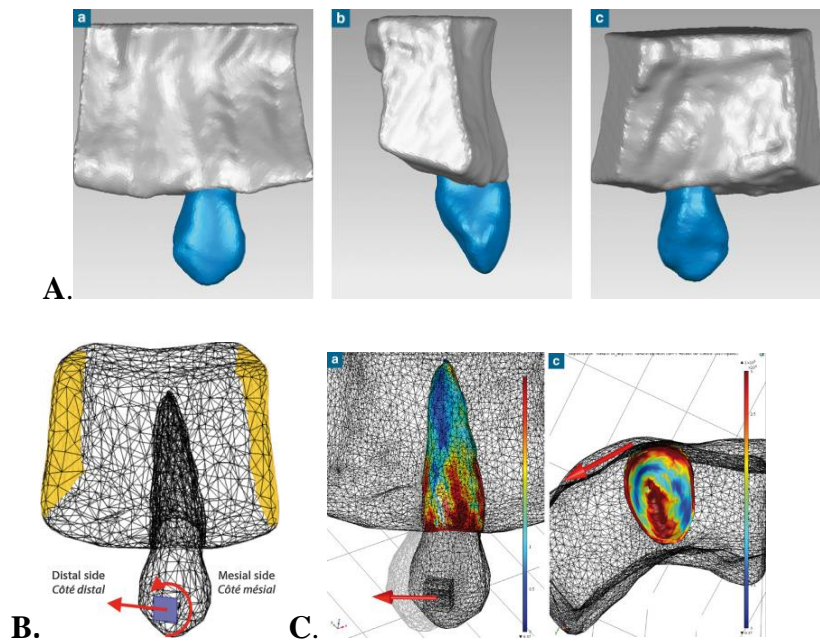
Fig.1.13 A. 3D reconstruction of tooth model extracted from a CBCT **B.** Meshed Model **C.** FEA results (Bouton et al., 2017)

1.1.4.2.1. Shortcomings and benefits of FEA

The analysis of results in FEA is very delicate because the entry of imprecise data, material information, and interpretation will produce erroneous outcomes. Furthermore, modeling human structures is demanding because of their compound anatomy and lack of broad information about their mechanical behaviors. Certain presumptions must be accepted. Henceforth results will be contingent on those assumptions and the expertise of the researcher.

Increasingly, reliable physical properties for structures such as, enamel, dentin, periodontal ligament, and cancellous and cortical bone, should further mimic the clinical settings. Moreover, during the process of load application, the tooth is pinned to the supporting bone, which is rigid and the nodes connecting the tooth to the bone are considered fixed. This postulation may introduce some error (Mohammed et al., 2014).

Despite the abovementioned limitations, the FEM has improved biomechanical research in orthodontics. It is a non-invasive, precise method that offers quantitative and thorough data on the physiological responses occurring in tissues (Kamble et al. 2012) with the benefit of controlling study variables (Viecilli, 2006).

1.1.4.2.2. Specific orthodontic applications of FEM

FEA has a wide-ranging variety of usages markedly in Orthodontics: craniofacial growth, periodontal stress and tooth movement, orthopedic forces, temporomandibular joint dynamics, orthognathic surgeries, orthodontic implants, brackets, and wire designs.

23

A. Tooth Movement

Direction and amount of tooth displacement during different types of tooth movements:

Molar protraction was investigated with a model testing for force application and mini-implants dimensions necessary for this movement (Kojima and Fukui, 2008; Liang et al., 2009; Nihara et al., 2015). Distalization was evaluated by several authors (E.-H. Sung et al., 2015; Yu et al., 2014) who evaluated antero-posterior movement of molars in the maxillary arch and compared effectiveness when changing mini-implants locations and force application. Maxillary expansion was assessed through the efficiency of different bone-borne appliances (H. K. Lee et al., 2012) and in surgically assisted palatal expansion (Han et al., 2009). Conclusions on treatment with clear aligners suggested that the absence of biomechanically supplementary composite attachments favors the undesired inclination of the tooth during the translation movements (Gomez et al., 2014) Maxillary protraction was compared between different designed tooth-borne and bone-borne appliances (K. Y. Kim et al., 2015; Yan et al., 2013). Incisors retraction was evaluated in a labial and lingual designs en masse retraction (Lombardo et al., 2014). Anchorage loss was also determined during the retraction of lingually or buccally inclined incisors (S.-J. Sung et al., 2010).

Areas most likely to present root resorption were evaluated in relation to the root shape of central incisors indicating that the maxillary central incisors with deviated root morphology are at higher risk of resorption (Kamble, Lohkare, Hararey, and Mundada, 2012).

The stress and displacement effects of three maxillary posterior intrusion mechanics with mini-implant anchorage were studied by Çifter et. al. (2011) using FEA. They applied a 300g force on

each posterior dental segment, distributed to the mini-implants in proportion to their calculated root surface areas.

The model was generated from CT images taken from a maxillary bone. Each tooth was located in the maxillary model aligned in respect of the periodontal membrane, cortical bone, and alveolar bone layers. The periodontal membrane was assumed to have a thickness of 0.25 mm evenly. The thickness of the cortical bone was 2 mm at the palatal alveolar bone and decreased from 2 to 1 mm from the top of the alveolar bone to the nasal floor of the buccal alveolar bone. The computer-aided design model of brackets, bands, and archwires with the same dimensions were generated with a laser surface scanner.

The results indicated that the most balanced intrusion and the most uniform stress distribution were obtained by concurrent force applications from the buccal and palatal sides. In setup with transpalatal arches and buccal force application, vestibular tipping movement and overall stress values were prominent. In all models, increased stress values were identified at the apical region of the first premolar roots and the apical region of the first molar mesial root. In summary, the results of this study suggest that the apical region of the first premolar roots and the apical region of the first molar mesial root should be considered to be prone to resorption during posterior intrusion treatment. Posterior intrusion systems with force application from counterbalancing sites lead to a more uniform stress distribution and balanced intrusion than the mechanics with a transpalatal arch. For a balanced intrusion, root surface areas should be considered when determining the appropriate forces.

B. Other than tooth movement

Craniofacial growth: According to Moss et al. (1985), FEM allows the analysis of the skull at a better resolution than previous techniques by discretizing the skull into adjacent finite elements. It is a delicate morphometric method and it can approximate the deformation of the structure under examination, in all directions and at every landmark, unlike the conventional cephalometric analysis (McIntyre et al., 2003).

Periodontal stress and tooth movement: Stress in PDL is linked with orthodontic tooth movement (Tanne K et al., 1987; Mestrovic et al., 2003; Kojima et al., 2011).

Orthopedic forces: FEA was used to study on mandible models including the temporomandibular joint (TMJ) to study biomechanical changes of the mandible from orthopedic chin cup action (Tanaka et al.,1994), and on maxillary models to analyze stresses distribution during rapid maxillary expansion via transverse orthopedic forces (Jafari et al., 2003).

Temporomandibular joint dynamics: Gupta et al. (2009), assessed in a study the stress generated in the TMJ after mandibular protraction and. This was investigated in a thesis research entitled "Inter-arch Elastics and Corresponding Stress on the Temporomandibular Joint and on the Mandibular Teeth: A Finite Element Analysis Study" (El-Helou et al. 2017).

Orthognathic surgeries: 3D simulation of outcomes and virtual surgical planning permits a new way in the interaction between patient and clinician. Soft tissue prediction resulting from bone repositioning after maxillofacial surgery was done in the research of Chabanas in 2003.

Orthodontic implants: FEA studies evaluated optimal dimensions of mini-implants for the maxillary posterior region and conceived that the optimal biomechanical conditions could be achieved with MIs having a diameter not exceeding 1.5mm in combination with ideally an increased length (preferably not less than 8mm) compatible with the safety of anatomical structures upon insertion (Jiang et al 2009).

Brackets and wire designs: One of the benefits of FEA is its ability to allow for mechanical experimentation of all designs in a reduced time and less need for prototypes and laboratory work (Huang et al., 2012).

1.2. Significance

FEA is a valuable mechanical way to assess tooth movements, by fractionating the geometry into its elements and validating the assumptions given to these elements from clinical data. The results are the closest to real clinical settings in the absence of a more direct but invasive approach.

Defining the properties of bone is of the utmost importance when FE analysis of a bony structure is contemplated. In previous FEA studies, bone variation was not accounted for as an element affecting the results. This study accounts for variations in cortical bone stiffness and thickness of real human beings, thereby creating a closer link between the virtual finite element

models and actual clinical variations. Most previous studies of the stress after different intrusion modalities, did not include palatal miniscrews in their mechanics and did not account for the effect of cortical bone thickness on the stresses. The inclusion of these parameters in our study shall allow conclusions and possible applications of the findings because of the introduced individual variation.

The definition of material properties especially of compact bone involved in tooth movement is essential. The role of cortical bone in impeding (Ten Hoeve and Mulie, 1977) or assisting (Rickets, 1980) tooth movement has been shown as a general determining factor. We aim to determine how cortical bone affects tooth movement by analyzing the effect of stiffness (related to bone density) variation taking at the same time account of the geometry and thickness of the cortex. In this context, the results should highlight which of the variables, stiffness, thickness, or both affect initial stress and displacement after the implementation of five modalities of posterior teeth intrusion.

On the basis of the designed study, the inclusion of individual human variation and the testing of different intrusion modalities shall move the research endeavors forward, both in accounting for the variation in material properties and setting the stage for time-dependent FEA, necessary to reach the ultimate goal of planning, simulating, and executing the proper mechanotherapy in the individual patient.

Moreover, such studies would be coupled with direct clinical assessments, beyond simple measurements of tooth displacement and including the assessment and correlation with biologic markers if crevicular fluid and patient response (pain level).

1.3. Specific aims

Aims related to the orthodontic intrusion of maxillary molars:

1. Compare the stress levels on the PDL of the maxillary buccal teeth in five different clinical intrusion setups against mini-screws placed at different locations and with different force applications.

2. Compare the initial displacement (primary intrusion and secondary effects) corresponding to the various intrusion setups.

3. Compare the stress and displacement under variable cortical bone material properties (stiffness and thickness).

Aims related to FEA application in orthodontics:

4. Develop a complete model for tooth movement accounting for material properties including the PDL and all the orthodontic gadgets (brackets, archwire, and miniscrews) to simulate true orthodontic mechanics.

5. Assess the response to forces according to the orthotropic properties of the bone (evaluate the response about variations in stiffness as per defined characteristics of maxillary bone biomechanics).

1.4. Hypothesis

In relation to the orthodontic intrusion of maxillary molars and premolars:

- Each intrusion modality has differential effects on teeth and different extent of secondary effects.

- Initial tooth displacement is related to the stress generated by the intrusion.

- The more force exerted the more displacement with higher stresses.

- Cortical bone stiffness and thickness influence the rate of tooth movement independently (thickness has a greater influence on displacement).

- Posterior intrusion systems with force application from buccal **and** palatal sites should be planned for more uniform stress distribution for better control of buccal tipping and lessen secondary effects.

In relation to the FEA application in orthodontics:

- Individual variation in the anatomy of the maxilla influences stresses generation.

- Interaction properties between the teeth can mimic the clinical situation.

CHAPTER 2

MATERIAL AND METHODS

2.1. Material

2.1.1. Anatomical record

A 3D model of the maxillary arch of an adult patient having all permanent teeth except the third molars was generated from a pre-treatment cranial CT scan (format: DICOM) selected from the Department of Radiology at the American University of Beirut Medical Center. The following characteristics were the basis for exclusion:

- Presence of any craniofacial anomaly (e.g. cleft lip/palate)

- Absence of medical conditions affecting bones in general and the maxilla in particular

- CT scan of patients undergoing orthodontic treatment

- Crowded or mal-aligned teeth

- Presence of deciduous teeth

- Missing or extracted teeth

CT scan imaging allows with its high contrast quality to differentiate trabecular from cortical bone and offers better resolution and contrast when compared to the regular CBCT which is more frequently requested in the dental clinical setting because of the reduced radiation.

The CT scan chosen was taken with a full head field of view with a resolution of $0.3 \times 0.3 \times 0.4$ mm with high contrast. Ideally, the scans should be attained with a cross-section of a minimum 0.25 mm distance to reach adequate resolution needed to construct the model. Accordingly, the

CT scan library at the hospital contains X-rays with a resolution between 0.4 and 0.6 mm. A radiograph was obtained without any details on the patient's identity. The scan revealed a well-aligned complete dentition, parallel roots, and a Class I occlusion with the midlines on, suggesting that the patient possibly had previous orthodontic treatment.

2.1.2. Individual Data Acquisition

Variables for individual variation were extracted from thickness and stiffness of interradicular maxillary cortical bone from 15 cadavers obtained from collaborators at the AMIN Texas University These measurements were extracted from a study by Peterson et al (2006), which was supported by The National Institutes of Health (NIH), National Institute of Dental and Craniofacial Research (NIDCR); Grant number K08 DE00403. Human tissue use conformed to the NIH, state, and federal standards.

This study entitled "Material Properties of the Dentate Maxilla" aimed to explore the changeability in the characteristics of the cortical bone of the dentate maxilla. The hypothesis was that important regional differences existed within the maxilla that would correspond to variations in function and development. Specimens were removed from the crania of 15 dentate human cadavers: 7 females (48–95 years of age) and 8 males (50– 89 years of age) with a median age of 58.9 years.

Cylindrical cortical bone specimens (4 mm in diameter) were harvested from 15 maxillary sites located in three distinct regions: (Fig.2.1)

- palate (four sites),
- alveolar bone (four sites),

- body of the maxilla (seven sites)
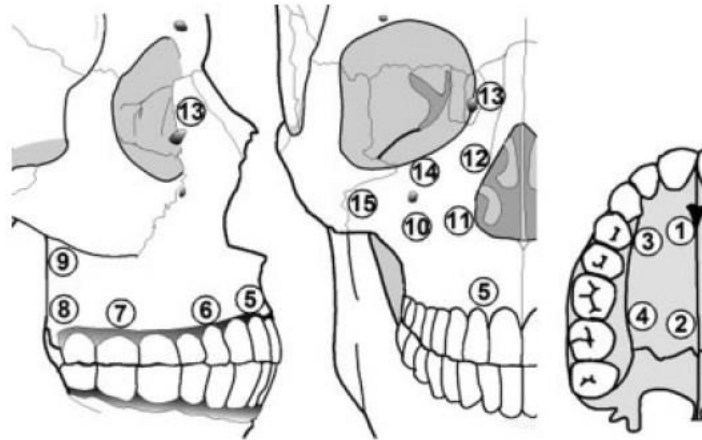
Fig.2.1. Cortical bone sites in the maxilla (numbered for reference) (Peterson et al., 2006).

Each bone specimen was measured using a digital caliper to determine the thickness of the bone cylinder. Apparent density was calculated based on Archimedes' buoyancy principle. Material property testing was performed using the pulse transmission technique. Using the linear elastic wave theory (Ashman et al., 1984; Dechow, Nail, Schwartz-Dabney, and Ashman, 1993), the specimen material properties were derived from various velocities with the following directions:

- **Maximum stiffness** (d3) matched with the direction of peak ultrasonic velocity and is parallel to the long axis of the three-pillars of the maxilla [zygomaticomaxillary, pterygomaxillary, and frontomaxillary] (Sicher and DuBrul, 1970).

- **Minimum stiffness** (d2): Perpendicular to the axis of maximum stiffness within the plane of the cortical plate.

- **Cortical thickness axis** (d1): Through the thickness of the cortical plate perpendicular to both (d2) and (d3).

Elastic modulus (E): measures of the ability of a structure to withstand deformation in a given direction, was defined by E1, E2, or E3 according to the axis direction.

Shear modulus (G): the measure of the stiffness in shear or angular deformation relative to applied shearing loads in a plane formed by the two axes (G12, G31, or G32).

Poisson's ratio (υ): the measure of the ability of a structure to resist deformation perpendicular to that of the applied load, (orientation for Poisson's ratios in the same manner as in describing the shear moduli (υ12, υ21, υ13, υ31, υ23, υ32)).

Significant differences were registered between sites in thickness and density that individually outlined regions of the maxilla. Altogether, where the cortical bone was slender, its density was high. Cortical bone near the incisors and canines (sites 3, 5, and 6) had greater thickness than at other maxillary alveolar sites, but its density and stiffness were intermediate.

The values for elastic moduli showed variances by direction (E3 >E2>E1). There were statistically significant differences between sites for E2 and E3. Most sites within the dentate maxilla were moderately anisotropic with ratios ranging from 0.69 to 0.85. Site 7 above the second molar and under the root of the zygomatic process had the densest and stiffest cortical bone in the buccal alveolar area. Palatal cortical bone areas had relatively higher stiffness than buccal areas (Table 2.1; Table 2.2).

Table 2.1. Density (mg/cm3), cortical thickness (mm) and ash weight (Peterson et al., 2006).

Site	N	Density		Thickness		Ash weight	
		Mean	SD	Mean	Mean	%	Mean
1	12	1.65	0.17	1.7	0.5	56	5
2	10	1.75	0.14	1.8	0.9	55	9
3	11	1.75	0.18	2.3	1.1	57	5
4	10	1.70	0.16	2.0	1.0	53	7
5	14	1.65	0.15	2.2	1.3	57	5
6	8	1.64	0.19	2.4	1.6	58	9
7	11	1.72	0.20	2.1	0.9	54	11
8	6	1.61	0.14	1.2	0.6	54	15
9	6	1.77	0.16	1.0	0.3	53	15
10	10	1.75	0.16	1.2	0.5	56	8
11	9	1.69	0.15	1.7	0.7	54	11
12	11	1.82	0.12	1.5	0.4	53	12
13	11	1.83	0.17	1.4	0.3	50	13
14	11	1.81	0.11	1.5	0.6	55	7
15	7	1.90	0.12	1.1	0.3	61	5
Grand mean		1.75	0.16	1.9	0.9	56	9
ANOVA		F	F	P	F	P	F
Sites		4.7	0.001	5.4	0.001	NS	NS

Table 2.2. Elastic moduli in GPa (Peterson et al., 2006).

Site	E_1		E_2		E_3	
	Mean	SD	Mean	SD	Mean	SD
1	8.3	1.9	11.3	2.7	14.1	2.9
2	8.9	1.9	11.9	2.3	16.5	4.0
3	10.3	2.0	13.6	2.1	17.3	3.4
4	8.9	2.9	10.9	2.7	15.6	3.7
5	10.0	3.3	11.0	2.7	14.3	3.8
6	7.2	1.5	8.7	2.3	12.2	1.9
7	9.8	2.4	11.3	3.0	16.0	4.3
8	6.9	1.1	8.8	1.0	10.5	1.3
9	9.8	2.3	11.7	1.4	15.6	2.8
10	7.6	2.3	10.7	3.3	14.2	4.2
11	9.0	1.9	11.2	2.2	16.4	3.6
12	10.0	1.7	13.5	1.6	17.6	3.4
13	9.9	3.0	12.8	2.8	17.0	3.3
14	9.4	1.6	13.3	2.1	17.8	2.3
15	9.2	1.5	14.0	1.7	18.7	3.4
Grand mean	9.1	2.3	11.7	2.7	15.6	3.7
ANOVA	F	P	F	P	F	P
Sites	1.51	NS	3.02	0.001	3.87	0.001

2.2. Methods

The chronological protocol from image capture to FE analysis is represented in a flow chart of 7 steps, developed in a FEA study of miniscrews (Ammar et al., 2011; Fig.2.2).
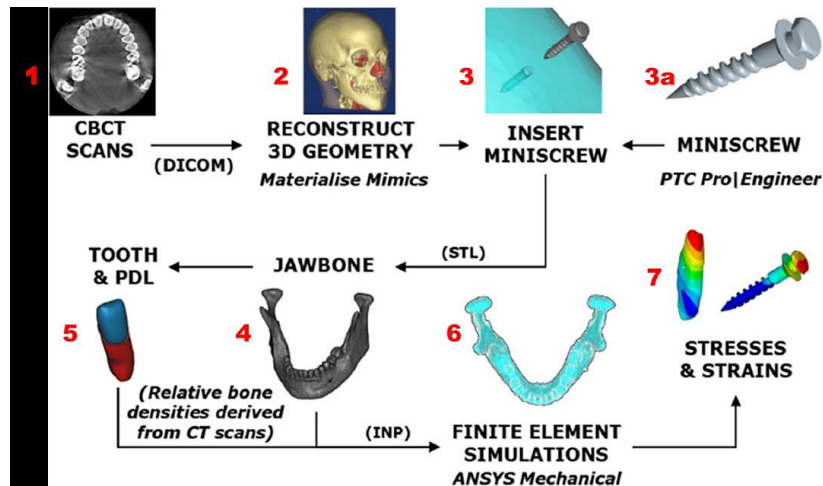
Fig.2.2. The approach for 3D patient-specific model reconstruction and dental finite element simulations (after Ammar et al, 2011).

Different software is used from the computer tomography image reconstruction (step 1) to the finite element simulations (step 6). Steps 1 to 5 correspond to the development of the 3D model; steps 6 and 7 relate to the FE analysis.

2.2.1. 3D Model

2.2.1.1 Image importing and model segmentation

The CT image was imported and segmented using the image processing and digital reconstruction software ScanIP™ 7.0 (Simpleware, Synopsys, Mountain view, CA, USA). Areas of interest (ROI) were chosen (included the maxillary bone and teeth) and non-significant ones deleted using the *crop tool* in ScanIP™.

Masks of every tooth, periodontal ligament as well as cortical and trabecular bone were created using manual and automated tools (see below). Automated segmentation was adopted for time management and allow reproducibility and reliable outcomes. Details of segmentation of all

masks will be spared since the same model used in the previous thesis was used with some additions and modifications.

Most importantly, '*Segmentation with Threshold'* tool that identifies voxels with Hounsfield units in a specific range to capture the voxels associated to the teeth was employed. Editing of the masks to eliminate excesses was achieved initially using automated filters to remove unconnected fragments ('*flood fill* 'command*),* to breakdown large fragments ('*morphological filters: Open and Erode'*), and to delete small fragments ('*Island remover'*). Details of Periodontal ligament mask will be developed since it is a soft tissue not identifiable on radiographs:
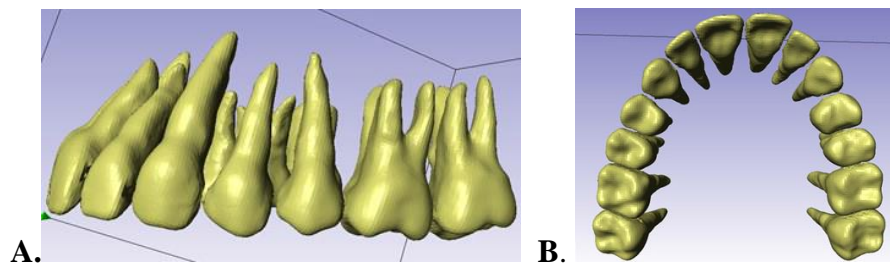
Fig.2.3. Finalized teeth mask: **A.** Lateral view; **B.** Axial view.

PDL Mask:

The periodontal ligament (PDL) cannot be captured on the CT scan. Therefore, the PDL mask was created with a thickness assumption of 0.3 mm (Bowers, 1963). Before this step, teeth were contacting the bone mask. The construction included 5 steps (Ammoury, Zeno; 2016):

- *Duplication* of the teeth mask

- Dilation of the new teeth masks (mask 9) by 1 voxel (0.3 to 0.4 mm) away from the surface of the tooth using the *morphological dilate tool.*

- Selecting the common area between the bone (mask 10) and the expanded teeth (mask 9), which will eventually represent the PDL (mask 11), using the '*Intersection Boolean operation tool*'.

Fig.2.4. PDL mask

A.

B.
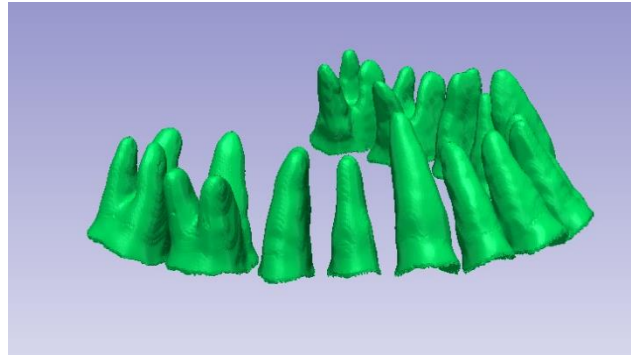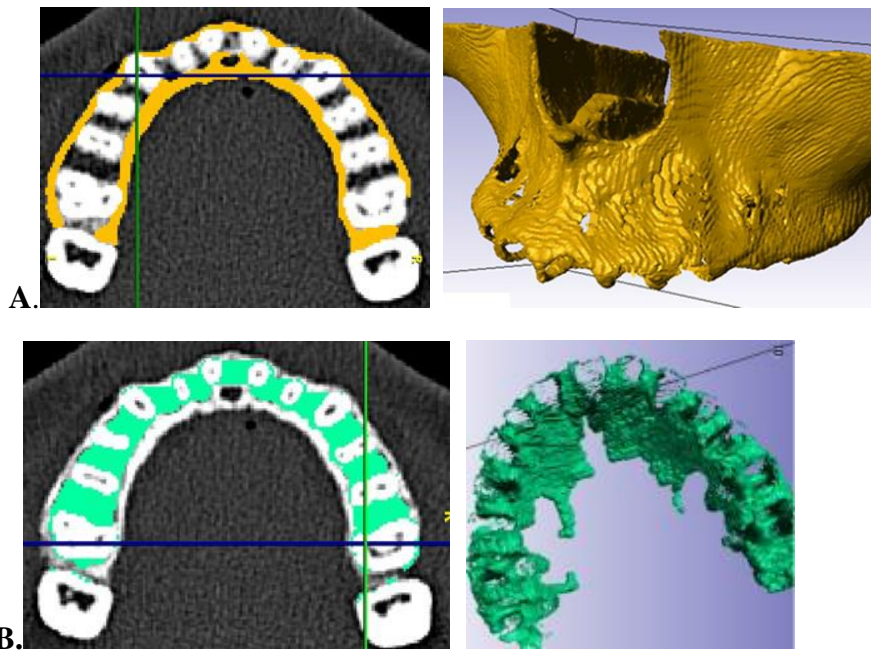
Fig.2.5 A. Cortical bone layer mask: 2D axial cut; **3**D view.
B. Trabecular bone (mask 5): Axial cut; **3**D view.

<u>2.2.1.2. CAD processing</u>

Autodesk® 3ds Max® Design software was used to sketch commercially available brackets (Mini-Twin bracket Orthos, SDS Ormco) and available miniscrews (OSAS - DEWIMED - Tuttlingen, Baden-Württemberg, Germany) with the following dimensions: 6 mm length, 1.5 mm diameter, reported as the ideal dimensions by Deguchi et al. (2006). The .max files were converted into .stl files and imported into the +CAD add-on module (Simpleware, Synopsys, Mountain view, CA, USA) to position the CAD geometry.
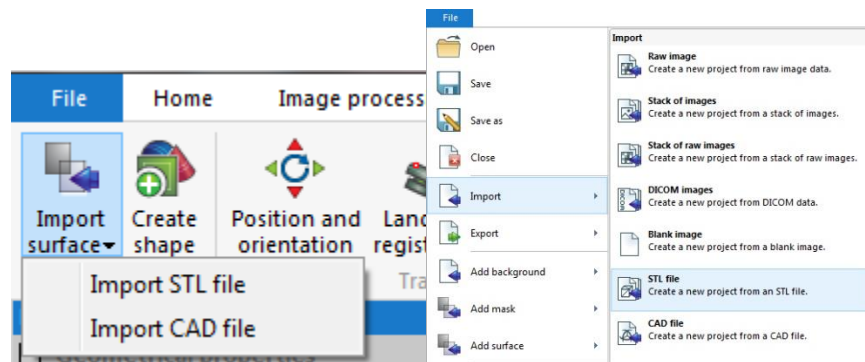
Fig.2.6. Process of importing CAD files (Brackets and mini-implants).

1- The brackets were positioned only on the right hemi-maxillary teeth crowns following the long axis of the tooth to define the point of application and direction of the load whenever it is applied on the brackets. To apply the force directly on the archwire in other modalities, a wire was inserted (Insert object, rectangular) fitted into the slot of all brackets of aligned teeth, equivalent to clinically used 0.021x0.025SS extending from right second molar to right central incisor. An axis system following the long axis of every tooth was created in Abaqus to simulate the movement of teeth along the archwire. Subsequently, specific boundary conditions allowing

39

for accurate tooth movement were assigned to 10 to 15 nodes located at the level of the brackets

position along with creation of interactions between adjacent surfaces.
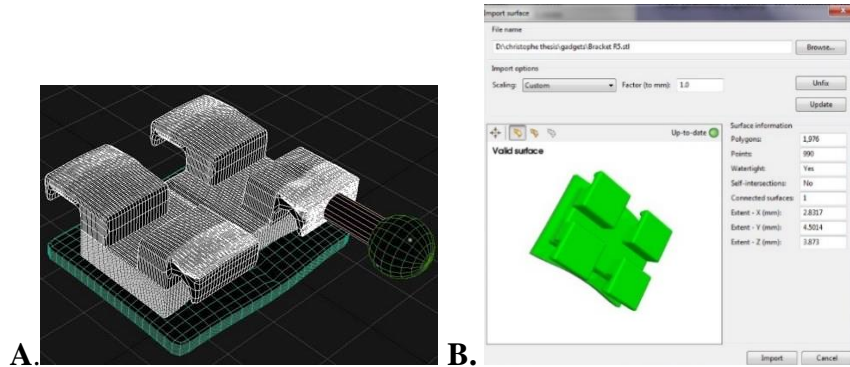
Fig.2.7. A. Bracket CAD sketched in Autodesk® 3ds Max® Design software
B. Bracket imported as a surface and fixed to fit dimensions of the maxilla model.
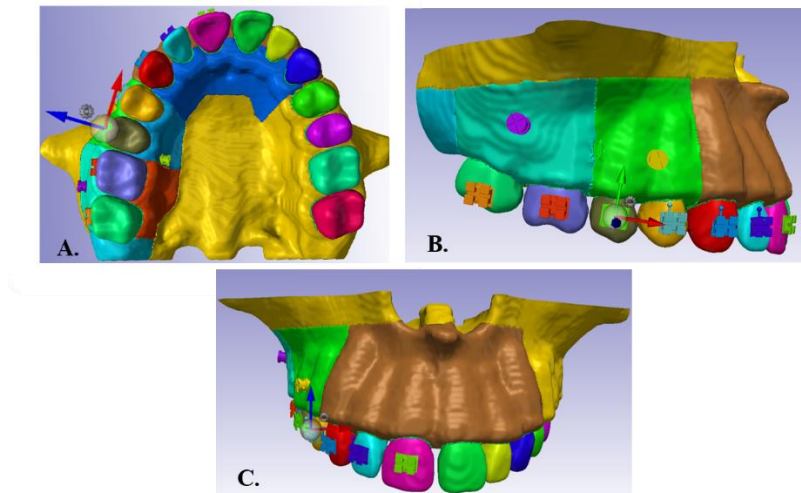
Fig.2.8. Positioning the brackets onto buccal surfaces of teeth
A. Axial View 3D model **B.** Lateral view 3D model **C.** Frontal view 3D model

2- The miniscrews were placed 5 mm apical to the cementoenamel junction (CEJ) at three buccal

interradicular spaces judged to have enough space for the MIs insertion, and to provide the

necessary forces for every intrusion modality to be tested:

1- Between the right second premolar and first molar when only one buccal miniscrew was used.

2- Between the first and the second right premolars and between first and second molars when two buccal miniscrews.

3- One miniscrew was inserted between the molars and one between the first molar and the second premolar.

Two positions were adopted for palatal MIs:

1- Between the right second premolar and first molar when only one palatal miniscrew was used.

2- Between the first and the second right premolars and between first and second molars when two palatal miniscrews were used.
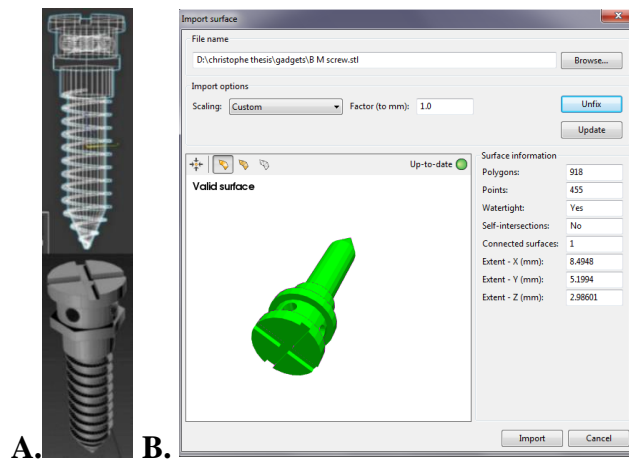
Fig.2.9. A. TAD CAD sketched in Autodesk® 3ds Max® Design software **B.** Mini-implant imported as a surface and fixed to fit dimensions of the maxilla model
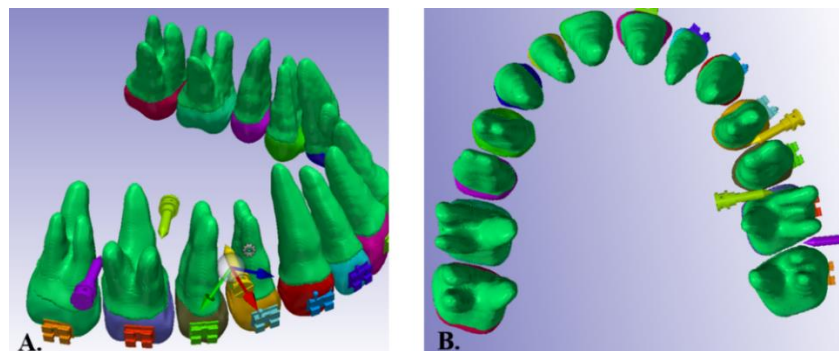
Fig.2.10. Positioning the Mini-implants between the roots.
A. Oblique view 3D model **B.** Axial View 3D

Successive cuboid shapes were created using the *Surface Tools* in Simpleware to form the final archwire, the latter was positioned into the free slots of the brackets simulating the clinical situation.

After completing the full length of the wire, the material property was assigned to simulate a stainless steel archwire.
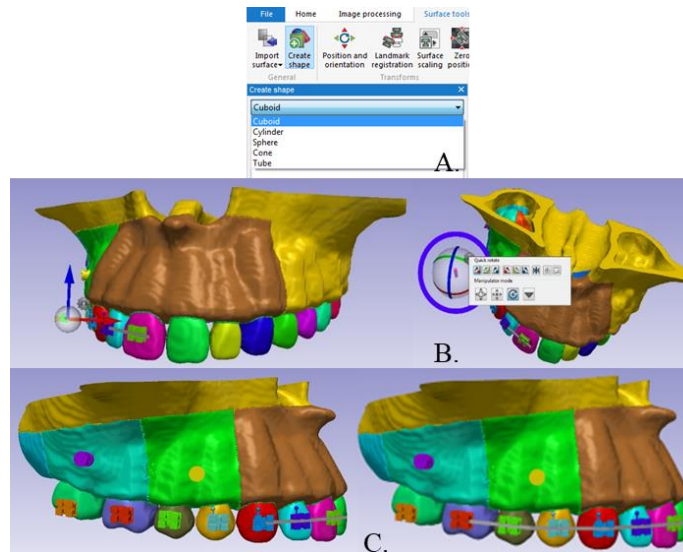
Fig.2.11. A. Process of creating shape of the wire section by section **B.** Repositioning the cubic shaped section of the archwire **C.** Fitted wire from anterior to posterior part into the inter-bracket span.

2.2.1.3. Individual variations

Anatomical variations in cortical bone stiffness and thickness were generated from the original prototype model to simulate clinical situations, the detailed individual data from 15 cadavers obtained by Peterson et al. 2006 (section 2.1.2) were used to replicate different bone characteristics found in human individual specimen.

Stiffness variation

The right side of the cortical bone's mask was divided into 7 areas of interest related to the mechanical model (4 buccal and 3 palatal areas) to be able to modify the stiffness and assign

42

an individual material property to each region matching the classification by Peterson et al (2006) (Fig.2.18).

For each area, a new mask was created via ScanIP™. Cuboid shape objects were created for the areas 3,4,6,7, and 8, using the 3D editing tool. As for area 5, two cuboid shape objects were used to select the cortical bone area spreading from the right to the left canines with the same cervical and apical borders as the previous objects; then they were combined using the 'Union Boolean operation' (Fig 3.18).
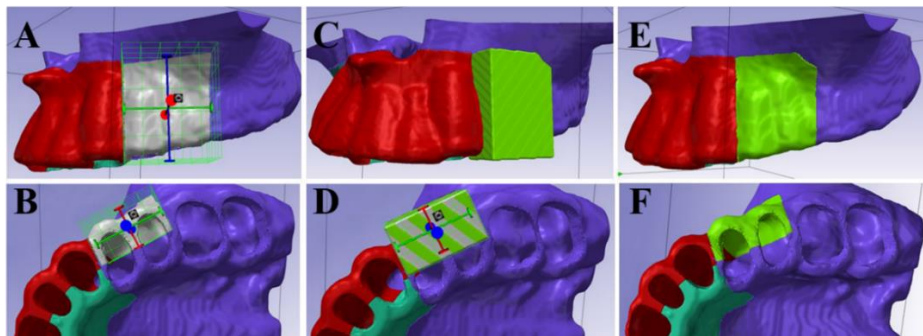
Fig.2.12. Creation of the buccal premolar cortical bone part. **A-B.** 3D editing tool used to create cuboid shape objects; **C-D.** Fill option used to form filled cuboid shaped mask; **E-F.** Intersection Boolean operation used with the original cortical bone mask to form the cortical bone part. (Ammoury et al., 2017)

Finally, each cortical bone part was assigned a material property from the individual values provided at the maxillary sites 1, 3, 4, 5, 6, 7 and 8 (fig 3.13.A).

- Palatal cortical bone at incisors area
- Palatal cortical bone at premolars area
- Palatal cortical bone at molars area
- Buccal cortical bone at incisors area
- Buccal cortical bone at premolars area
- Buccal cortical bone at molars area
- Buccal cortical bone at the tuberosity area

A.
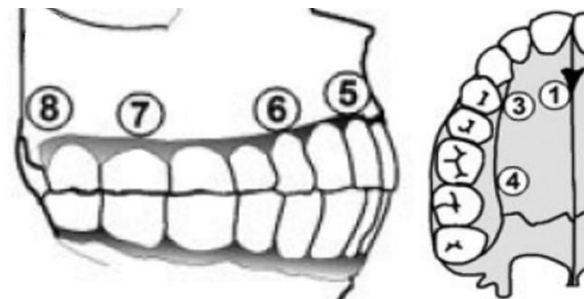
Fig.2.13. A. Maxillary buccal and palatal areas defined by Peterson et al. (2006)

B.
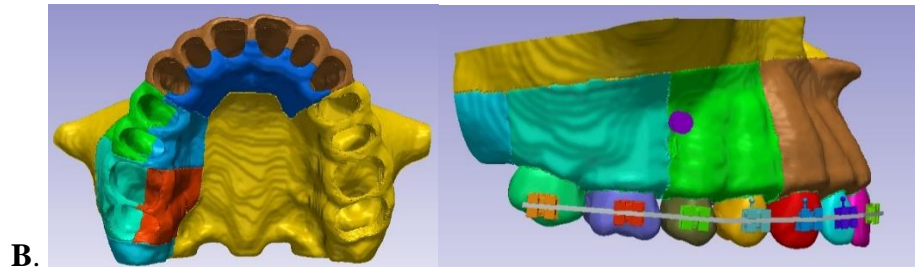
Fig.2.13. B. The 3D Model after cortical bone division.

Thickness variation

Separate models each corresponding to a single cadaver were meshed using Simpleware

ScanIP™ 7.0 by replicating thickness values provided by Peterson et al. (2006) in the template

model (with cortical bone parts).

Only cadavers with all values available were used, and if any single value was missing,

the average thicknesses from the total sample were used for the corresponding areas.

Initially, the cortical bone thickness of each part was measured in the template model at 9 sites

dispersed around the bone part surface. In each site, 25 to 30 thickness measurements were made

on the 2D axial cut sections using ScanIP™ 7.0. A minimum of 200 cortical bone thickness

measurements was performed for each cortical bone part (Fig 3.20).

Next, the total average was calculated and later used to calculate the amounts of

expansion or reduction needed for each mask by subtracting the template model thickness from

the cadaver thickness at the same location. Knowing that the pixel size is 0.2 mm (after

resampling), the value obtained is multiplied by 0.2 to determine the number of pixels needed to

attain the cadaver's thickness. To avoid changing the outer contour of the model, the thickness

variation was implemented at the expense of the trabecular bone.
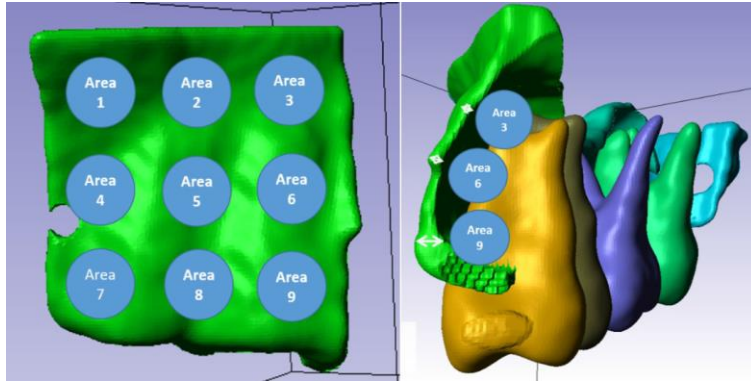
Fig.2.14. Areas of thickness measurements in the buccal cortical bone part at the premolar area.

Depending on the need to expand or reduce the cortical bone thickness, two methods were used:

- Scenario 1: Template Model Thickness < Cadaver Thickness (Fig.2.21).
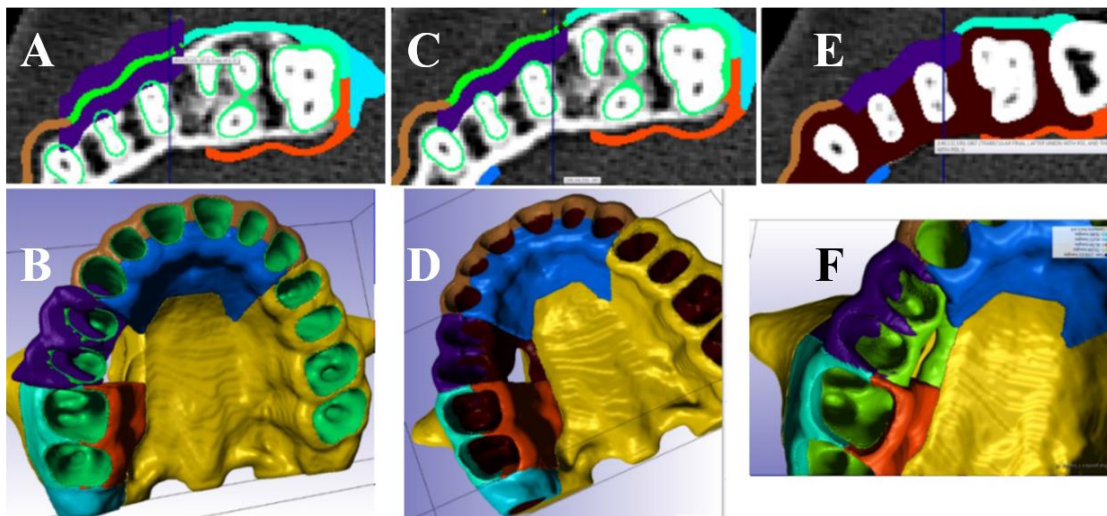
Fig.2.15. The technique applied to increase cortical bone thickness. **A-B.** 2D and 3D images after dilating the premolar cortical bone part by 14 pixels; **C.** After applying "Intersection Boolean operation" with trabecular bone mask; **D-E-F.** 2D and 3D images after union with "original cortical bone part".

- Scenario 2: Template Model Thickness > Cadaver Thickness (Fig.2.22)
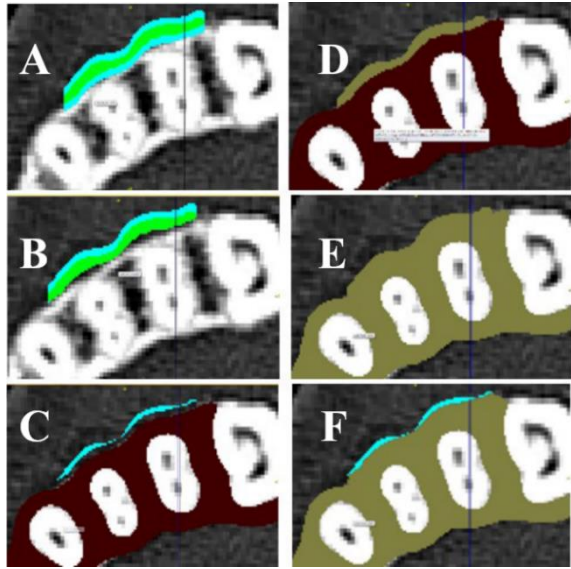
Fig.2.16. The technique applied to decrease cortical bone thickness. **A.** The buccal premolar cortical bone part dilated by 3 (dilation occurs on both sides of the cortical bone). **B.** Delete the increase that occurred at the inner cortical surface by subtracting the trabecular bone mask from the dilated cortical part; **C.** Application of *Morphological Erode* filter by 3 (mask a); **D-E.** Duplicate trabecular bone mask and then unite it with the original cortical bone part (mask b); **F.** Subtract the mask a (eroded cortical bone part) from the mask b (combined trabecular and original cortical bone part).

After applying the above-mentioned steps on the seven areas of each model, twelve 3D models were generated, each corresponding to one cadaver (Fig.2.23)
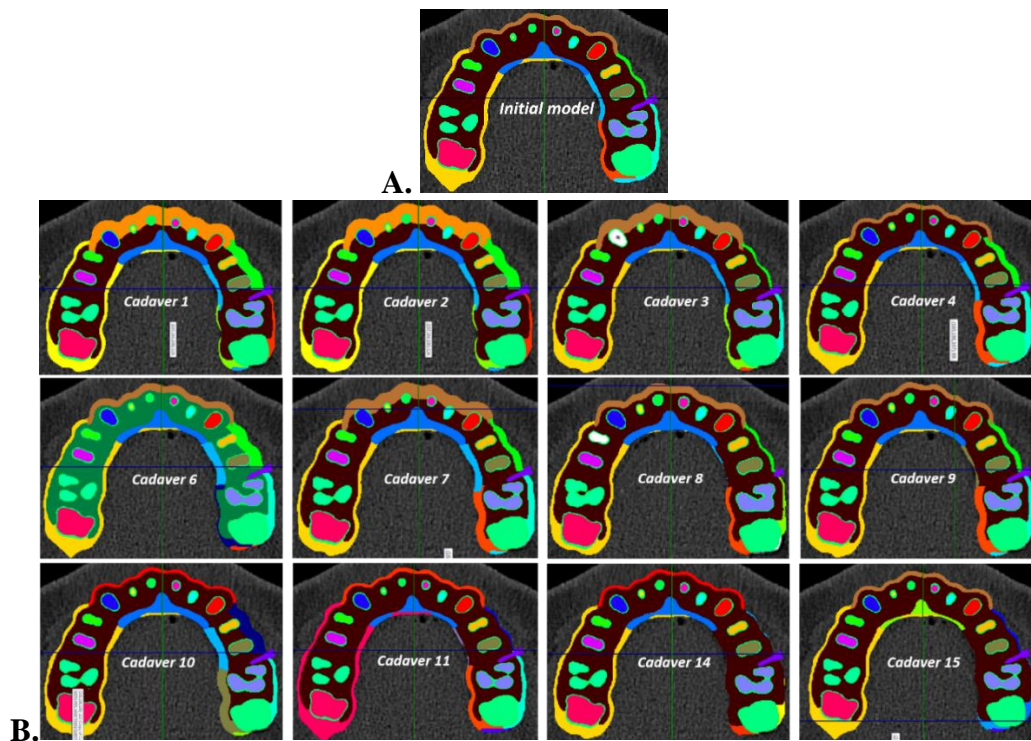
Fig.2.17 A.TAD level axial cut of the original template model; **B.** Similar cuts individualized models corresponding to 12 cadavers with modified cortical bone thickness.

2.2.2. Finite Element Analysis (FEA)

2.2.2.1. Mesh size

FEA offers estimated outcomes since theoretical representation is usually complex. The number of elements in a meshed model, dictates the accuracy and precision of the estimation, with one drawback of increase in time during the simulation if the number of elements is greater than necessary. Though, the number of elements does not always relate to the accuracy of the solution. For this reason, a convergence study was previously done in the research by Ammoury et. al (2017) to determine the least number of elements that provide the most precise solution by running a convergence testing by varying the mesh size in ScanIP™ 7.0 before exporting the FE models. Accordingly, 10 identical FE models differing only in mesh coarseness (19, 25, 28, 31, 34, 36, 40, 43, 47 and 50), with tetrahedral element sizes ranging from 0.2 to 1.3 mm, were exported in "inp." format. And ran in Abaqus, with the same settings applied for the loading. Results were compared using a color-coded map of displacement to determine the location of the maximum displacement. Afterward, the maximum nodal displacement at the crown of the right second molar was recorded and later plotted against the mesh size. In the results, no significant variations existed between the different meshes. This result indicated that similar accuracy outcomes could be obtained in the models with element sizes of 0.2 to 1.3 mm (Fig.2.24 and Fig.2.25). Thus, the chosen mesh size was of 0.604 mm (corresponding to coarseness level 36), avoiding large size models that would increase the simulation time, without compromising on the precision of the results (Ammoury et al., 2017).
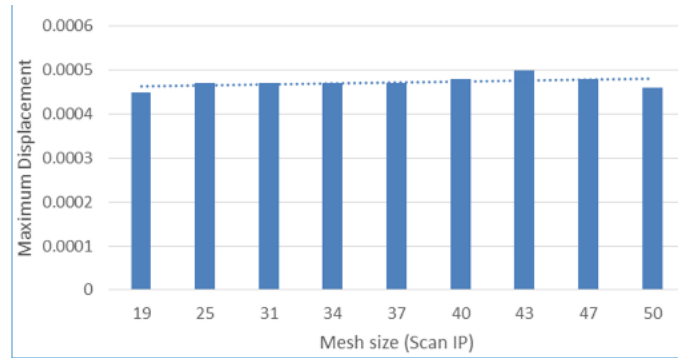
Fig.2.18. Scatter plot showing the results of the convergence testing (total displacements at the second molar assessed in 9 models with various mesh coarseness size).

After defining contact pairs between the connected parts of the models in the configuration settings menu, 13 models (one template model on which stiffness was varied and twelve models with thickness variation) were exported from ScanIP as inp. file format. The master model comprised a total of 170798 nodes and 854698 linear tetrahedral elements (Fig 3.26). Fig.2.26:
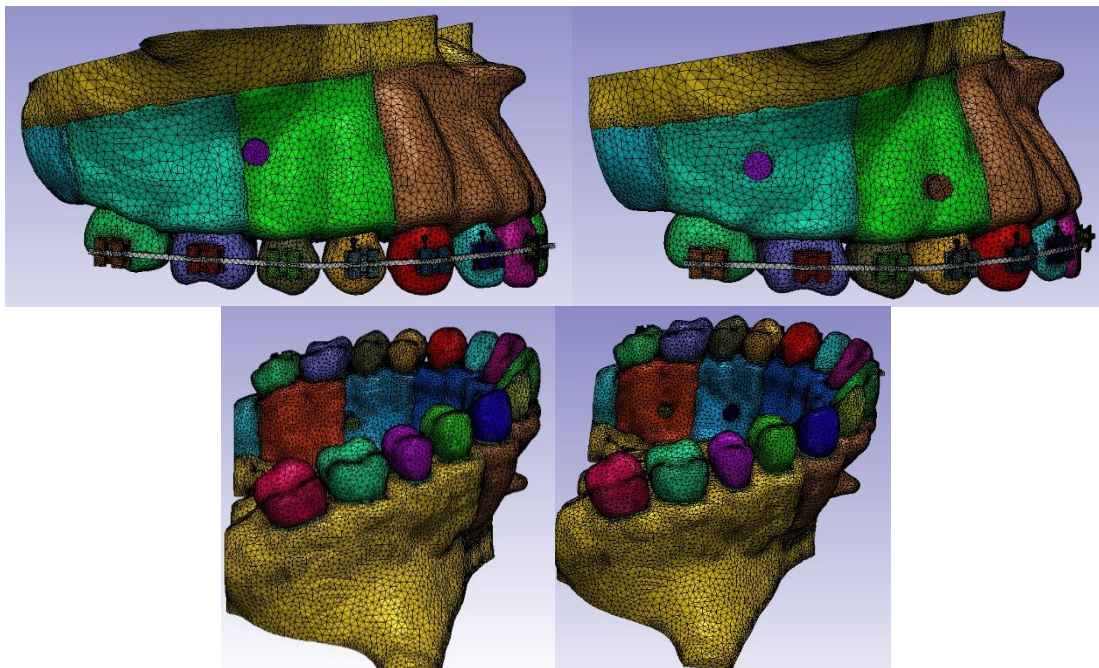
Fig.2.19. Meshed template models.

The initial parameters of tissue response set the accuracy of FEA results (Middletton et al. 1996). Consequently, Strait et al. (2005) recommended obtaining specific elastic properties data about the species and skeletal elements of the subjects to be analyzed. Presumptions on all those elements are made based on scientific computations commonly used in FEA applications in orthodontics. Material properties (Young's Modulus of Elasticity and Poisson's ratios) of trabecular bone, teeth, brackets, and miniscrew were defined from available data in the literature (Table 3.3). Except for the cortical bone, all materials used in this study were homogeneous, isotropic, and linearly elastic (Field et al., 2009; Lim et al., 2003; Tanne et al., 1987). The material property of the PDL was assigned based on the work of Kojima and Fukui (2012).

Table 2.3. Young Modulus and Poisson's ratio

	Young's modulus (MPa)	Poisson's ratio
Teeth	20 000	0.3
Periodontal ligament (PDL)	0.68	0.45
Trabecular bone	1500	0.33
Cortical bone	Variable	0.33
Brackets and Miniscrew	200 000	0.3
Field et al., 2009 ; Kojima et al., 2012; Lim et al., 2003; Tanne et al., 1987		

Cortical bone stiffness was modified according to Peterson et al. (2006) to replicate bone features that originated in real patients' cadavers. Individual material properties provided at the maxillary sites 1, 3, 4, 5, 6, 7 and 8 were incorporated into the template FE model. For stiffness variation, unlike other elements of the model, the cortical bone parts were assigned orthotropic material properties providing more detailed information about its behavior under different loads.

In material science and solid mechanics, material properties of an orthotropic material differ when measured from different directions.

Therefore, engineering constants (defined in section 2.1.2.) of Young's modulus of elasticity: E1, E2, E3, Shear Modulus of elasticity G12, G31, G32 and Poisson's ratio υ12, υ13, υ23 were all incorporated into each cortical bone part (Table 3.4).

Table 2.4. Orthotropic material properties at the site of "buccal cortical bone at incisors area (5)" in the 15 cadavers. **E1 - E2 - E3:** Components of normal stiffness; **v12- v13 - v32:** Poisson's ratio; **G12- G31 - G23:** Shear stiffness

	Site 5 (buccal incisors)								
	E1	**E2**	**E3**	**v12**	**v13**	**v32**	**G12**	**G31**	**G23**
Patient 1	17140	16918	21567	0.327	0.368	0.123	6603	6889	7175
Patient 2	6762	9888	12219	0.261	0.277	0.489	2879	2667	2455
Patient 3	11380	10731	16861	0.397	0.2	0.357	3990	5426	6862
Patient 4	8343	10246	14033	0.477	0.413	0.116	3229	3701	4173
Patient 6	10825	10006	13323	0.52	0.307	0.264	3453	4626	5799
Patient 7	17129	17209	21765	0.341	0.385	0.365	6411	6594	6777
Patient 9	9188	9143	11113	0.445	0.454	0.227	3198	3443	3688
Patient 10	8301	9263	12943	0.485	0.467	0.066	3098	3490	3882
Patient 11	8993	10380	16675	0.493	0.366	0.176	3292	4141	4990
Patient 14	7129	9636	10967	0.237	0.175	0.424	3114	3362	3610
Patient 15	8550	9582	10798	0.307	0.22	0.343	3395	3792	4189

Peterson et al. (2006) confirmed that the direction of maximum stiffness was parallel to the long axis of the three pillars of the maxilla and perpendicular to the fronto-maxillary suture, furthermore, they found that in the 15 maxillary cortical bone areas studied, 7 areas (4 of which included in our model) have a distinct vertical direction of maximum stiffness.

Orthotropic material properties were then assigned to each area assigned by defining each element stiffness in the 3 dimensions.

3: Parallel to the long axis of the three-pillars of the maxilla

2: Within the plane of the cortical plate

1: Through the thickness of the cortical plate

To rule out the effect of stiffness, the same isotropic material properties were assigned to all cortical bone parts when the thickness was varied.

<u>2.2.2.3. Interactions</u>

Insufficient literature is available in FEA research regarding the application of interactions between teeth contact to simulate clinical orthodontic tooth movement. To precisely represent the load's transmission through contact point surface, models were subjected to teeth separation on ScanIP (manually using the *unpaint tool*) by a distance equal to 0.2 to 0.4 mm (1 to 2 pixels).

In Abaqus, a separation from the teeth between the exported surfaces allowed for the definition of "surface to surface" interactions between the adjacent surfaces. Yet, it was necessary to apply adjustments to increase the sensibility of interactions to obtain load transmission through teeth as separate entities in Abaqus where the "surface to surface interaction" works only for surfaces in contact with each other. Therefore, we altered the tolerance of each surface to surface interaction to 0.4 to allow communication of nodes at a distance up to 0.4 mm (to account for the maximum distance separating the teeth which is equal to 0.3 mm) (Fig.2.29).
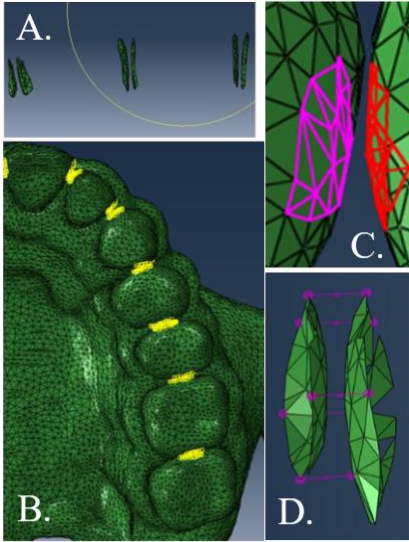
Fig.2.20. Surface to surface interactions (Master/slave): **A.** Individual surfaces as viewed in Abaqus; **B.** "Surface to surface" interactions (in yellow) defined between the adjacent surfaces. **C and D** Zoomed in a picture of the two interactions used.
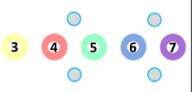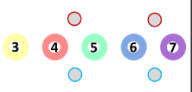
2.2.2.4. Loading set-ups

For simplification purposes, the archwire was created and full-size and passive, therefore duplicating the clinical intrusion prior to mechanics in intrusion. An optimal orthodontic force of 400 grams equivalent to 3.92 Newtons was applied, divided into 200 grams buccally and 200 grams palatally.

Load

Five prototype models representing five intrusion modalities were generated (Table 3.5)

Table 2.5. Summary of the intrusion modalities adopted.

Model	1	2	3	4	5
MIs	1B, 2 P	2 B, 2 P	2 B, 1 P	2 B, 2 P	2 B, 2 P
Buccal MIs position between	2nd PM and 1st M	- 2nd PM and 1st M - Ms	-PMs - Ms	-PMs - Ms	-PMs - Ms
Palatal MIs position between	-PMs - Ms	-PMs - Ms	2nd PM and 1st M	-PMs - Ms	-PMs - Ms
Force applied on	archwire	archwire	brackets	brackets	archwire

B: Buccal; **P:** Palatal; **Blue outlined circle:** MI with load applied on brackets; **Red outlined circle:** MI with load applied on archwire.

Intrusion modality 1 (Fig.2.21):

Three mini-implants were inserted in the interradicular bone at an angle of 30° (Deguchi et al., 2006) relative to the surface of the cortical bone with the neck/thread interface coincident with the external contour of the cortical bone. One MI placed buccally between the second premolar and the first molar, and two were located palatally, one between the molars and another one between premolars.

Buccal loading was applied in two directions from the interbracket archwire length between first and second premolars (100 grams) and between the second premolar and first molar (100 grams). On the palatal side, the load to the premolars was directed from the anterior MI and the load to the molars was shouldered by the posterior MI (50 grams/ tooth).

Fig.2.21. Clinical picture showing the first intrusion modality.

Intrusion modality 2 (Fig.2.22):

Four MIs were anchored: two buccal placed one between the molars and the second between the first molar and the second premolar; two palatal mini-implants, one between the molars and another one between the premolars. Buccal loading was directed from the interbracket span between the brackets (100 grams/ archwire span). On the palatal side, load to the premolars and molars was directed to the palatal MIs (50 grams/ tooth).

Fig.2.22. Clinical picture showing the second intrusion modality
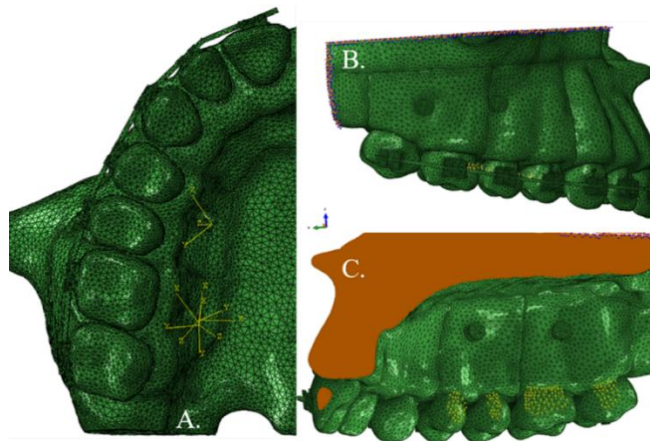
Fig.2.23. Datum axis system used to define the direct load direction **A.** Occlusal view of palatal datum axis. **B**. Sagittal view of buccal load **C.** palatal midsagittal cut displaying palatal load

Intrusion modality 3 (Fig.2.24):

Three mini-implants were used: two buccal placed one between the premolars one between the molars, and one palatal between the first molar and the second premolar. Buccal

loading was divided in four components and directed from the brackets of the premolars and the molars (50 grams/ tooth). On the palatal side, load to premolars and molars was directed to the palatal mini-implant (50 grams/ tooth).

Fig.2.24 Clinical picture showing the third intrusion modality.

Intrusion modality 4 (Fig.2.25):

Of four MIs used, two were buccal and two palatal placed in a parallel one between the premolars one between the molars. Buccal loading was identical to that in the second modality and palatal loading as in the first modality.

Fig.2.25. Clinical picture showing the fourth intrusion modality.
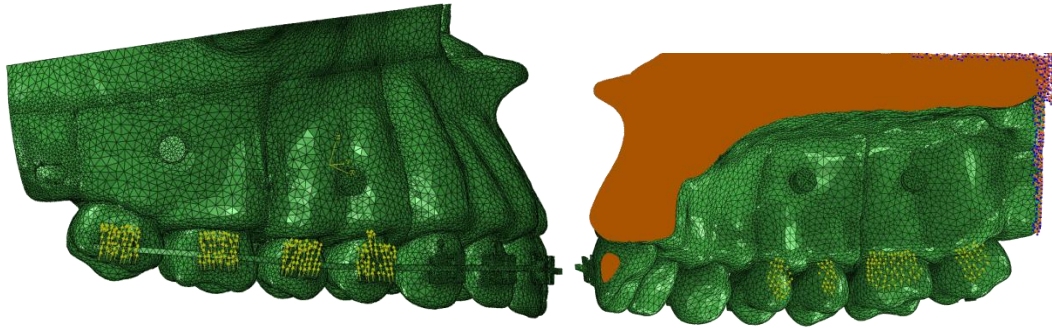
Fig.2.26. Load in fourth intrusion setup. (Buccally: 50 grams/ 1200 nodes/ bracket- Palatally: 50 grams/ 15 nodes/ palatal aspect, premolars directed to anterior mini-implant and molars directed to posterior mini-implant).

Intrusion modality 5 (Fig.2.27):

MIs placement was the same as in modality 5. Division of load was similar to the third modality. The difference was in the buccal force application on the archwire; 50 grams applied from the wire to the anterior mini-implant section between:

1- the canine and the first premolar

2- the first premolar and the second premolar

50 grams applied from the wire to the posterior mini-implant section between:

3- the second premolar and the first molar

4- the first molar and the second molar

Fig.2.27. Clinical picture showing the fifth intrusion modality.

56
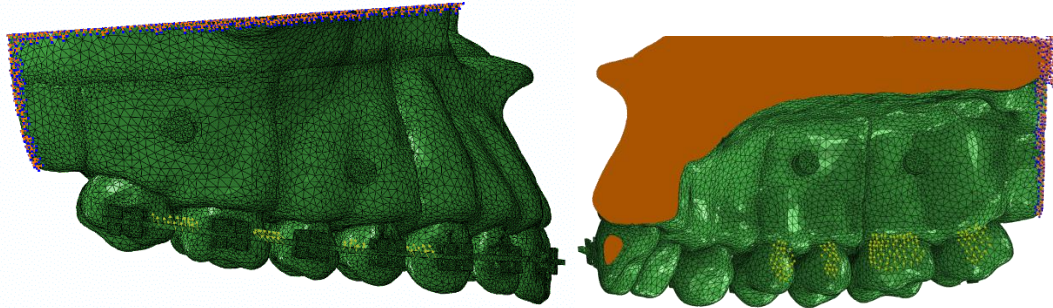
Fig.2.28. Load in fifth intrusion setup.

Force application on the archwire

In Abaqus, a condensed mechanical force was created on the wire nodes set, distributed around 15 nodes at every inter-bracket span, and nodes sets each composed of around 15 nodes at every palatal aspect of the premolars and molars subjected to the intrusive load. The applied force (100 grams =3.92 Newton) was divided equally on all the nodes of the set (Buccally: 100 grams/ 15 nodes/ Archwire span- Palatally: 50 grams/ 15 nodes/ palatal aspect).

Force application on the brackets

A condensed mechanical force was created on brackets' nodes set, composed of around 1200 nodes each, and placed at the center of the crowns, and palatally the same distribution described previously was employed. The applied force (100 grams =3.92 Newton) was divided equally on all the nodes of the set (Buccally: 50 grams/ 1200 nodes/ bracket- Palatally: 50 grams/ 15 nodes/ palatal aspect).

A.   **B.**
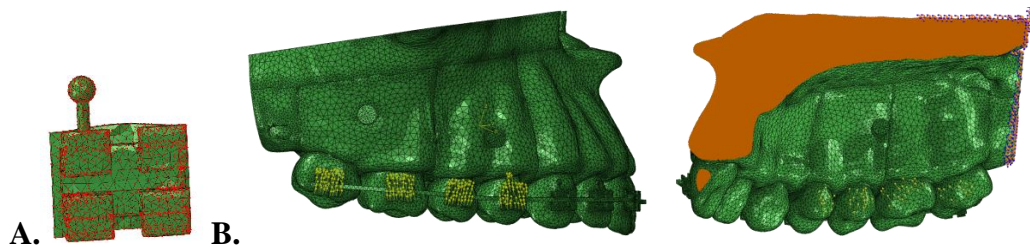
Fig.2.29. A. Nodal set on the canine's bracket **B.** Load in third intrusion setup.

A datum axis system was constructed using 3 points: the origin of the axis system located at the center of the miniscrew head; a second point located at the center of the bracket helped define the X-axis; and a third point was placed perpendicular to the X-axis. The direction of the direct loading force followed the X-axis with no components in the Y and Z axes (Fig.2.30).
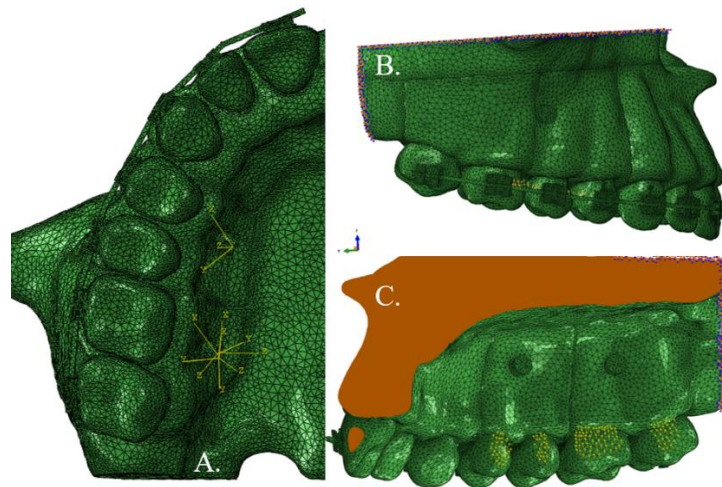
Fig.2.30. Datum axis system used to define the direct load direction **A.** Occlusal view of palatal datum axis. **B**. Sagittal view of buccal load **C.** palatal midsagittal cut displaying palatal load

2.2.2.5. Data collection and export

Boundary conditions

a- Because the upper and posterior parts of the maxillary bone are fused to the cranial base bones (frontal, ethmoid, sphenoid, malar and nasal bones) and therefore are wedged in all directions,

b- FEA studies accounted for a small part of the maxillary surrounding area studied.

Boundary conditions were applied to help completely immobilize the upper and posterior regions of the maxilla (Figs. 3.31).
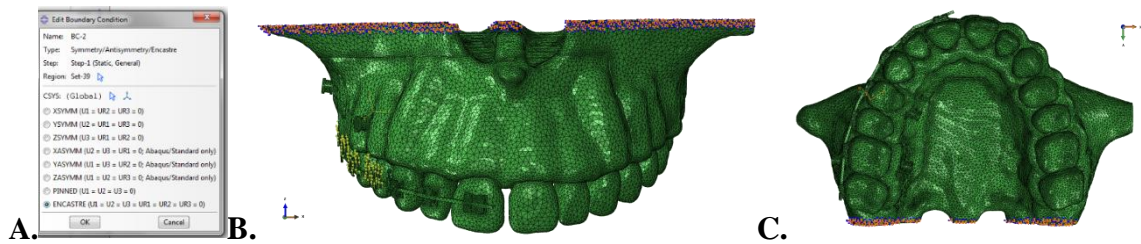
Fig.2.31. A. Boundary condition (BC) applied to superior and posterior part of the maxilla (Encastre) **B.** Superior BC **C.** Posterior BC

Sets

Findings in FEA are interpreted by methods of color mapped representations and arrows, but numerical data is necessary to perform statistical analysis including individual variations. It is possible to collect numerical data on stress, strain, displacement and other variables at every node and element.

For stress data collection, a set that contains randomly chosen elements evenly scattered along every surface of the periodontal ligament in every tooth was created on every aspect (mesial, distal, buccal and, palatal) of the canine, first and second premolars, and, first and second molars) of each tooth:. A total of 20 sets for every model, each containing between 100 to 350 elements (depending on area size and excluding the transition line between the surfaces) was created to obtain numerical data for stress. Furthermore, to collect initial displacement data, additional nodal sets of around 15 to 25 nodes were created at every tooth at the level of cusp tips and the apical regions (total of 5 sets in every model) (Fig.2.32-33).
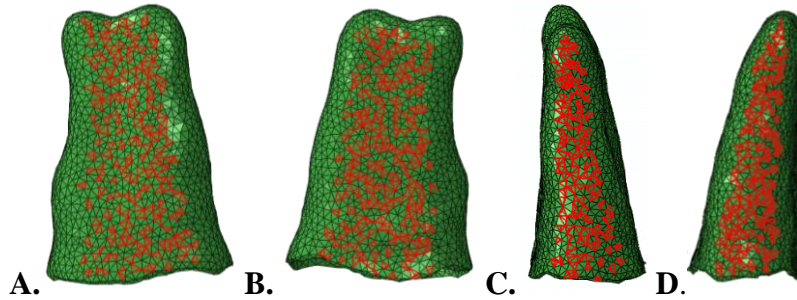
Fig.2.32 Selection of element sets (stress) on the second premolar: **A.** Distal; **B.** Mesial **C.** Palatal; **D.** Buccal.
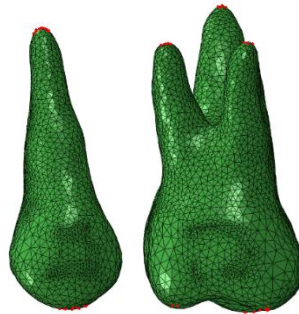
Fig.2.33 Selection of node sets (stress) on the second premolar and first molar

After running the finite element analysis, the stress and displacement results were exported as DAT. files into excel where the averages were calculated. Subsequently, the averages were displayed in final datasheets.

Five datasheets corresponding to the 10 parts of the study were obtained:

- Part 1: Stiffness variation applied to first intrusion modality

- Part 2: Stiffness variation applied to second intrusion modality

- Part 3: Stiffness variation applied to third intrusion modality

- Part 4: Stiffness variation applied to fourth intrusion modality

- Part 5: Stiffness variation applied to fifth intrusion modality

- Part 6: Thickness variation applied to first intrusion modality

- Part 7: Thickness variation applied to second intrusion modality

- Part 8: Thickness variation applied to third intrusion modality

- Part 9: Thickness variation applied to fourth intrusion modality

- Part 10: Thickness variation applied to fifth intrusion modality

Stress and displacement data were repeated for the first two cadavers to evaluate intra-examiner reliability.

2.2.3. Statistical analysis

Descriptive statistics were generated for the stress in the subsamples of stiffness and thickness variations and tooth displacement in the five treatment modalities. Mean and standard deviations for each tooth (canine [3]), first and second premolars [4 and 5] and first and second molars [6 and 7]) at each surface (buccal, mesial, distal, and palatal) were reported. The Shapiro-Wilk normality test was employed to assess the normality of distribution of the outcome variables.

The stress resulting from the stiffness and thickness variations, and the amount of tooth displacement were compared between the 5 teeth at each surface within each treatment modality using the one-way analysis of variance (ANOVA), followed by Bonferroni post-hoc analyses for multiple comparisons. Homogeneity of variances was tested for each set of comparisons, and when violated, Welch's robust ANOVA and Games-Howell post hoc tests were reported instead. When the data were not normally distributed, the Kruskal-Wallis one-way analysis of variance followed by pairwise comparison (for non-parametric data) was used.

For comparisons of stress and tooth displacement between modalities, the repeated measures ANOVA was utilized followed by pairwise comparison. The Pearson product-moment correlation coefficient (and its equivalent non-parametric Spearman correlation coefficient) was

performed to test correlations between the stress amounts at the mesial, distal, palatal, and buccal surfaces of the periodontal ligament of each tooth and:

- Stiffness and thickness (S1, S2, S3) of the corresponding palatal and buccal cortical bone areas.

- Tooth displacement (in terms of intrusion (Axis 3) and secondary effects (Axis 1+2)) for each tooth.   All statistical analyses were performed using SPSS and the level of significance was set at P≤0.05.

CHAPTER 3

RESULTS

The intraclass correlation coefficient of stress and displacement data for repeated measurements were greater than 0.9.

3.1. Stiffness Variation / Stress comparison among the teeth and modalities

3.1.1. Part 1: Stiffness variation / Intrusion modality 1

The Levene's test results were only statistically significant for the stress amounts at the buccal surface, and non-significant for the stresses at the mesial, distal, and palatal surfaces (Table 3.1). Therefore, the Welch ANOVA and Games-Howell tests were used for the buccal surface and the ANOVA and the Bonferroni tests were used for the other surfaces.

The highest stresses was registered on the second premolar specifically on its buccal aspect, and progressively decreasing on the first premolar (4) then the first molar (6) with both teeth at the extremities having lower stress values: the canine (3) and second molar (7). All the stresses were statistically significantly different between the teeth. No statistical difference was observed between the distal and the palatal aspects of the premolars. (Table 3.2, Table 3.3; Fig 3.1).

Table 3.1: Descriptive statistics for the stress generated on the 4 surfaces of the buccal teeth (Stiffness variation/1st modality)

Statistics	Buccal		Distal		Mesial		Palatal		Total
	Mean	SD	Mean	SD	Mean	SD	Mean	SD	
Canine (3)	1.033	2.4E-05	1.070	2.3E-05	1.035	2.2E-05	1.000	1.9E-05	4.138
First premolar (4)	1.360	4.4E-05	1.381	3.7E-05	1.393	2.9E-05	1.410	2.5E-05	5.544
Second premolar (5)	1.666	6.9E-05	1.379	4.3E-05	1.516	4.3E-05	1.437	3.2E-05	5.997
First molar (6)	1.292	3.0E-04	0.880	3.5E-05	1.459	3.3E-05	1.260	2.0E-05	4.891
Second molar (7)	0.438	6.5E-05	0.324	3.1E-05	0.455	3.3E-05	0.403	3.1E-05	1.619

Stresses in kPa; **SD**: Standard deviation

Table 3.2: ANOVA: Comparison of stress among the 5 teeth at each surface (Stiffness/1ˢᵗ modality)

	3	4	5	6	7	p-value
Buccal †	1.033	1.360	1.666	1.292	0.438	**0.000***
Distal	1.070	1.381	1.379	0.880	0.324	**0.000***
Mesial	1.035	1.393	1.516	1.459	0.455	**0.000***
Palatal	1.000	1.410	1.437	1.260	0.403	**0.000***

†Welch's ANOVA *p* values reported because
assumption of homogeneity of variances was violated; *Significant at *p* <0.05

Table 3.3: Pairwise comparisons for stress between the teeth at each surface (Post-Hoc tests: Bonferroni)

	3-4	3-5	3-6	3-7	4-5	4-6	4-7	5-6	5-7	6-7
Buccal†	0.000*	0.000*	0.094	0.000*	0.000*	0.941	0.000*	0.013*	0.000*	0.000*
Distal	0.000*	0.000*	0.000*	0.000*	1.000	0.000*	0.000*	0.000*	0.000*	0.000*
Mesial	0.000*	0.000*	0.000*	0.000*	0.000*	0.000*	0.000*	0.002*	0.000*	0.000*
Palatal	0.000*	0.000*	0.000*	0.000*	0.212	0.000*	0.000*	0.000*	0.000*	0.000*

†Games-Howell post hoc p values reported when the assumption of homogeneity of variance violated.
*Significant at p <0.05
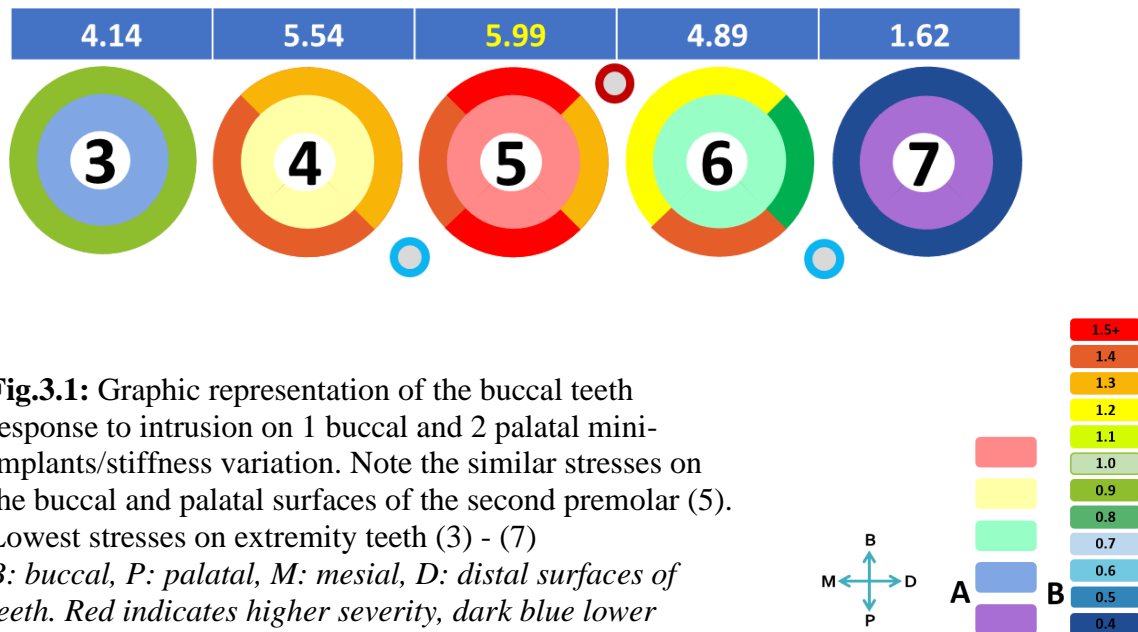
Fig.3.1: Graphic representation of the buccal teeth response to intrusion on 1 buccal and 2 palatal mini-implants/stiffness variation. Note the similar stresses on the buccal and palatal surfaces of the second premolar (5). Lowest stresses on extremity teeth (3) - (7)
B: buccal, P: palatal, M: mesial, D: distal surfaces of teeth. Red indicates higher severity, dark blue lower severity as per used FEA scale.

3.1.2. Part 2: Stiffness variation / Intrusion modality 2

As in modality 1, results revealed statistical significance for the stress amounts at the buccal surface, and non-significant for the stresses at the mesial, distal, and palatal surfaces, (Table 3.4). Accordingly, the Welch ANOVA and Games-Howell tests were used for the buccal surface and the ANOVA and Bonferroni tests were applied for the rest of the surfaces.

The highest stress was recorded on the second premolar (4.529 kPa) and the first premolar (4.330 kPa), stresses posteriorly (6-7) are higher than in modality 1 (Fig 4.2). All stresses were statistically significant between teeth for every surface. Comparing between teeth revealed no statistical significance between the extremity teeth (1-7), between the premolars (4-5) except for their buccal aspect, and between the second premolar and the first molar (5-6) (Table 3.5, Table 3.6).

Table 3.4: Descriptive statistics for the stress generated on the 4 surfaces of the buccal teeth (Stiffness variation/2nd modality)

Statistics	Buccal		Distal		Mesial		Palatal		Total
	Mean	**SD**	**Mean**	**SD**	**Mean**	**SD**	**Mean**	**SD**	
3	0.730	2.7E-05	0.797	3.6E-05	0.765	3.4E-05	0.832	2.6E-05	3.124
4	0.929	5.1E-05	1.076	6.1E-05	1.101	4.3E-05	1.224	5.3E-05	4.330
5	1.118	6.7E-05	1.098	9.6E-05	1.146	6.1E-05	1.166	7.4E-05	4.529
6	1.064	1.0E-04	0.814	6.9E-05	1.098	2.1E-04	0.965	2.6E-04	3.941
7	0.719	1.7E-04	0.471	6.7E-05	0.489	6.2E-05	0.426	3.5E-05	2.105

Stresses in kPa; **SD**: Standard deviation

Table 3.5: ANOVA: Comparison of stress among the 5 teeth at each surface (Stiffness/2nd modality)

	3	**4**	**5**	**6**	**7**	**p-value**
Buccal †	0.730	0.929	1.118	1.064	0.719	**0.000***
Distal	0.797	1.076	1.098	0.814	0.471	**0.000***
Mesial	0.765	1.101	1.146	1.098	0.489	**0.000***
Palatal	0.832	1.224	1.166	0.965	0.426	**0.000***

†Welch's ANOVA p values reported because assumption of homogeneity of variances was violated; *Significant at $p < 0.05$

Table 3.6: Pairwise comparisons for stress between the teeth at each surface (Post-Hoc tests: Bonferroni)

	3-4	3-5	3-6	3-7	4-5	4-6	4-7	5-6	5-7	6-7
Buccal†	0.000*	0.000*	0.000*	0.999	0.000*	0.009*	0.014*	0.577	0.000*	0.000*
Distal	0.010*	0.004*	1.000	0.254	1.000	0.034*	0.000*	0.016*	0.000*	0.095
Mesial	0.332	0.010*	0.022*	0.570	1.000	1.000	0.001*	1.000	0.000*	0.000*
Palatal	0.000*	0.020*	1.000	0.724	1.000	0.015*	0.000*	0.431	0.000*	0.042*

†Games-Howell post hoc p values reported when the assumption of homogeneity of variance violated.
*Significant at p <0.05

Fig.3.2: Graphic representation of the buccal teeth response to intrusion on 2 buccal (posterior) and 2 palatal mini-implants/stiffness variation. Note the similar stresses on the buccal, mesial and distal surfaces of the second premolar (5). Lowest stresses on extremity teeth (3) - (7)
B: buccal, P: palatal, M: mesial, D: distal surfaces of teeth. Red indicates higher severity, dark blue lower severity as per used FEA scale.
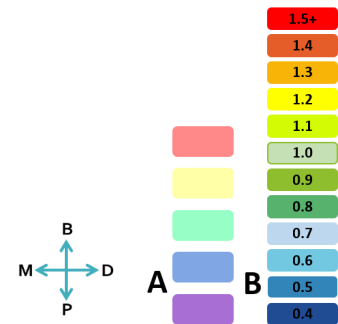
3.1.3. Part 3: Stiffness variation /Intrusion modality 3

The stress amounts were only statistically significant at the palatal surface, and non-significant for the stresses at the mesial, distal, and buccal surfaces (Levene's test) (Table 3.4). The Welch ANOVA and Games-Howell tests were thus applied for the palatal surface and the ANOVA and Bonferroni tests for the mesial, distal, and buccal surfaces.

The first premolar sustained the highest stress specifically its buccal aspect with stress concentrated more anterior (relatively lower values when compared to previous modalities). All stresses were statistically different when comparing each tooth among them.

Pairwise comparison revealed no statistical difference between the first and the second premolars. (Table 3.7, Table 3.8; Fig.3.4).

Table 3.7: Descriptive statistics for the stress generated on the 4 surfaces of the buccal teeth (Stiffness variation/3rd modality)

Statistics	Buccal		Distal		Mesial		Palatal		Total
	Mean	**SD**	**Mean**	**SD**	**Mean**	**SD**	**Mean**	**SD**	
3	0.927	3.5E-05	0.922	3.5E-05	0.854	3.7E-05	0.821	3.8E-05	3.524
4	1.122	4.4E-05	0.994	4.4E-05	1.039	4.5E-05	1.011	2.1E-05	4.167
5	1.154	5.1E-05	0.968	4.3E-05	1.063	5.3E-05	0.972	5.0E-05	4.157
6	0.911	6.7E-05	0.684	3.7E-05	1.018	4.2E-04	0.845	3.6E-04	3.458
7	0.587	5.7E-05	0.570	6.0E-05	0.591	3.8E-05	0.577	4.7E-05	2.325

Stresses in kPa; **SD**: Standard deviation

Table 3.8: ANOVA: Comparison of stress among the 5 teeth at each surface (Stiffness/3rd modality)

	3	4	5	6	7	**p-value**
Buccal	0.927	1.122	1.154	0.911	0.587	**0.000***
Distal	0.922	0.994	0.968	0.684	0.570	**0.000***
Mesial	0.854	1.039	1.063	1.018	0.591	**0.000***
Palatal†	0.821	1.011	0.972	0.845	0.577	**0.000***

†*Results obtained with Welch ANOVA* values reported because assumption of homogeneity of variances was violated; *Significant at $p < 0.05$
3: canine; 4, 5: first, second premolars; 6, 7: first, second molars.

Table 3.9: Pairwise comparisons for stress between the teeth at each surface (Post-Hoc tests: Bonferroni)

	3-4	3-5	3-6	3-7	4-5	4-6	4-7	5-6	5-7	6-7
Buccal	0.000*	0.000*	1.000	0.000*	1.000	0.000*	0.000*	0.000*	0.000*	0.000*
Distal	0.004*	0.196	0.000*	0.000*	1.000	0.000*	0.000*	0.000*	0.000*	0.000*
Mesial	0.000*	0.000*	0.000*	0.000*	1.000	1.000	0.000*	0.175	0.000*	0.000*
Palatal†	0.073	0.000*	0.553	0.000*	0.97	0.133	0.000*	0.000*	0.000*	0.000*

†Games-Howell post hoc p values reported when assumption of homogeneity of variance violated.
*Significant at p <0.05.
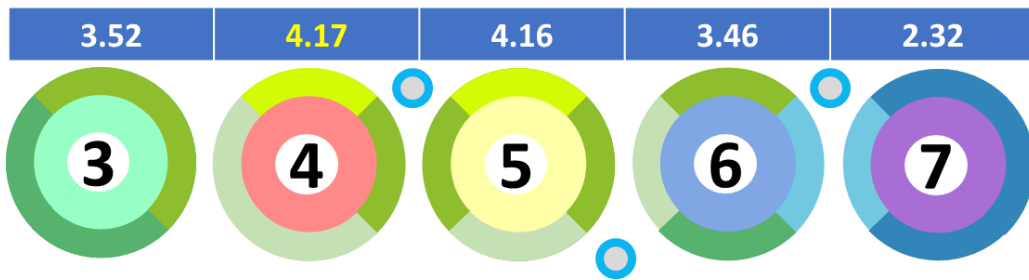
Fig.3.3: Graphic representation of the buccal teeth response to intrusion on 2 buccal and 1 palatal mini-implants/stiffness variation. Note the similar stresses on the first (4) and the second premolar (5). Lowest stresses on extremity teeth (3) - (7)
B: buccal, P: palatal, M: mesial, D: distal surfaces of teeth. Red indicates higher severity, dark blue lower severity as per used FEA scale.
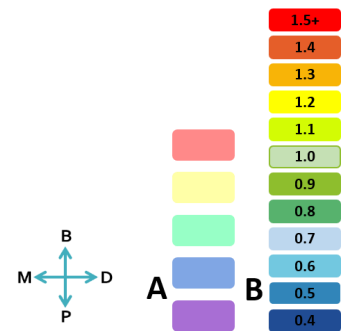
3.1.4. Part 4: Stiffness variation / Intrusion modality 4

In the stiffness variation applied to the fourth and fifth intrusion modalities, the data were not normally distributed, therefore the equivalent of ANOVA for non-parametric data was used (Kruskal-Wallis).

All stresses were statistically significantly different when comparing each tooth to its adjacent, decreasing in magnitude from the first premolar (4) to the second molar (7). Stress was concentrated more anteriorly. (Table 3.11, Table 3.2; Fig.3.4).

Table 3.10: Descriptive statistics for the stress generated on the 4 surfaces of the buccal teeth (Stiffness variation/4th modality)

Statistics	Buccal		Distal		Mesial		Palatal		total
	Mean	SD	Mean	SD	Mean	SD	Mean	SD	
Canine (3)	0.957	1.9E-05	1.037	1.7E-05	1.162	1.9E-05	1.258	1.7E-05	4.414
First premolar (4)	0.942	2.2E-05	1.039	2.0E-05	1.237	2.1E-05	1.405	2.2E-05	4.622
Second premolar (5)	0.801	2.3E-05	0.930	1.8E-05	1.077	2.1E-05	1.314	2.6E-05	4.122
First molar (6)	0.425	2.2E-05	0.665	2.1E-05	0.920	1.9E-05	1.149	3.0E-05	3.158
Second molar (7)	0.422	2.9E-05	0.452	3.8E-05	0.536	3.6E-05	0.599	5.8E-05	2.009

Stresses in kPa; **SD**: Standard deviation

68

Table 3.11: ANOVA: Comparison of stress among the 5 teeth at each surface (Stiffness/4th modality)

	3	4	5	6	7	p-value
Buccal	0.957	0.942	0.801	0.425	0.422	**0.000***
Distal	1.037	1.039	0.930	0.665	0.452	**0.000***
Mesial	1.162	1.237	1.077	0.920	0.536	**0.000***
Palatal	1.258	1.405	1.314	1.149	0.599	**0.000***

Kruskal-Wallis one-way analysis of variance for non-parametric data.
*Significant at $p < 0.05$

Table 3.12: Pairwise comparisons for stress between the teeth at each surface. (Post-Hoc tests: Bonferroni)

	3-4	3-5	3-6	3-7	4-5	4-6	4-7	5-6	5-7	6-7
Buccal	1.000	**0.040***	**0.000***	**0.000***	0.504	**0.000***	**0.000***	0.160	0.154	1.000
Distal	1.000	0.178	**0.001***	**0.000***	0.138	**0.000***	**0.000***	1.000	**0.013***	1.000
Mesial	1.000	1.000	**0.013***	**0.000***	**0.013***	**0.000***	**0.000***	1.000	**0.012***	1.000
Palatal	**0.015***	1.000	0.989	**0.011***	0.989	**0.000***	**0.000***	**0.015***	**0.000***	1.000

*Significant at p <0.05.
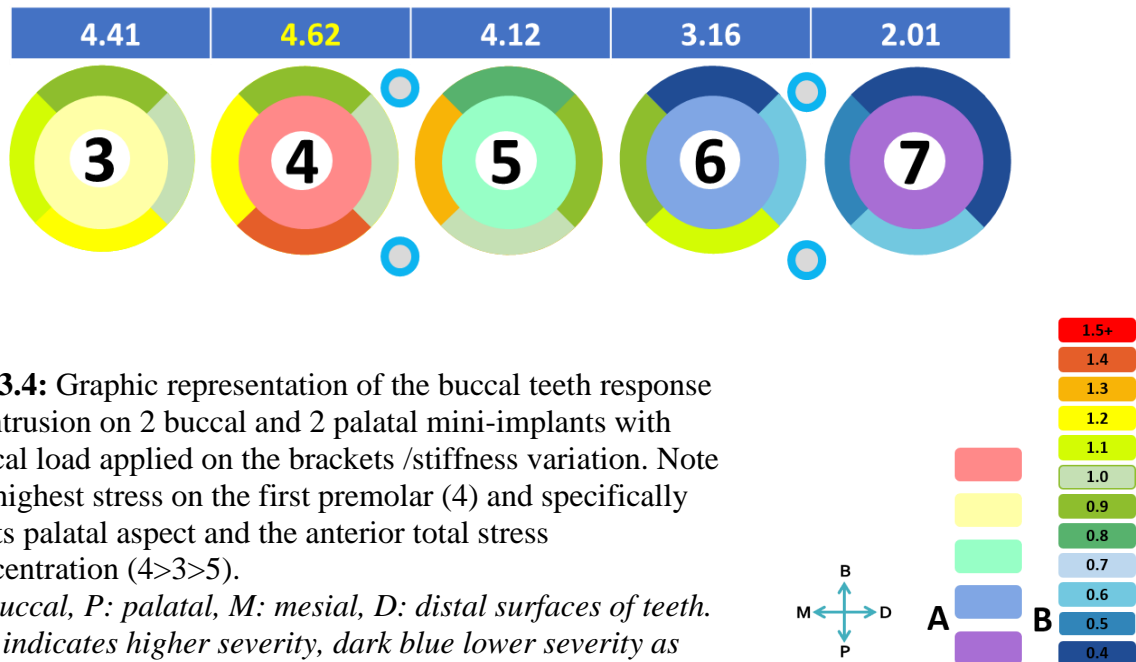
Fig.3.4: Graphic representation of the buccal teeth response to intrusion on 2 buccal and 2 palatal mini-implants with buccal load applied on the brackets /stiffness variation. Note the highest stress on the first premolar (4) and specifically on its palatal aspect and the anterior total stress concentration (4>3>5).
B: buccal, P: palatal, M: mesial, D: distal surfaces of teeth. Red indicates higher severity, dark blue lower severity as per used FEA scale.

3.1.5. Part 5: Stiffness variation / Intrusion modality 5

All stresses were statistically significantly different when comparing between teeth surfaces. The fashion of stress distribution was similar to that of the fourth modality but with higher values. Statistical significant difference was registered between the extremity teeth (3-7) between the first premolar and both first and second molars (4-5/4-7) and between the second premolar and the second molar (5-7) (Table 3.14, Table 3.15; Fig.3.5).

Table 3.13: Descriptive statistics for the stress generated on the 4 surfaces of the buccal teeth (Stiffness variation/ 5th modality)

Statistics	Buccal		Distal		Mesial		Palatal		total
	Mean	SD	Mean	SD	Mean	SD	Mean	SD	
Canine (3)	1.612	3.1E-05	1.469	2.6E-05	1.478	2.7E-05	1.298	2.2E-05	5.856
First premolar (4)	1.718	4.3E-05	1.468	3.3E-05	1.616	3.3E-05	1.461	6.1E-05	6.264
Second premolar (5)	1.519	5.4E-05	1.214	3.4E-05	1.456	3.9E-05	1.366	3.4E-05	5.556
First molar (6)	1.020	6.2E-05	0.750	2.4E-05	1.285	4.0E-05	1.054	2.7E-05	4.108
Second molar (7)	0.445	4.1E-05	0.421	3.7E-05	0.570	3.1E-05	0.635	6.2E-05	2.070

Stresses in kPa; **SD**: Standard deviation

Table 3.14: Comparison of stress among the 5 teeth at each surface (Stiffness/5th modality)

	3	4	5	6	7	p-value
Buccal	1.612	1.718	1.519	1.020	0.445	**0.000***
Distal	1.469	1.468	1.214	0.750	0.421	**0.000***
Mesial	1.478	1.616	1.456	1.285	0.570	**0.000***
Palatal	1.298	1.461	1.366	1.054	0.635	**0.000***

Kruskal-Wallis one-way analysis of variance for non-parametric data.
*Significant at $p < 0.05$

Table 3.15: Pairwise comparisons for stress between the teeth at each surface (Post-Hoc tests: Bonferroni)

	3-4	3-5	3-6	3-7	4-5	4-6	4-7	5-6	5-7	6-7
Buccal	0.962	1.000	**0.018***	**0.000***	**0.023***	**0.000***	**0.000***	0.813	**0.008***	1.000
Distal	1.000	0.138	**0.000***	**0.000***	0.178	**0.001***	**0.000***	1.000	**0.013***	1.000
Mesial	0.474	1.000	**0.044***	**0.000***	**0.044***	**0.000***	**0.000***	0.474	**0.003***	1.000
Palatal	0.042	1.000	0.824	**0.008***	1.000	**0.000***	**0.000***	**0.009***	**0.000***	1.000

*Significant at p <0.05

| 5.86 | 6.26 | 5.56 | 4.11 | 2.07 |

Fig.3.5: Graphic representation of the buccal teeth response to intrusion on 2 buccal and 2 palatal mini-implants with buccal load applied on the archwire /stiffness variation. Note the highest stress on buccal aspects of the most anterior teeth (4>3>5).
B: buccal, P: palatal, M: mesial, D: distal surfaces of teeth.
Red indicates higher severity, dark blue lower severity as per used FEA scale.

3.1.6. Comparison between the five modalities of intrusion/ Stiffness variation

The results showed statistically significant differences (P<0.05) for all modalities on all the teeth (Table 3.16).

Comparison of outcomes are presented considering the similarities and differences in modality through the following scheme:

1	1 / 2 / 5	force applied to the wire
2	3 / 4	force is exerted on the brackets
3	4 / 5	4- force on brackets; 5- force on archwire

- M 1 and 2 are comparable in terms of Von mises stresses on the second premolars (anterior pull on MI) and first molar (despite the additional force on the second MI).

- Between M1 and M5, almost all stresses are statistically different (except for surfaces on the second PREMOLAR and first M) even though the position of the MIs differs between these 2 modalities *suggesting that the amount of force dictated the resultant Von Mises Stress.*

- M2-M5: NS difference on molars since the posterior pull in both is evenly distributed

- M3-M4: the only difference was the number in palatal MIs, (NS difference posteriorly): *one hypothesis is that the number of palatal MIs does not influence the amount of stresses on the posterior section.*

- M4-M5: NS on the second molar only, *application of force whether on wire or brackets affects the stresses on teeth.*

Table 3.16: Repeated measures ANOVA for comparison of stress among different modalities/ Stiffness Variation

Tooth		M1		M2		M3		M4		M5		p-value
		Mean	SD	Mean	SD	Mean	SD	Mean	SD	Mean	SD	
Canine	B3	1.033	2.45E-05	0.730	2.69E-05	0.927	3.50E-05	0.957	1.91E-05	1.612	3.09E-05	**0.000***
	D3	1.070	2.34E-05	0.797	3.57E-05	0.922	3.51E-05	1.037	1.74E-05	1.469	2.64E-05	**0.000***
	M3	1.035	2.24E-05	0.765	3.42E-05	0.854	3.71E-05	1.162	1.91E-05	1.478	2.65E-05	**0.000***
	P3	1.000	1.91E-05	0.832	2.59E-05	0.821	3.77E-05	1.258	1.70E-05	1.298	2.23E-05	**0.000***
1st premolar	B4	1.360	4.43E-05	0.929	5.12E-05	1.122	4.35E-05	0.942	2.22E-05	1.718	4.29E-05	**0.000***
	D4	1.381	3.73E-05	1.076	6.09E-05	0.994	4.36E-05	1.039	2.00E-05	1.468	3.32E-05	**0.000***
	M4	1.393	2.86E-05	1.101	4.32E-05	1.039	4.53E-05	1.237	2.09E-05	1.616	3.34E-05	**0.000***
	P4	1.410	2.54E-05	1.224	5.32E-05	1.011	2.06E-04	1.405	2.16E-05	1.461	6.15E-05	**0.000***
2nd premolar	B5	1.666	6.90E-05	1.118	6.66E-05	1.154	5.14E-05	0.801	2.33E-05	1.519	5.41E-05	**0.000***
	D5	1.379	4.31E-05	1.098	9.60E-05	0.968	4.30E-05	0.930	1.82E-05	1.214	3.44E-05	**0.000***
	M5	1.516	4.31E-05	1.146	6.08E-05	1.063	5.34E-05	1.077	2.09E-05	1.456	3.92E-05	**0.000***
	P5	1.437	3.23E-05	1.166	7.37E-05	0.972	4.97E-05	1.314	2.61E-05	1.366	3.43E-05	**0.000***
1st molar	B6	1.292	2.98E-04	1.064	1.00E-04	0.911	6.66E-05	0.425	2.15E-05	1.020	6.23E-05	**0.000***
	D6	0.880	3.47E-05	0.814	6.95E-05	0.684	3.69E-05	0.665	2.08E-05	0.750	2.42E-05	**0.000***
	M6	1.459	3.28E-05	1.098	2.08E-04	1.018	4.21E-05	0.920	1.94E-05	1.285	3.97E-05	**0.000***
	P6	1.260	2.03E-05	0.965	2.64E-04	0.845	3.60E-05	1.149	3.03E-05	1.054	2.71E-05	**0.001***
2nd molar	B7	0.438	6.55E-05	0.719	1.68E-04	0.587	5.74E-05	0.422	2.90E-05	0.445	4.05E-05	**0.000***
	D7	0.324	3.13E-05	0.471	6.70E-05	0.570	6.00E-05	0.452	3.85E-05	0.421	3.74E-05	**0.000***
	M7	0.455	3.25E-05	0.489	6.21E-05	0.591	3.85E-05	0.536	3.61E-05	0.570	3.11E-05	**0.000***
	P7	0.403	3.15E-05	0.426	3.53E-05	0.577	4.70E-05	0.599	5.77E-05	0.635	6.15E-05	**0.000***

B: Buccal, D: Distal, M: Mesial, P: Palatal.

Table 3.17: Pairwise comparison among modalities/ Stiffness Variation

		M1-M2	M1-M3	M1-M4	M1-M5	M2-M3	M2-M4	M2-M5	M3-M4	M3-M5	M4-M5
Canine	B3	0.000*	0.000*	0.000*	0.000*	0.000*	0.000*	0.000*	0.003*	0.000*	0.000*
	D3	0.000*	0.000*	0.000*	0.000*	0.000*	0.000*	0.000*	0.000*	0.000*	0.000*
	M3	0.000*	0.000*	0.000*	0.000*	0.000*	0.000*	0.000*	0.000*	0.000*	0.000*
	P3	0.000*	0.000*	0.000*	0.000*	1.000	0.000*	0.000*	0.000*	0.000*	0.000*
1st premolar	B4	0.000*	0.000*	0.000*	0.000*	0.000*	1.000	0.000*	0.000*	0.000*	0.000*
	D4	0.000*	0.000*	0.000*	0.000*	0.054	0.880	0.000*	0.001*	0.000*	0.000*
	M4	0.000*	0.000*	0.000*	0.000*	0.005*	0.000*	0.000*	0.000*	0.000*	0.000*
	P4	0.000*	0.001*	1.000	0.129	0.052	0.000*	0.000*	0.001*	0.000*	0.158
2nd premolar	B5	0.000*	0.000*	0.000*	0.000*	0.968	0.000*	0.000*	0.000*	0.000*	0.000*
	D5	0.000*	0.000*	0.000*	0.000*	0.035*	0.003*	0.061	0.013*	0.000*	0.000*
	M5	0.000*	0.000*	0.000*	0.000*	0.041*	0.028*	0.000*	1.000	0.000*	0.000*
	P5	0.000*	0.000*	0.000*	0.000*	0.000*	0.000*	0.000*	0.000*	0.000*	0.000*
1st molar	B6	0.122	0.015*	0.000*	0.146	0.004*	0.000*	1.000	0.000*	0.000*	0.000*
	D6	0.060	0.000*	0.000*	0.000*	0.000*	0.000*	0.820	0.388	0.000*	0.000*
	M6	0.001*	0.000*	0.000*	0.000*	1.000	0.123	0.072	0.000*	0.000*	0.000*
	P6	0.029*	0.000*	0.000*	0.000*	1.000	0.343	1.000	0.000*	0.000*	0.000*
2nd molar	B7	0.000*	0.000*	1.000	1.000	0.079	0.000*	0.001*	0.000*	0.000*	0.026
	D7	0.000*	0.000*	0.000*	0.000*	0.007*	1.000	0.048*	0.000*	0.000*	0.000*
	M7	0.125	0.000*	0.000*	0.000*	0.000*	0.031*	0.000*	0.000*	0.000*	0.001*
	P7	0.019*	0.000*	0.000*	0.000*	0.000*	0.000*	0.000*	0.046*	0.000*	0.000*

3.2. Thickness Variation / Stress comparison among teeth and modalities

3.2.1. Part 6: Thickness variation / Intrusion modality 1

The stress amounts at teeth surfaces were not statistically significant (Levene's test) for the mesial, distal, buccal, and palatal surfaces (Table 3.18-19-20). Therefore, the ANOVA and Bonferroni tests were used.

For the first modality, all stresses were statistically significantly different between teeth (Table 3.19). Comparison of surfaces among teeth revealed that: the only palatal surface was significant when comparing canine to premolars, mesial when comparing canine to the first molar and distal when comparing canine to second molar and no statistical difference between premolars. The highest stress value was on the second premolar (5) and on the medial teeth (4-5-6) in comparison with the extremity teeth: the canine (3) and second molar (7) (Table 3.20; Fig 3.6).

Table 3.18: Descriptive statistics for the stress generated on the 4 surfaces of the buccal teeth (Thickness variation/ 1st modality)

Statistics	Buccal		Distal		Mesial		Palatal		Total
	Mean	SD	Mean	SD	Mean	SD	Mean	SD	
Canine (3)	1.019	1.1E-04	1.081	1.5E-04	1.029	5.9E-05	0.948	5.3E-05	**4.078**
First premolar (4)	1.245	6.2E-05	1.279	2.4E-04	1.282	4.0E-05	1.410	4.4E-05	**5.216**
Second premolar (5)	1.419	8.6E-05	1.307	1.4E-04	1.406	1.4E-04	1.397	1.6E-05	**5.529**
First molar (6)	1.172	2.3E-04	0.895	5.8E-05	1.298	6.2E-05	1.200	1.1E-04	**4.564**
Second molar (7)	0.386	4.8E-05	0.312	4.2E-05	0.596	1.9E-04	0.375	5.7E-05	**1.668**

Stresses in kPa; **SD**: Standard deviation

Table 3.19: Comparison of stress among the 5 teeth at each surface (Thickness/ 1st modality)

	3	4	5	6	7	p-value
Buccal	1.019	1.245	1.419	1.172	0.386	**0.000***
Distal	1.081	1.279	1.307	0.895	0.312	**0.000***
Mesial	1.029	1.282	1.406	1.298	0.596	**0.000***
Palatal	0.948	1.410	1.397	1.200	0.375	**0.000***

Kruskal-Wallis one-way analysis of variance for non-parametric data.
*Significant at $p < 0.05$

Table 3.20: Pairwise comparisons for stress between the teeth at each surface (Post-Hoc tests: Bonferroni)

	3-4	3-5	3-6	3-7	4-5	4-6	4-7	5-6	5-7	6-7
Buccal	0.188	**0.000***	0.230	0.709	0.108	1.000	**0.000***	0.087	**0.000***	**0.000***
Distal	1.000	0.132	0.946	**0.003***	1.000	**0.010***	**0.000***	**0.000***	**0.000***	0.538
Mesial	0.050	**0.000***	**0.022***	0.924	1.000	1.000	**0.000***	1.000	**0.000***	**0.000***
Palatal	**0.000***	**0.000***	0.924	0.924	1.000	0.098	**0.000***	0.137	**0.000***	**0.008***

*Significant at p < 0.05

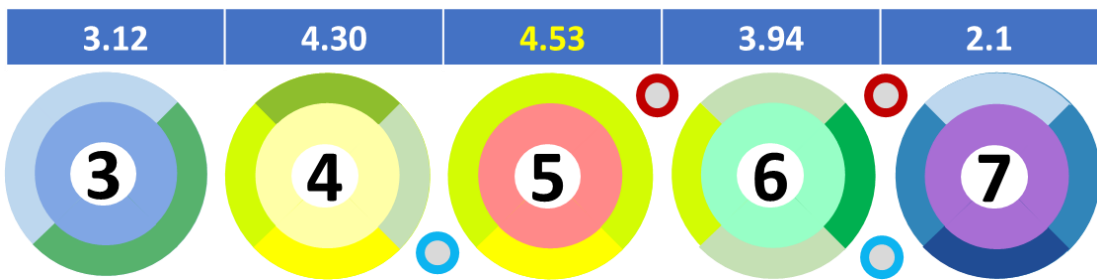**Fig.3.6:** Graphic representation of the buccal teeth response to intrusion on 1 buccal and 2 palatal mini-implants/thickness variation. Note the similar stresses on palatal surfaces of the first and second premolars (5). Lowest stresses on extremity teeth (3) - (7)
B: buccal, P: palatal, M: mesial, D: distal surfaces of teeth. Red indicates higher severity, dark blue lower severity as per used FEA scale.

3.2.2. Part 7: Thickness variation / Intrusion modality 2

The Levene's test results were statistically significant only for the stress amounts at the buccal and mesial surfaces, and non-significant for the mesial, distal, and palatal surfaces, (Table 3.22). Therefore, the Welch ANOVA and Games-Howell tests were used for the buccal and mesial surfaces.

For comparison between teeth, only the buccal and mesial surfaces were statistically significantly different specifically the canine in comparison with the premolars (3-4/3-5) and the second premolar versus the second molar (3-7). (Table 3.23)

Table 3.21: Descriptive statistics for the stress generated on the 4 surfaces of the buccal teeth (Thickness variation/2nd modality)

Statistics	Buccal		Distal		Mesial		Palatal		Total
	Mean	SD	Mean	SD	Mean	SD	Mean	SD	
Canine (3)	0.833	1.25E-04	0.893	1.65E-04	0.828	1.01E-04	0.826	1.15E-04	3.380
First premolar (4)	1.075	2.57E-04	1.089	2.65E-04	1.085	2.08E-04	1.019	2.28E-04	4.268
Second premolar (5)	1.246	3.98E-04	1.047	4.49E-04	1.158	2.98E-04	1.143	3.05E-04	4.594
First molar (6)	0.896	3.15E-04	0.883	1.63E-04	1.110	1.76E-04	1.091	2.15E-04	3.980
Second molar (7)	0.751	1.62E-04	0.726	3.45E-04	0.800	1.55E-04	1.006	4.11E-04	3.284

Stresses in kPa; **SD**: Standard deviation

Table 3.22: Comparison of stress among the 5 teeth at each surface (Thickness/ 2nd modality)

	3	4	5	6	7	p-value
Buccal†	0.833	1.075	1.246	0.896	0.751	**0.003***
Distal	0.893	1.089	1.047	0.883	0.726	0.085
Mesial†	0.828	1.085	1.158	1.110	0.800	**0.000***
Palatal	0.826	1.019	1.143	1.091	1.006	0.111

Kruskal-Wallis one-way analysis of variance for non-parametric data.
†*Results obtained with Welch ANOVA* values reported because assumption of homogeneity of variances was violated; *Significant at $p < 0.05$

Table 3.23: Pairwise comparisons for stress between the teeth at each surface (Games-Howell)

|	3-4	3-5	3-6	3-7	4-5	4-6	4-7	5-6	5-7	6-7
Buccal	0.084	0.042*	0.970	0.677	0.752	0.594	0.018*	0.190	0.015*	0.662
Mesial	0.016*	0.030*	0.002*	0.987	0.962	0.998	0.014*	0.990	0.022*	0.002*

*Significant at p <0.05
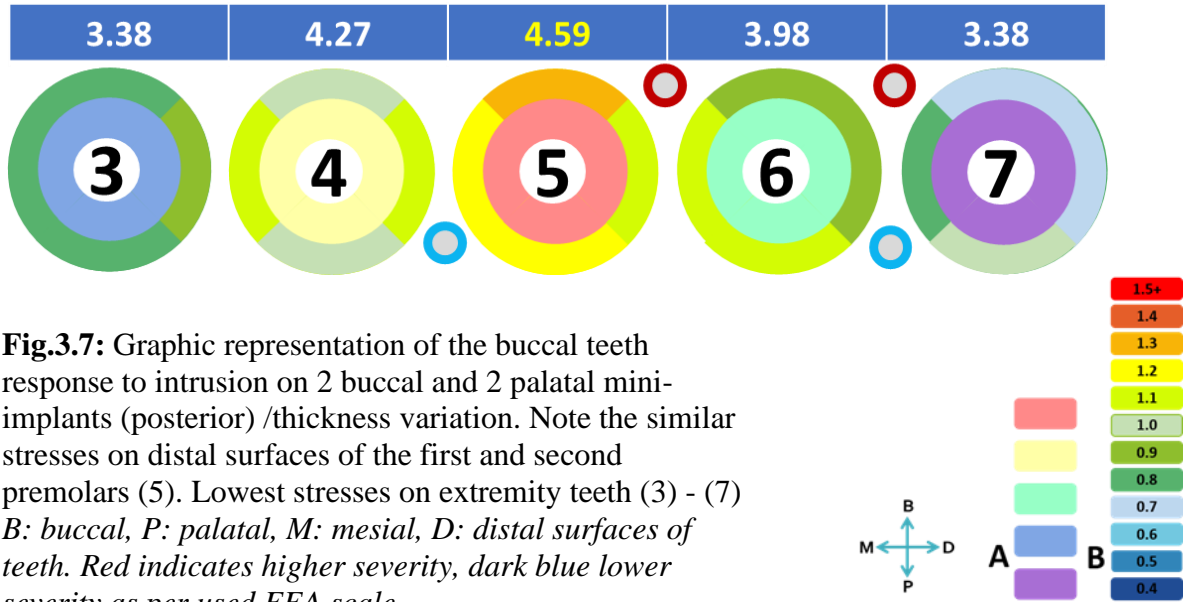
Fig.3.7: Graphic representation of the buccal teeth response to intrusion on 2 buccal and 2 palatal mini-implants (posterior) /thickness variation. Note the similar stresses on distal surfaces of the first and second premolars (5). Lowest stresses on extremity teeth (3) - (7) *B: buccal, P: palatal, M: mesial, D: distal surfaces of teeth. Red indicates higher severity, dark blue lower severity as per used FEA scale.*

3.2.3. Part 8: Thickness variation / Intrusion modality 3

The second premolar sustained the highest stress specifically its buccal aspect with stress concentrated more anterior (5>4>3). All stresses were statistically significantly different between teeth. Comparison between surfaces indicated statistically significant difference in all aspects of the canine and the second premolar (3-5), the first and second premolars and the second molar (4-7/5-7) (Table 3.25, Table 3.26; Fig.3.8).

Table 3.24: Descriptive statistics for the stress generated on the 4 surfaces of the buccal teeth (Thickness variation/3rd modality)

Statistics	Buccal		Distal		Mesial		Palatal		total
	Mean	SD	Mean	SD	Mean	SD	Mean	SD	
Canine (3)	0.870	5.0E-05	0.854	5.2E-05	0.833	4.7E-05	0.813	3.9E-05	3.370
First premolar (4)	1.066	8.4E-05	0.913	2.6E-04	1.031	7.9E-05	1.019	8.8E-05	4.029
Second premolar (5)	1.217	2.8E-05	1.082	7.3E-05	1.067	3.0E-04	1.079	7.7E-05	4.444
First molar (6)	0.935	6.5E-05	0.688	5.8E-05	0.966	5.3E-05	0.851	1.1E-04	3.440
Second molar (7)	0.655	7.3E-05	0.550	1.6E-04	0.661	8.3E-05	0.594	4.3E-05	2.460

Stresses in kPa; **SD**: Standard deviation

Table 3.25: Comparison of stress among the 5 teeth at each surface (Thickness/3rd modality)

	3	4	5	6	7	p-value
Buccal	0.870	1.066	1.217	0.935	0.655	**0.000***
Distal	0.854	0.913	1.082	0.688	0.550	**0.000***
Mesial	0.833	1.031	1.067	0.966	0.661	**0.000***
Palatal	0.813	1.019	1.079	0.851	0.594	**0.000***

Kruskal-Wallis one-way analysis of variance for non-parametric data.
*Significant at $p < 0.05$

Table 3.26: Pairwise comparisons for stress between the teeth at each surface (Post-Hoc tests: Bonferroni)

|	3-4	3-5	3-6	3-7	4-5	4-6	4-7	5-6	5-7	6-7
Buccal	0.040*	0.000*	1.000	0.386	0.816	0.700	0.000*	0.004*	0.000*	0.017*
Distal	1.000	0.036*	0.700	0.013*	1.000	0.012*	0.000*	0.000*	0.000*	1.000
Mesial	0.032*	0.000*	0.288	0.924	1.000	1.000	0.000*	0.496	0.000*	0.001*
Palatal	0.005*	0.000*	1.000	0.656	1.000	0.158	0.000*	0.013*	0.000*	0.037*

*Significant at p <0.05
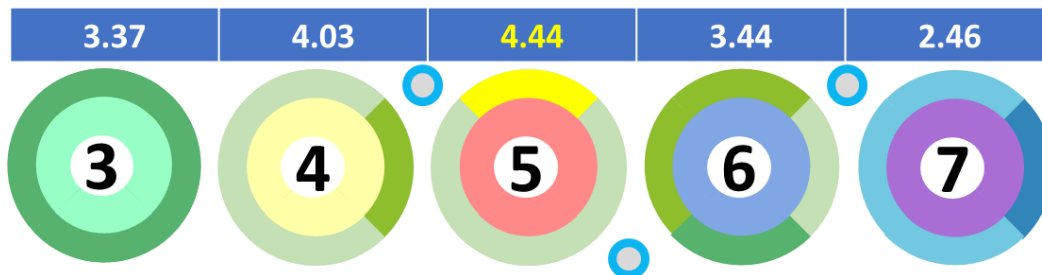
Fig.3.8: Graphic representation of the buccal teeth response to intrusion on 2 buccal and 1 palatal mini-implants/thickness variation. Note the concentration of stress on the anterior segment (5>4>3)
B: buccal, P: palatal, M: mesial, D: distal surfaces of teeth.
Red indicates higher severity, dark blue lower severity as per used FEA scale.
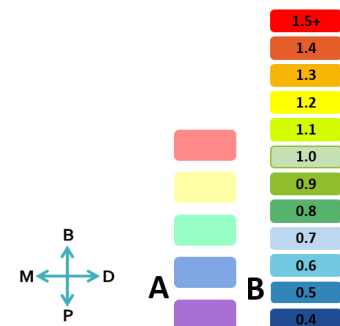
3.2.4. Part 9: Thickness variation / Intrusion modality 4

The first premolar sustained the highest stress specifically its palatal aspect with stress concentrated more anterior (4>3>5). Comparison between stresses on teeth, revealed statistically significantly difference (Table 3.28). Pairwise comparison between teeth was statistically significant between the canines and molars (3-6/3-7), first premolar and molars (4-6/4-7), and second premolar and second molar (5-7) (Table 3.29; Fig.3.9).

Table 3.27: Descriptive statistics for the stress generated on the 4 surfaces of the buccal teeth (Thickness variation/4th modality

Statistics	Buccal		Distal		Mesial		Palatal		total
	Mean	SD	Mean	SD	Mean	SD	Mean	SD	
Canine (3)	1.110	9.5E-05	1.126	7.7E-05	1.230	7.0E-05	1.332	7.5E-05	4.799
First premolar (4)	1.091	1.1E-04	1.240	1.2E-04	1.355	1.2E-04	1.452	1.0E-04	5.138
Second premolar (5)	1.010	9.5E-05	1.084	9.0E-05	1.171	8.3E-05	1.278	7.3E-05	4.543
First molar (6)	0.586	1.3E-04	0.698	1.3E-04	0.773	1.0E-04	0.843	1.3E-04	2.901
Second molar (7)	0.587	1.4E-04	0.617	1.4E-04	0.659	1.5E-04	0.687	1.6E-04	2.550

Stresses in kPa; **SD**: Standard deviation

Table 3.28: Comparison of stress among the 5 teeth at each surface (Thickness/4th modality)

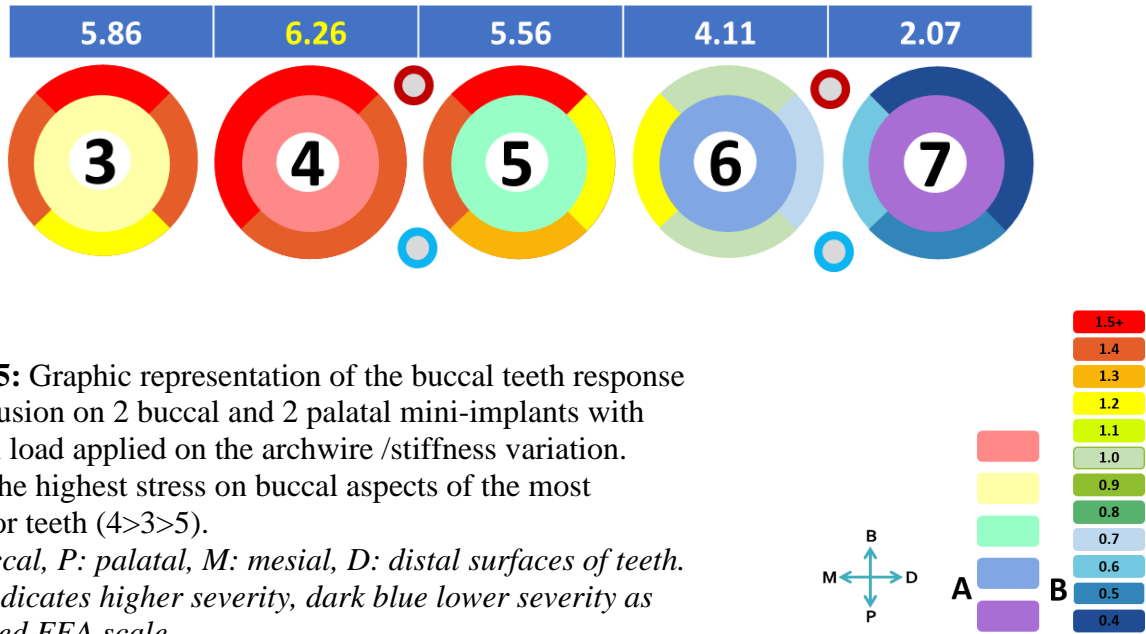|	3	4	5	6	7	p-value
Buccal	1.110	1.091	1.010	0.586	0.587	**0.000***
Distal	1.126	1.240	1.084	0.698	0.617	**0.000***
Mesial	1.230	1.355	1.171	0.773	0.659	**0.000***
Palatal	1.332	1.452	1.278	0.843	0.687	**0.000***

Kruskal-Wallis one-way analysis of variance for non-parametric data.
*Significant at $p < 0.05$

Table 3.29: Pairwise comparisons for stress between the teeth at each surface (Post-Hoc tests: Bonferroni)

	3-4	3-5	3-6	3-7	4-5	4-6	4-7	5-6	5-7	6-7
Buccal	1.000	1.000	**0.000***	**0.000***	1.000	**0.000***	**0.000***	**0.007***	**0.009***	1.000
Distal	1.000	1.000	**0.003***	**0.000***	0.568	**0.000***	**0.000***	**0.024***	**0.002***	1.000
Mesial	1.000	1.000	**0.002***	**0.000***	0.280	**0.000***	**0.000***	0.056	**0.004***	1.000
Palatal	1.000	1.000	**0.004***	**0.000***	0.234	**0.000***	**0.000***	0.085	**0.002***	1.000

*Significant at p <0.05
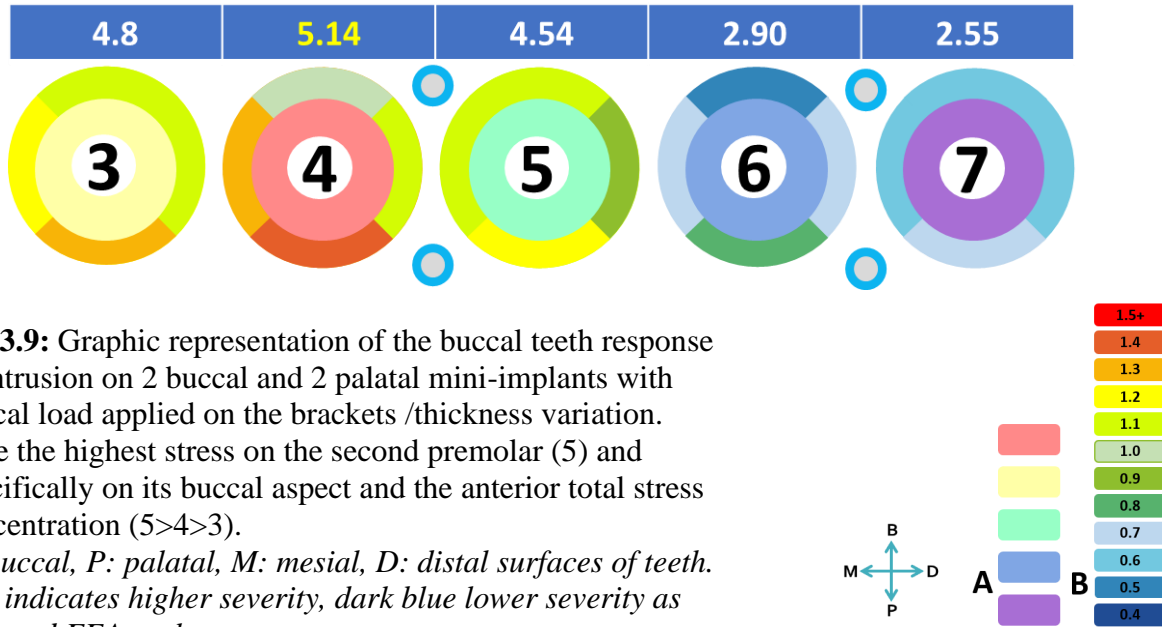
Fig.3.9: Graphic representation of the buccal teeth response to intrusion on 2 buccal and 2 palatal mini-implants with buccal load applied on the brackets /thickness variation. Note the highest stress on the second premolar (5) and specifically on its buccal aspect and the anterior total stress concentration (5>4>3).
B: buccal, P: palatal, M: mesial, D: distal surfaces of teeth. Red indicates higher severity, dark blue lower severity as per used FEA scale.

3.2.5. Part 10: Thickness variation / Intrusion modality 5

The first premolar sustained the highest stress specifically its palatal aspect with stress concentrated more anterior (4>3>5), pattern of stress distribution was similar to that of the modality 4 but with higher values. All stresses were statistically significantly different between teeth. Pairwise comparison between teeth was statistically significant between the canines and molars (3-6/3-7), first premolar and molars (4-6/4-7), and second premolar and second molar (5-7) (Table 3.31, Table 3.32; Fig.3.10).

Table 3.30: Descriptive statistics for the stress generated on the 4 surfaces of the buccal teeth (Thickness variation/ 5ᵗʰ modality)

Statistics	Buccal		Distal		Mesial		Palatal		total
	Mean	SD	Mean	SD	Mean	SD	Mean	SD	
Canine (3)	1.747	9.9E-05	1.611	7.4E-05	1.619	8.4E-05	1.459	7.6E-05	6.436
First premolar (4)	1.849	4.4E-05	1.605	6.1E-05	1.716	4.9E-04	1.606	8.3E-05	6.776
Second premolar (5)	1.670	5.7E-05	1.351	6.2E-05	1.595	1.5E-04	1.523	9.2E-05	6.138
First molar (6)	1.159	3.6E-05	0.910	5.9E-05	1.417	6.3E-05	1.200	6.5E-05	4.686
Second molar (7)	0.583	6.4E-05	0.559	7.8E-05	0.710	7.9E-05	0.785	9.0E-05	2.637

Stresses in kPa; **SD**: Standard deviation

Table 3.31: Comparison of stress among the 5 teeth at each surface (Thickness/ 5th modality)

	3	4	5	6	7	p-value
Buccal	1.747	1.849	1.670	1.159	0.583	**0.000***
Distal	1.611	1.605	1.351	0.910	0.559	**0.000***
Mesial	1.619	1.716	1.595	1.417	0.710	**0.000***
Palatal	1.459	1.606	1.523	1.200	0.785	**0.000***

Kruskal-Wallis one-way analysis of variance for non-parametric data.
*Significant at $p < 0.05$

Table 3.32: Pairwise comparisons for stress between the teeth at each surface (Post-Hoc tests: Bonferroni)

	3-4	3-5	3-6	3-7	4-5	4-6	4-7	5-6	5-7	6-7
Buccal	1.000	1.000	**0.011***	**0.000***	0.141	**0.000***	**0.000***	0.288	**0.001***	0.924
Distal	1.000	0.074	**0.000***	**0.000***	0.177	**0.000***	**0.000***	0.923	**0.008***	0.923
Mesial	1.000	1.000	0.177	**0.000***	0.700	**0.001***	**0.000***	0.324	**0.000***	0.553
Palatal	0.324	1.000	0.194	**0.001***	1.000	**0.000***	**0.000***	**0.010***	**0.000***	0.924

*Significant at p <0.05
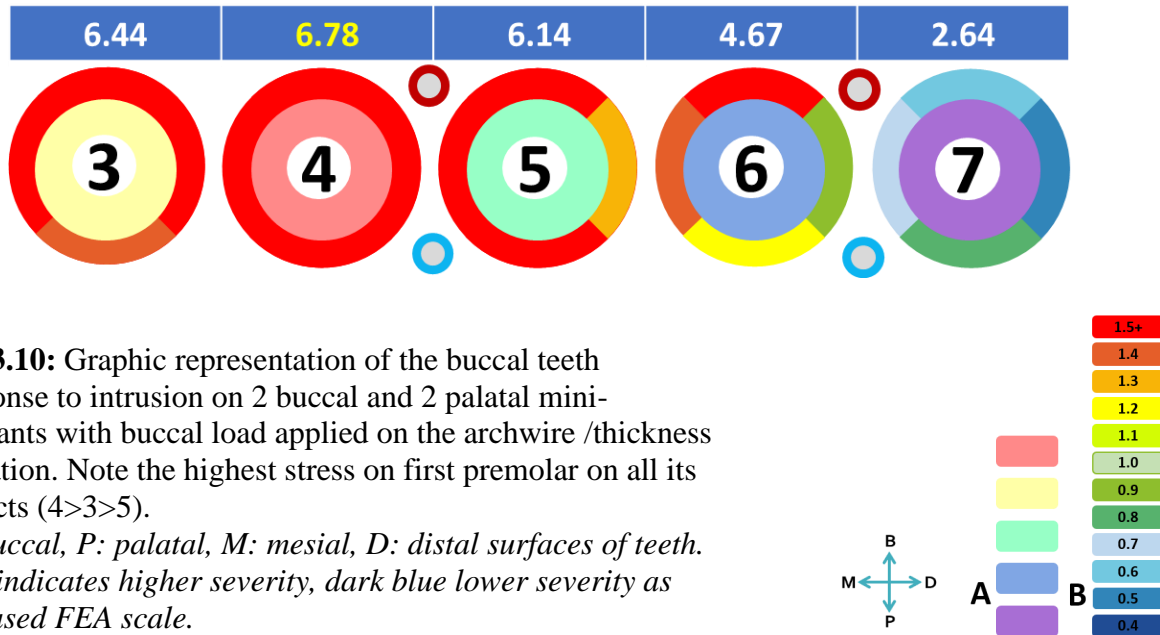
Fig.3.10: Graphic representation of the buccal teeth response to intrusion on 2 buccal and 2 palatal mini-implants with buccal load applied on the archwire /thickness variation. Note the highest stress on first premolar on all its aspects (4>3>5).
B: buccal, P: palatal, M: mesial, D: distal surfaces of teeth.
Red indicates higher severity, dark blue lower severity as per used FEA scale.

3.2.6. Thickness Variation/ Comparison between the five modalities of intrusion

The results showed statistically significant differences for all modalities among all the teeth. The p-values were all below 0.05 except for the mesial surface of the second molar (M7) in all modalities (Table 3.33).

- M 1 and 2 are comparable in terms of Von mises stresses on the second premolars (anterior pull on MI) and first molar (despite the additional force on the second MI).
- Between M1 and M5, almost all stresses are statistically different (except for surfaces on the second premolar and first molar) even though the position of the MIs differs between these 2 modalities *suggesting that the amount of force dictated the resultant Von Mises Stress*.
- M2-M5: NS difference on molars since the posterior pull in both is evenly distributed
- M3-M4: the only difference was the number in palatal MIs, (NS difference posteriorly): *one hypothesis is that the number of palatal MIs does not influence the amount of stresses on the posterior section.*
- M4-M5: NS on the second molar only, *application of force whether on wire or brackets affects the stresses on teeth.*

Table 3.33: Repeated measures ANOVA for comparison of stress among different modalities/ Thickness Variation

Tooth		M1		M2		M3		M4		M5		p-value
		Mean	SD	Mean	SD	Mean	SD	Mean	SD	Mean	SD	
Canine	B3	1.019	1.13E-04	0.850	1.34E-04	0.870	4.97E-05	1.110	9.52E-05	1.747	9.86E-05	**0.000***
	D3	1.081	1.51E-04	0.909	1.67E-04	0.854	5.16E-05	1.126	7.65E-05	1.611	7.36E-05	**0.000***
	M3	1.029	5.85E-05	0.842	1.09E-04	0.833	4.66E-05	1.230	7.00E-05	1.619	8.36E-05	**0.000***
	P3	0.948	5.31E-05	0.845	1.27E-04	0.813	3.87E-05	1.332	7.52E-05	1.459	7.58E-05	**0.000***
1st premolar	B4	1.245	6.22E-05	1.086	2.47E-04	1.066	8.38E-05	1.091	1.11E-04	1.849	4.43E-05	**0.000***
	D4	1.279	2.42E-04	1.107	2.60E-04	0.913	2.62E-04	1.240	1.17E-04	1.605	6.13E-05	**0.000***
	M4	1.282	3.99E-05	1.098	2.03E-04	1.031	7.91E-05	1.355	1.21E-04	1.716	4.87E-04	**0.001***
	P4	1.410	4.41E-05	1.036	2.25E-04	1.019	8.77E-05	1.452	1.03E-04	1.606	8.27E-05	**0.000***
2nd premolar	B5	1.419	8.62E-05	1.269	3.88E-04	1.217	2.82E-05	1.010	9.49E-05	1.670	5.70E-05	**0.000***
	D5	1.307	1.38E-04	1.072	4.37E-04	1.082	7.32E-05	1.084	8.98E-05	1.351	6.23E-05	**0.041***
	M5	1.406	1.41E-04	1.173	2.89E-04	1.067	3.03E-04	1.171	8.25E-05	1.595	1.46E-04	**0.000***
	P5	1.397	1.61E-05	1.161	2.98E-04	1.079	7.66E-05	1.278	7.35E-05	1.523	9.23E-05	**0.002***
1st molar	B6	1.172	2.34E-04	0.905	3.02E-04	0.935	6.47E-05	0.586	1.32E-04	1.159	3.56E-05	**0.000***
	D6	0.895	5.84E-05	0.892	1.59E-04	0.688	5.76E-05	0.698	1.31E-04	0.910	5.89E-05	**0.000***
	M6	1.298	6.20E-05	1.126	1.76E-04	0.966	5.25E-05	0.773	1.04E-04	1.417	6.35E-05	**0.000***
	P6	1.200	1.06E-04	1.103	2.09E-04	0.851	1.13E-04	0.843	1.31E-04	1.200	6.53E-05	**0.001***
2nd molar	B7	0.386	4.78E-05	0.757	1.55E-04	0.655	7.26E-05	0.587	1.36E-04	0.583	6.39E-05	**0.001***
	D7	0.312	4.24E-05	0.745	3.35E-04	0.550	1.63E-04	0.617	1.37E-04	0.559	7.75E-05	**0.009***
	M7	0.596	1.89E-04	0.807	1.50E-04	0.661	8.30E-05	0.659	1.45E-04	0.710	7.90E-05	**0.026***
	P7	0.375	5.74E-05	1.023	3.96E-04	0.594	4.34E-05	0.687	1.57E-04	0.785	8.98E-05	**0.001***

Table 3.34: Pairwise comparison among modalities/ Thickness Variation

		M1-M2	M1-M3	M1-M4	M1-M5	M2-M3	M2-M4	M2-M5	M3-M4	M3-M5	M4-M5
Canine	B3	**0.019***	**0.002***	0.405	**0.000***	1.000	**0.009***	**0.000***	**0.000***	**0.000***	**0.000***
	D3	**0.049***	**0.001***	1.000	**0.000***	1.000	0.065	**0.000***	**0.000***	**0.000***	**0.000***
	M3	**0.002***	**0.000***	**0.000***	**0.000***	1.000	**0.000***	**0.000***	**0.000***	**0.000***	**0.000***
	P3	0.136	**0.000***	**0.000***	**0.000***	1.000	**0.000***	**0.000***	**0.000***	**0.000***	**0.000***
1st premolar	B4	0.382	**0.000***	**0.018***	**0.000***	1.000	1.000	**0.000***	1.000	**0.000***	**0.000***
	D4	1.000	**0.028***	1.000	**0.010***	0.219	1.000	**0.001***	**0.045***	**0.000***	**0.000***
	M4	0.063	**0.000***	0.999	0.103	1.000	0.087	**0.028***	**0.000***	**0.004***	0.304
	P4	**0.003***	**0.000***	0.505	**0.000***	1.000	**0.004***	**0.000***	**0.000***	**0.000***	**0.000***
2nd premolar	B5	1.000	**0.000***	**0.000***	**0.000***	1.000	0.656	0.067	**0.000***	**0.000***	**0.000***
	D5	0.916	**0.008***	**0.012***	1.000	1.000	1.000	0.612	1.000	**0.000***	**0.000***
	M5	0.170	**0.048***	**0.010***	0.131	1.000	1.000	**0.020***	1.000	**0.000***	**0.000***
	P5	0.202	**0.000***	**0.001***	**0.007***	1.000	1.000	0.064	**0.000***	**0.000***	**0.000***
1st molar	B6	0.573	**0.048***	**0.000***	1.000	1.000	0.159	0.186	**0.000***	**0.000***	**0.000***
	D6	1.000	**0.000***	**0.004***	1.000	**0.012***	0.217	1.000	1.000	**0.000***	**0.001***
	M6	0.105	**0.000***	**0.000***	**0.014***	0.204	**0.001***	**0.002***	**0.000***	**0.000***	**0.000***
	P6	1.000	**0.000***	**0.000***	1.000	0.072	**0.027***	1.000	1.000	**0.000***	**0.000***
2nd molar	B7	**0.000***	**0.000***	**0.001***	**0.000***	1.000	0.580	0.150	0.126	**0.000***	1.000
	D7	**0.010***	**0.003***	**0.000***	**0.000***	1.000	1.000	1.000	1.000	1.000	0.220
	M7	0.186	1.000	1.000	0.254	0.402	0.885	0.953	1.000	0.478	1.000
	P7	**0.002***	**0.003***	**0.000***	**0.000***	**0.041***	0.412	0.878	0.419	**0.000***	0.239

3.3. Stress values comparison within each modality: stiffness/ thickness

Statistically significant differences were found at the level of the premolars (S/T S4 and 5) and the first molar (S/T S6) (p-value <0.05) in the first modality (Table 3.35), but none in modality 2, (Table 3.36). In the third modality, all stresses on teeth were significantly different between stiffness (S) and thickness (T) values except for the first molars stress (Table 3.37), while differences were significant for all five teeth in modality 4 (Table 3.38). In modality 5, the main difference was on the second molar (S/T S 7) (Table 3.39).

Modality 1				
S/T S3	S/T S4	S/T S5	S/T S6	S/T S7
P-value				
0.252	0.005	0.000	0.000	0.955

Table.4.35. Stress comparison between stiffness and thickness variation in the first modality

Modality 2				
S/T S3	S/T S4	S/T S5	S/T S6	S/T S7
P-value				
0.051	0.332	0.075	0.965	0.331

Table.4.36. Stress comparison between stiffness and thickness variation in the second modality

Modality 3				
S/T S3	S/T S4	S/T S5	S/T S6	S/T S7
P-value				
0.000	0.000	0.000	0.080	0.013

Table.4.37. Stress comparison between stiffness and thickness variation in the third modality

Modality 4				
S/T S3	S/T S4	S/T S5	S/T S6	S/T S7
P-value				
0.000	0.020	0.000	0.000	0.000

Table.4.38. Stress comparison between stiffness and thickness variation in the fourth modality

Modality 5				
S/T S3	S/T S4	S/T S5	S/T S6	S/T S7
P-value				
0.314	0.360	0.489	0.357	0.019

Table.4.39. Stress comparison between stiffness and thickness variation in the fifth modality

S/T: Stiffness/thickness
S3: Stress 3/ **S4:** Stress 4/ **S5:** Stress 5/ **S6:** Stress 6/ **S7:** Stress 7

3.4. Displacement comparison between teeth

Descriptive statistics were planned to evaluate initial displacement in all three directions of movement in both stiffness and thickness variation (**Axis 1**= x= Bucco-lingual direction/ **Axis**

2= y= Antero-posterior direction/ **Axis 3**= z= Vertical direction) considering that axis 1 and 2 represent secondary effects of intrusion (axis 3). (Tables.3.40/44).

3.4.1. Stiffness variation

The first modality displayed the highest intrusion value on the second premolar (5) (1.060 mm) and the first premolar (4) (0.950 mm), with statistically significant differences between all the teeth. The second molar (7) exhibits the least intrusion (0.319 mm) (Table 3.41).

Modality 2 was similar to the first one; the highest displacement being on the second premolar (5), but at a lower amount (0.817 mm). The displacement of the canine (3), first premolar (4) and first molar (6) were of lower values than in modality 1 (0.565 mm, 0.738 mm, and 0.692 mm respectively). On the opposite, the second molar intruded more (0.489 mm) when compared to the first modality (0.319 mm).

The comparison between modalities 1 and 5, showed greater intrusion of the canine in the latter (1.062 mm) and the maximal intrusion on the first premolar (4) (1.154 mm). The second molars were similar at 0.319 mm of initial displacement. The comparison between modalities 4 and 5, revealed the higher intrusion on the second molar.

In modality 3, the same pattern of intrusion was observed with lower values as in the first modality (0.754 mm and 0.736 mm respectively on 5 and 4). The second molar (7) intrusion was 0.412 mm compared to less intrusion on the first molar (6) (0.349 mm) with intrusion concentrated anteriorly 3, 4 and 5 with 0.739, 0.784 and 0.701 mm, respectively.

Whereas, the highest intrusion was on the second premolar for modality 3 (0.754 mm), compared to 0.784 mm in modality 4. Both setups 3 and 4 exhibited close amount of intrusion

for the first molar (0.585 versus 0.483) and the second molar (0.412 mm and 0.349 mm;

respectively).

Premolars intrusion was higher in modality 4 than in modality 5 but followed same

pattern for teeth intrusion (4>3>5). The second molar intruded more in model 4 (0.349 mm) but

the second molar intruded more in modality 5 (0.665 mm). Difference between teeth and models

was significant in all aspects (Table 3.40).

Pairwise comparison displayed no statistical significance between the molars (6-7), between the

premolars (4-5) in the first two modalities and between the canine and the first premolar (3-4)

(Table 3.42)

Table 3.40. Descriptive statistics for tooth initial displacement/ Stiffness variation (in mm)
Axis 1= x= Bucco-lingual direction
Axis 2= y= Antero-posterior direction
Axis 3= z= Vertical direction

		M1		M2		M3		M4		M5	
		Mean	SD	Mean	SD	Mean	SD	Mean	SD	Mean	SD
3	Axis 1	0.307	2E-05	0.099	2E-05	0.345	1E-05	0.283	3E-06	0.087	4E-06
	Axis 2	-0.135	1E-05	-0.068	3E-05	-0.137	6E-06	-0.098	6E-06	-0.146	8E-06
	Axis 3	0.744	3E-05	0.565	8E-05	0.636	3E-05	0.739	1E-05	1.062	2E-05
4	Axis 1	0.102	2E-05	-0.007	1E-05	0.211	2E-05	0.310	7E-06	-0.004	9E-06
	Axis 2	-0.251	2E-05	-0.159	1E-05	-0.193	1E-05	-0.120	1E-05	-0.241	1E-05
	Axis 3	0.950	2E-05	0.738	3E-05	0.736	3E-05	0.784	1E-05	1.154	2E-05
5	Axis 1	0.523	5E-05	0.041	2E-05	0.194	4E-05	0.174	6E-06	0.019	8E-06
	Axis 2	-0.237	2E-05	-0.128	1E-05	-0.178	2E-05	-0.111	9E-06	-0.224	1E-05
	Axis 3	1.060	3E-05	0.817	4E-05	0.754	3E-05	0.701	1E-05	1.024	3E-05
6	Axis 1	-0.046	2E-05	-0.058	2E-05	-0.023	9E-06	0.145	1E-05	0.027	2E-05
	Axis 2	-0.044	9E-06	-0.044	1E-05	-0.072	7E-06	0.018	9E-06	-0.077	9E-06
	Axis 3	0.773	2E-05	0.692	1E-04	0.585	7E-05	0.483	1E-05	0.665	3E-05
7	Axis 1	-0.032	7E-06	0.009	8E-06	0.143	1E-05	0.109	1E-05	0.142	2E-05
	Axis 2	-0.001	5E-06	-0.042	7E-06	-0.103	7E-06	-0.029	4E-06	-0.029	7E-06
	Axis 3	0.319	3E-05	0.489	6E-05	0.412	3E-05	0.349	3E-05	0.318	3E-05

Table 3.41. Comparison of INTRUSION among the teeth (intramodality in millimeter) and comparison of Intrusion among different modalities (intermodality in millimeter) /Stiffness variation.

	3		4		5		6		7		
	Mean	SD	Mean	SD	Mean	SD	Mean	SD	Mean	SD	P-value†
M 1	0.744	3E-05	0.950	2E-05	*1.060*	3E-05	0.759	4E-05	0.319	3E-05	**0.000***
M 2	0.565	8E-05	0.738	3E-05	*0.817*	4E-05	0.692	1E-04	0.489	6E-05	**0.000***
M 3	0.636	3E-05	0.736	3E-05	*0.754*	3E-05	0.585	7E-05	0.412	3E-05	**0.000***
M 4	0.739	1E-05	*0.784*	1E-05	0.701	1E-05	0.483	1E-05	0.349	3E-05	**0.000***
M 5	1.062	2E-05	*1.154*	2E-05	1.024	3E-05	0.665	3E-05	0.318	3E-05	**0.000***
P-Value¥	**0.000***		**0.000***		**0.000***		**0.000***		**0.000***		

†Kruskal-Wallis one-way analysis of variance
¥ Repeated measures ANOVA

Table 3.42. Pairwise comparison between teeth in every modality/ Stiffness variation

	3-4	3-5	3-6	3-7	4-5	4-6	4-7	5-6	5-7	6-7
M1	0.102	**0.000***	1.000	0.237	1.000	0.237	**0.000***	**0.001***	**0.000***	0.102
M2	0.172	**0.000***	0.790	1.000	0.417	1.000	**0.002***	0.078	**0.000***	**0.018***
M3	0.172	**0.017***	1.000	0.056	1.000	**0.007***	**0.000***	**0.000***	**0.000***	0.813
M4	0.989	1.000	**0.015***	**0.000***	**0.017***	**0.000***	**0.000***	0.936	**0.010***	1.000
M5	0.767	1.000	**0.022***	**0.000***	**0.022***	**0.000***	**0.000***	0.767	**0.007***	1.000

Table 3.43. Pairwise comparison between modalities/ Stiffness variation

	M1-M2	M1-M3	M1-M4	M1-M5	M2-M3	M2-M4	M2-M5	M3-M4	M3-M5	M4-M5
3	**0.000***	**0.000***	1.000	**0.000***	**0.022***	**0.000***	**0.000***	**0.000***	**0.000***	**0.000***
4	**0.000***	**0.000***	**0.000***	**0.000***	1.000	**0.000***	**0.000***	**0.000***	**0.000***	**0.000***
5	**0.000***	**0.000***	**0.000***	**0.001***	**0.001***	**0.000***	**0.000***	**0.000***	**0.000***	**0.000***
6	0.781	**0.000***	**0.000***	**0.001***	0.198	**0.001***	1.000	**0.004***	**0.007***	**0.000***
7	**0.001***	**0.000***	**0.009***	1.000	**0.003***	**0.000***	**0.000***	**0.000***	**0.000***	**0.000***

3.4.2. Thickness variation

Modality 1 displayed the highest intrusion values on the second (5) (1.071 mm) and the first (4) (0.962 mm) premolars, with statistically significant difference among teeth. The second molar (7) intruded the least (0.344 mm) (Table 3.45), as reflected in the stiffness variation.

The comparison between the modalities 1 and 2, revealed a greater intrusion on the second premolar (5) in model 1, decreasing in both modalities respectively on teeth 4, 6, 3 and 7. The second molar intruded more in the second modality (0.513 versus 0.344 mm).

In model 5, the highest displacement was registered on the first premolar (4) with 1.167 mm with stress localized anteriorly (1.035 mm on the canine (3)), and lowest on the molars (0.657 mm on the first molar (6)), in model 2, distribution of intrusion was more uniform.

Displacement values were close between modalities 3 and 4 (4>5>3>6>7). In the third setup, intrusion was high on 4 and 5 (0.766 mm and 0.772 mm respectively). The second molar intruded more (0.489 mm).

Less intrusion was observed on the second molar (7) in the fourth modality (0.421) with intrusion concentrated anteriorly on the 3, 4 and 5, with 0.734, 0.756 and 0.727 millimeters, respectively.

Intrusion in modality 4 was greater anteriorly among the first premolar (1.167 mm) and the second premolar (1.049 mm), and more uniformly distributed in comparison with the fifth setup.

Differences between teeth in all modalities was significant in all aspects (Table 3.46/47). Pairwise comparisons displayed no statistical significance between the molars (6-7), between the premolars (4-5), between the canine and the first premolar (3-5), and between the canine and the first molar (3-6) (Table 3.45).

When comparing modalities, no significant statistical difference was noted between modalities 2 and 3, 2 and 4, and, 3 and 4 on all teeth (Table 3.47).

Table 3.44. Descriptive statistics for tooth initial displacement/ Thickness variation (in mm)
Axis 1= x= Bucco-lingual direction
Axis 2= y= Antero-posterior direction
Axis 3= z= Vertical direction

		M1		M2		M3		M4		M5	
		Mean	SD	Mean	SD	Mean	SD	Mean	SD	Mean	SD
3	Axis 1	0.316	4E-05	0.049	2E-05	0.428	3E-04	0.286	7E-05	0.086	2E-05
	Axis 2	-0.146	2E-05	-0.066	1E-05	-0.151	4E-05	-0.096	2E-05	-0.143	6E-05
	Axis 3	0.753	1E-04	0.585	1E-04	0.694	3E-04	0.734	2E-04	1.035	2E-04
4	Axis 1	0.110	1E-05	0.033	1E-05	0.245	4E-04	0.309	1E-04	-0.004	3E-06
	Axis 2	-0.258	5E-05	-0.180	1E-04	-0.195	5E-05	-0.137	3E-05	-0.257	9E-05
	Axis 3	0.962	2E-04	0.660	2E-04	0.776	2E-04	0.756	3E-05	1.167	3E-04
5	Axis 1	0.537	8E-05	0.102	5E-05	0.158	4E-05	0.174	3E-05	0.021	1E-05
	Axis 2	-0.240	7E-05	-0.121	3E-05	-1.693	6E-04	-0.122	1E-05	-0.231	8E-05
	Axis 3	1.071	8E-05	0.820	2E-04	0.772	7E-05	0.727	3E-04	1.049	2E-04
6	Axis 1	-0.051	2E-05	-0.022	1E-05	-0.024	4E-06	0.176	1E-04	0.045	5E-05
	Axis 2	-0.047	6E-06	-0.039	3E-05	-0.066	2E-05	-0.076	1E-04	-0.074	1E-05
	Axis 3	0.789	1E-04	0.518	2E-04	0.596	7E-05	0.568	2E-04	0.657	1E-04
7	Axis 1	-0.032	7E-06	0.111	5E-05	0.171	3E-05	0.181	2E-04	0.148	7E-05
	Axis 2	-0.146	6E-06	-0.118	3E-05	-0.100	3E-05	-0.147	2E-04	-0.025	7E-06
	Axis 3	0.344	1E-04	0.513	2E-04	0.489	1E-04	0.421	2E-04	0.329	8E-05

Table 3.45. Comparison of INTRUSION among the teeth (intramodality in mm). Comparison of Intrusion among different modalities (intermodality) /Thickness variation

	3		4		5		6		7		
	Mean	SD	Mean	SD	Mean	SD	Mean	SD	Mean	SD	P-value†
M1	0.753	1E-04	0.962	2E-04	*1.071*	8E-05	0.756	1E-04	0.344	1E-04	**0.000***
M2	0.585	1E-04	0.660	2E-04	*0.820*	2E-04	0.518	2E-04	0.513	2E-04	0.471
M3	0.694	3E-04	*0.776*	2E-04	0.772	7E-05	0.596	7E-05	0.489	1E-04	**0.000***
M4	0.734	2E-04	*0.756*	3E-05	0.727	3E-04	0.568	2E-04	0.421	2E-04	**0.000***
M5	1.035	2E-04	*1.167*	3E-04	1.049	2E-04	0.657	1E-04	0.329	8E-05	**0.000***
P-value¥	**0.000***		**0.000***		**0.000***		**0.000***		**0.000***		

†Kruskal-Wallis one-way analysis of variance
¥ Repeated measures ANOVA

Table 3.46. Pairwise comparison between teeth in every modality (Bonferroni)/ Thickness variation

	3-4	3-5	3-6	3-7	4-5	4-6	4-7	5-6	5-7	6-7
M1	0.151	**0.005***	1.000	0.069	1.000	0.132	**0.000***	**0.004***	**0.000***	0.923
M3†	0.915	0.884	0.776	0.187	1.000	**0.044***	**0.001***	**0.000***	**0.000***	0.058
M4†	0.998	1.000	0.332	**0.021***	0.996	**0.014***	**0.001***	0.454	**0.041***	1.000
M5	1.000	1.000	0.108	**0.000***	1.000	**0.003***	**0.000***	0.091	**0.000***	0.496

†Games-Howell post hoc p values reported when assumption of homogeneity of variance violated

Table 3.47. Pairwise comparison between modalities/ Thickness variation

	M1-M2	M1-M3	M1-M4	M1-M5	M2-M3	M2-M4	M2-M5	M3-M4	M3-M5	M4-M5
3	0.001*	1.000	1.000	0.002*	1.000	0.861	0.000*	1.000	0.014*	0.005*
4	0.000*	0.009*	0.006*	0.156	0.293	0.913	0.004*	1.000	0.005*	0.006*
5	0.069	0.000*	0.011*	1.000	1.000	1.000	0.621	1.000	0.022*	0.001*
6	0.004*	0.086	0.351	0.649	1.000	1.000	0.183	1.000	0.945	0.597
7	0.004*	0.275	1.000	1.000	1.000	1.000	0.109	1.000	0.001*	0.500

3.5. Comparison of displacement values upon stiffness versus thickness variation

Comparison of intrusion distribution on teeth, revealed significant statistical difference second molars (S/TU3 7) for modality 2 (Table 3.49) and the first premolar (S/TU3 6) (table 3.50) and both first premolar and molar on the last one (S/TU3 4-6) (table 3.52). Results suggest less effect of stiffness and thickness on intrusion than on stress distribution.

	Modality 1				
	S/TU3 3	S/TU3 4	S/TU3 5	S/TU3 6	S/TU3 7
P-value	0.687	0.857	0.873	0.720	0.905

Table.4.48. Intrusion comparison between stiffness and thickness variation in the first modality

	Modality 2				
	S/TU3 3	S/TU3 4	S/TU3 5	S/TU3 6	S/TU3 7
P-value	0.896	0.721	0.585	0.681	0.037

Table.4.49. Intrusion comparison between stiffness and thickness variation in the second modality

	Modality 3				
	S/TU3 3	S/TU3 4	S/TU3 5	S/TU3 6	S/TU3 7
P-value	0.876	0.014	0.743	0.067	0.205

Table.4.50. Intrusion comparison between stiffness and thickness variation in the third modality

	Modality 4				
	S/TU3 3	S/TU3 4	S/TU3 5	S/TU3 6	S/TU3 7
P-value	0.586	0.876	0.747	0.685	0.923

Table.4.51. Intrusion comparison between stiffness and thickness variation in the fourth modality

	Modality 5				
	S/TU3 3	S/TU3 4	S/TU3 5	S/TU3 6	S/TU3 7
P-value	0.572	0.015	0.384	0.001	0.859

Table.4.52. Intrusion comparison between stiffness and thickness variation in the fifth modality

S/T: Stiffness/thickness
U3 3: Stress 3/ **U3 4:** Stress 4/ **U3 5:** Stress 5/ **U3 6:** Stress 6/ **U3 7:** Stress 7

3.6. Correlations

3.6.1. Between Bone properties and stress

3.6.1.1. Stiffness Variation

3.6.1.1.1. Canine

Except for a high correlation between the buccal aspects of the bone and the stress on the canine in the second model (r=0.915), there were no significant correlations between the stresses at the canine in all modalities and the stiffness components of the corresponding cortical bone areas (S1Pinc- S2Pinc - S3Pinc- S1Binc - S2Binc - S3Binc), (Table 3.53).

Table 3.53. Correlations between stresses and stiffness values of the cortical bone at palatal and buccal incisors and canine areas for the five modalities

		3 Stress M1	3 Stress M2	3 Stress M3	3 Stress M4	3 Stress M5
S1Pinc	Pearson Correlation	.422	-.236	.243	.259	.331
	Sig. (2-tailed)	.224	.485	.498	.469	.351
S2Pinc	Pearson Correlation	.033	.009	-.085	-.052	-.031
	Sig. (2-tailed)	.928	.979	.816	.886	.932
S3Pinc	Pearson Correlation	-.133	.076	-.226	-.188	-.209
	Sig. (2-tailed)	.715	.824	.53	.604	.563
S1Binc	Pearson Correlation	-.273	-.132	-.242	-.314	-.262
	Sig. (2-tailed)	.445	.698	.500	.377	.464
S2Binc	Pearson Correlation	-.190	.903	-.142	-.192	-.160
	Sig. (2-tailed)	.598	.000**	.695	.595	.658
S3Binc	Pearson Correlation	-.361	.915	-.319	-.339	-.317
	Sig. (2-tailed)	.305	.000**	.369	.338	.372

**. Correlation is significant at the 0.01 level (2-tailed).
*. Correlation is significant at the 0.05 level (2-tailed).

3.6.1.1.2. Premolars

On the contrary, high ($-0.68 < r < 0.72$) and significant correlations (p-value <0.05) existed between stress amounts at the first premolar and the second premolar on all surfaces, and

the S3Ppmol in the fourth modality, and a correlation between the premolars and the palatal

aspect of the bone in the third (r=-0.0662)), fourth and fifth (r=0.884) modalities (Table 3.54).

Table 3.54: Correlations between stresses and stiffness values of the cortical bone at palatal and buccal premolar areas in the five intrusion modalities.

		4 Stress M1	5 Stress M1	4 Stress M2	5 Stress M2	4 Stress M3	5 Stress M3	4 Stress M4	5 Stress M4	4 Stress M5	5 Stress M5
S1Ppmol	Pearson Correlation	-.334	-.019	.232	.416	-.561	-.445	-.714	-.678	-.342	-.401
	Sig. (2-tailed)	.345	.958	.493	.204	.092	0.197	0.020*	0.031*	0.333	0.251
S2Ppmol	Pearson Correlation	-.417	-.117	.490	.636	-.587	-.538	-.702	-.617	-.609	-.525
	Sig. (2-tailed)	.231	.747	.126	.035*	.074	.109	.023*	.058	.062	.119
S3Ppmol	Pearson Correlation	-.618	-.261	.386	.560	-.375	-.752	-.913	-.834	-.767	-.744
	Sig. (2-tailed)	.057	.466	.241	.073	.286	.012*	.000**	.003**	.010*	.014*
S1Bpmol	Pearson Correlation	.351	.304	-.586	-.434	.104	.366	.230	.254	.225	.261
	Sig. (2-tailed)	.319	.394	.058	.183	.775	.298	.523	.478	.531	.467
S2Bpmol	Pearson Correlation	.545	.282	-.652	-.662	.331	.625	.704	.680	.588	.594
	Sig. (2-tailed)	.103	.429	.030*	.027*	.350	.053	.023*	.031*	.074	.070
S3Bpmol	Pearson Correlation	.085	-.155	-.477	-.0570	.844	.096	.315	.207	.225	.138
	Sig. (2-tailed)	.816	.669	.138	.067	.002**	.792	.375	.567	.532	.705

**. Correlation is significant at the 0.01 level (2-tailed).
*. Correlation is significant at the 0.05 level (2-tailed).

3.6.1.1.3. Molars

Stress on both molars (6 and 7) highly and negatively correlated with buccal cortical bone

stiffness (SBmol) at this location and it was statistically significant with Pearson correlation

coefficients ranging from -0.728 and -0.912. A similar negative correlation was present between

the second molars of models 3 and 4 and palatal cortical bone stiffness (SPmol) (Table 3.55).

Table 3.55: Correlations between stresses and stiffness values of the cortical bone at palatal and buccal molar areas in the five intrusion modalities.

		6 Stress M1	7 Stress M1	6 Stress M2	7 Stress M2	6 Stress M3	7 Stress M3	6 Stress M4	7 Stress M4	6 Stress M5	7 Stress M5
S1Pmol	Pearson Correlation	.121	-.369	-.501	-.536	.181	-.281	-.251	-.685	.228	-.632
	Sig. (2-tailed)	.740	.294	.117	.090	.616	.431	.484	.029*	.526	.050*
S2Pmol	Pearson Correlation	.092	-.388	-.418	-.488	.136	-.224	-.39	-.754	.233	-.596
	Sig. (2-tailed)	.801	.268	.201	.128	.708	.533	.265	.012*	.517	.069
S3Pmol	Pearson Correlation	-.239	-.653	0-.572	-.653	-.167	-.482	-.586	-.874	-.033	-.730
	Sig. (2-tailed)	.505	.041*	.066	.029*	.646	.158	.075	.001*	.928	.016*
S1Bmol	Pearson Correlation	-.825	-.817	.219	.381	-.639	-.843	-.429	-.489	-.541	-.583
	Sig. (2-tailed)	.003*	.004*	.517	.247	.047*	.002*	.216	.152	.106	.077
S2Bmol	Pearson Correlation	-.485	-.825	.317	.388	-.35	-.696	-.608	-.896	-.235	-.872
	Sig. (2-tailed)	.155	.003*	.342	.239	.322	.025*	.062	.000*	.513	.001*
S3Bmol	Pearson Correlation	-.728	-.912	.352	.450	-.606	-.834	-.778	-.883	-.496	-.894
	Sig. (2-tailed)	.017*	.000*	.289	.165	.063	.003*	.008*	.001*	.145	.000*

**. Correlation is significant at the 0.01 level (2-tailed).
*. Correlation is significant at the 0.05 level (2-tailed).

3.6.1.2. Thickness Variation

3.6.1.2.1. Canine

Except for the correlation of stress on the canine for the first (3 Stress M1) and the fifth (3 Stress M5) modalities with the buccal aspect of the cortical bone (TBinc), there was a significant positive correlation between all variables of bone properties (TPinc, TBinc) and stress values on the canines (3 Stress M1, M3, M4, and M5) with the highest correlation between "3 Stress M3" and TPinc (r=0.810) (Table 3.56).

93

Table 3.56. Correlations between stresses and thickness values of the cortical bone at palatal and buccal incisors and canine areas for the five modalities

		3 Stress M1	3 Stress M2	3 Stress M3	3 Stress M4	3 Stress M5
TPinc	Pearson Correlation	.703	-.196	.810	.621	.637
	Sig. (2-tailed)	.011*	.541	.001*	.031*	.026*
TBinc	Pearson Correlation	.261	-.479	.587	.578	.554
	Sig. (2-tailed)	.412	.115	.045*	.049*	.062

**. Correlation is significant at the 0.01 level (2-tailed).
*. Correlation is significant at the 0.05 level (2-tailed).

3.6.1.2.2. Premolars

The only significant correlations were noted between the stress on the first premolar in model 3 (4 Stress M3) and the palatal aspect of the cortical bone (TPpmol) (r=0.872), and between the second premolar of the last modality (5 Stress M4) and the palatal aspect of the cortical bone (r=0.689) (Table 3.57).

Table 3.57. Correlations between stresses and thickness values of the cortical bone at palatal and buccal premolars areas for the five intrusive modalities.

		4 Stress M1	5 Stress M1	4 Stress M2	5 Stress M2	4 Stress M3	5 Stress M3	4 Stress M4	5 Stress M4	4 Stress M5	5 Stress M5
	Pearson Correlation	.097	-.016	-.397	-.517	.494	.455	.872	.564	.224	.689
TPpmol	Sig. (2-tailed)	.763	.961	.201	.085	.103	.137	.000*	.056	.484	.013*
	Pearson Correlation	-.130	-.066	-.424	-.544	.494	.667	0.968	.606	.247	0.928
TPBpmol	Sig. (2-tailed)	.754	.563	.193	.084	.103	.051	.795	.059	.500	.013

**. Correlation is significant at the 0.01 level (2-tailed).
*. Correlation is significant at the 0.05 level (2-tailed).

Except for the stress on molars in modality 5 and the stress acting on the buccal aspect (TBmol) of the first modality, all first and second molars stresses (6 Stress, 7 Stress) correlated significantly and positively with the cortical bone properties on the palatal and buccal sides (TPmol, TBmol) with the highest value (r=0.933) between stress on the second molar of the first modality (7 Stress M1) and the palatal cortex (TPmol) (Table 3.58).

Table 3.58. Correlations between stresses and thickness values of the cortical bone at palatal and buccal molars areas for the five intrusive modalities.

		6 Stress M1	7 Stress M1	6 Stress M2	7 Stress M2	6 Stress M3	7 Stress M3	6 Stress M4	7 Stress M4	6 Stress M5	7 Stress M5
TPmol	Pearson Correlation	.659	.933	-.448	-.459	.701	.727	.863	.672	.525	.567
	Sig. (2-tailed)	.020*	.000*	.144	.133	.011*	.007*	.000*	.017*	.080	.054
TBmol	Pearson Correlation	.538	.454	-.484	-.701	.649	.709	.705	.845	.390	.444
	Sig. (2-tailed)	.071	.138	.111	.011*	.022*	.010*	.010*	.001*	.211	.149

**. Correlation is significant at the 0.01 level (2-tailed).
*. Correlation is significant at the 0.05 level (2-tailed).

3.6.2. Between Bone properties and displacement

3.6.2.1. Stiffness Variation

3.6.2.1.1. Canine

The Pearson correlation product applied on bone properties and displacement divided into pure intrusion (U3) and secondary effects (U1+U2), displayed no interdependence at the level of the canines in all modalities (Table 3.59).

Table 3.59. Correlations between displacement and stiffness values of the cortical bone at palatal and buccal canine areas for the five intrusive modalities.

		3 U1+U2 M1	3 U3 M1	3 U1+U2 M2	3 U3 M2	3U1+U2 M3	3 U3 M3	3 U1+U2 M3	3 U3 M3	3 U1+U2 M4	3 U3 M4
	Pearson Correlation	.398	.293	-.228	-.050	.497	.227	-.313	.245	-.158	.289
S1Pinc	Sig. (2-tailed)	.255	.411	.499	.884	.144	.529	.379	.494	.662	.418
	Pearson Correlation	.107	.089	.070	.002	.105	-.117	-.103	-.087	.268	-.097
S2Pinc	Sig. (2-tailed)	.769	.808	.838	.996	.774	.748	.778	.811	.453	.789
	Pearson Correlation	.023	.002	.119	-.012	-.019	-.246	-.067	-.200	.371	-.243
S3Pinc	Sig. (2-tailed)	.949	.996	.727	.972	.959	.494	.855	.579	.291	.498
	Pearson Correlation	-.118	-.182	.397	-.299	-.258	-.285	.626	-.404	.508	-.346
S1Binc	Sig. (2-tailed)	.746	.616	.227	.373	.471	.425	.053	.247	.133	.327
	Pearson Correlation	-.162	.011	.316	-.193	-.244	-.184	.511	-.282	.428	-.242
S2Binc	Sig. (2-tailed)	.654	.976	.345	.570	.498	.611	.131	.430	.217	.500
	Pearson Correlation	-.245	-.068	.525	-.314	-.375	-.367	.517	-.428	.562	-.409
S3Binc	Sig. (2-tailed)	.495	.853	.097	.347	.286	.297	.126	.218	.091	.241

3.6.2.1.2. Premolars

For the first modality, initial displacement including secondary effects (U1+U2) correlated negatively with the buccal aspect of the cortical bone (S2Bpmol, S3Bmol) for the first premolar (r=-0.8), whereas for the second premolar (5 U1+U2), correlated positively with the palatal aspect (S1Ppmol, S3Ppmol) (r=0.702 and 0.644) and negatively with the buccal aspect (S1Bpmol) in both intrusion (r=-0.720) and secondary effects (r=0.831).

For the rest of the modalities (M3, M4, and M5), high correlations were concentrated between the palatal aspect of the cortical bone (S3Ppmol) and all initial displacements at the level of the first and second premolars with the highest on the first premolar (r=-0.912) (Table 3.60).

3.6.2.1.3. Molars

The only correlated variables in the first modality were found between the secondary effects of the second molar (7 U1+U2) and the palatal cortical bone (S1, S2, S3Pmol) highest on S2Pmol (r=0.912). Secondary effects on the first molar in the fourth and fifth modalities (M3, M4), highly and negatively correlated with the palatal aspect of the cortical bone (r=-0.948), (Table 3.61)

Table.4.60. Correlations between displacement and stiffness values of the cortical bone at palatal and buccal premolars areas for the five intrusive modalities

		4 U1+U2 M1	4 U3 M1	5 U1+U2 M1	5 U3 M1	4 U1+U2 M2	4 U3 M2	5 U1+U2 M2	5 U3 M2	4 U1+U2 M3	4 U3 M3	5 U1+U2 M3	5 U3 M3	4 U1+U2 M4	4 U3 M4	5 U1+U2 M4	5 U3 M4	4 U1+U2 M5	4 U3 M5	5 U1+U2 M5	5 U3 M5
S1Pmol	Pearson Correlation	.276	-.204	.702	-.023	-.329	-.198	-.177	-.034	.248	-.654	.778	-.486	.258	-.673	.439	-.613	.337	-.443	.403	-.349
	Sig. (2-tailed)	.440	.571	.024*	.949	.323	.559	.603	.921	.489	.040*	.008**	.155	.472	.033*	.205	.059	.340	.200	.248	.323
S2Pmol	Pearson Correlation	.569	-.277	.538	-.107	-.391	-.036	-.253	.166	.114	-.714	.583	-.571	.582	-.701	.662	-.615	.582	-.584	.619	-.491
	Sig. (2-tailed)	.086	.438	.108	.768	.234	.917	.454	.626	.755	.020*	.077	.084	.078	.024*	.037*	.059	.077	.076	.056	.150
S3Pmol	Pearson Correlation	.547	-.465	.644	-.256	-.351	-.036	-.299	.163	.132	-.901	.689	-.763	.682	-.912	.819	-.849	.745	-.795	.799	-.706
	Sig. (2-tailed)	.102	.176	.044*	.475	.290	.915	.372	.632	.717	.000**	.028*	.010*	.030*	.000**	.004**	.002**	.013*	.006**	.006**	.022*
S1Bmol	Pearson Correlation	-.404	-.571	-.831	-.720	.349	-.004	-.172	-.091	-.377	.016	-.773	-.250	-.209	.116	-.298	-.037	.136	-.151	.071	-.291
	Sig. (2-tailed)	.247	.084	.003**	.019*	.293	.991	.612	.790	.283	.965	.009**	.486	.563	.749	.402	.919	.707	.678	.846	.415
S2Bmol	Pearson Correlation	-.803	-.172	-.487	-.323	.235	-.045	.117	-.205	-.138	.156	-.372	.000	-.740	.261	-.703	.090	-.353	.181	-.392	.064
	Sig. (2-tailed)	.005**	.634	.153	.363	.487	.896	.731	.545	.704	.667	.290	.999	.014*	.466	.023*	.804	.316	.617	.263	.860
S3Bmol	Pearson Correlation	-.843	-.488	-.482	-.609	-.186	-.496	.546	-.633	-.225	-.102	-.339	-.290	-.539	.019	-.473	-.173	-.104	-.095	-.127	-.222
	Sig. (2-tailed)	.002**	.152	.158	.062	.585	.121	.082	.036*	.532	.779	.338	.416	.108	.958	.168	.632	.774	.794	.726	.538

Table.4.61. Correlations between displacement and stiffness values of the cortical bone at palatal and buccal molars areas for the five intrusive modalities

		6 U1+U2 M1	6 U3 M1	7 U1+U2 M1	7 U3 M1	6 U1+U2 M2	6 U3 M2	7 U1+U2 M2	7 U3 M2	6 U1+U2 M3	6 U3 M3	7 U1+U2 M3	7 U3 M3	6 U1+U2 M4	6 U3 M4	7 U1+U2 M4	7 U3 M4	6 U1+U2 M5	6 U3 M5	7 U1+U2 M5	7 U3 M5
S1Pmol	Pearson Correlation	-.262	.069	.865	-.252	.032	-.320	.107	-.447	-.445	.484	-.413	-.264	-.868	-.064	-.964	-.657	-.785	.194	-.957	-.485
	Sig. (2-tailed)	.465	.851	.001**	.483	.925	.338	.755	.168	.198	.156	.235	.461	.001**	.860	.000**	.039*	.007**	.590	.000**	.156
S2Pmol	Pearson Correlation	-.335	.084	.912	-.239	.174	-.273	.074	-.412	-.432	.771	-.224	-.190	-.948	-.118	-.719	-.735	-.847	.240	-.824	-.480
	Sig. (2-tailed)	.344	.817	.000**	.507	.609	.416	.829	.208	.212	.009**	.533	.599	.000**	.746	.019*	.015*	.002**	.504	.003**	.160
S3Pmol	Pearson Correlation	-.030	-.246	.828	-.528	-.073	-.291	.120	-.536	-.164	.502	.133	-.477	-.819	-.388	-.457	-.881	-.615	-.054	-.625	-.699
	Sig. (2-tailed)	.935	.494	.003**	.116	.831	.386	.725	.089	.651	.139	.715	.164	.004**	.268	.184	.001**	.059	.881	.053	.024*
S1Binc	Pearson Correlation	.318	-.059	-.629	.187	-.757	-.395	.328	-.612	.404	-.532	.150	.173	.688	.104	.429	.570	.640	-.145	.564	.392
	Sig. (2-tailed)	.370	.870	.051	.606	.007**	.229	.325	.045*	.247	.113	.680	.633	.028*	.776	.215	.085	.046*	.689	.090	.263
S2Binc	Pearson Correlation	.342	-.113	-.493	.097	-.006	-.107	.691	-.474	.354	-.562	.133	.079	.586	.091	.330	.474	.548	-.141	.449	.304
	Sig. (2-tailed)	.333	.756	.147	.790	.986	.755	.018*	.141	.315	.091	.715	.828	.075	.803	.352	.166	.101	.698	.193	.394
S3Binc	Pearson Correlation	.408	-.224	-.482	-.004	-.174	-.051	.528	-.637	.414	-.580	.235	-.043	.587	-.130	.414	.346	.632	-.327	.473	.162
	Sig. (2-tailed)	.242	.533	.158	.991	.609	.881	.095	.035*	.234	.079	.513	.907	.074	.720	.234	.328	.060*	.357	.167	.654

97

3.6.2.2.   Thickness Variation

3.6.2.2.1. Canine

The initial displacement correlated with the palatal aspect of cortical bone (TPinc) in

modality 1 (r=0.813) and modality 2 (r=616), (Table 3.62).

Table 3.62. Correlations between displacement and thickness values of the cortical bone at palatal and buccal canine areas for the five intrusive modalities.

		3 U1+U2 M1	3 U3 M1	3 U1+U2 M2	3 U3 M2	3 U1+U2 M3	3 U3 M3	3 U1+U2 M4	3 U3 M4	3 U1+U2 M5	3 U3 M5
TPinc	Pearson Correlation	.267	.813	.065	.346	.467	.616	.328	-.117	-.497	.272
	Sig. (2-tailed)	.401	.001**	.841	.271	.126	.033**	.299	.717	.100	.393
TBinc	Pearson Correlation	.062	.211	.033	-.095	-.140	-.032	.307	.201	-.440	.252
	Sig. (2-tailed)	.849	.510	.918	.768	.664	.921	.333	.530	.152	.429

**. Correlation is significant at the 0.01 level (2-tailed).
*. Correlation is significant at the 0.05 level (2-tailed).

3.6.2.2.2. Premolars

In the first modality, there were strong correlations between the secondary effects on load

(U1+U2) and both sides of the cortices palatally (TPpmol) and buccally (TBpmol), with r=-0.736

and r=-0.835, respectively on the first premolars. Intrusion (U3) correlated positively with the

cortical bone with r=0.659 for TPpmol and r=0.633 for TBpmol, (Table 3.63).

3.6.2.2.3. Molars

No significant correlations were found between the displacement at the molars in all

modalities and the thickness components of the corresponding cortical bone areas (TPmol,

TBmol), (Table 3.64).

Table.4.63. Correlations between displacement and thickness values of the cortical bone at palatal and buccal premolars areas for the five intrusive modalities

		4 U1+U2 M1	4 U3 M1	5 U1+U2 M1	5 U3 M1	4 U1+U2 M2	4 U3 M2	5 U1+U2 M2	5 U3 M2	4 U1+U2 M3	4 U3 M3	5 U1+U2 M3	5 U3 M3	4 U1+U2 M4	4 U3 M4	5 U1+U2 M4	5 U3 M4	4 U1+U2 M5	4 U3 M5	5 U1+U2 M5	5 U3 M5
TPpmol	Pearson Correlation	-.736	.659	-.356	.152	.218	.251	-.105	-.362	-.080	.154	.194	.009	.341	-.118	-.162	.337	-.264	.281	.054	.528
	Sig. (2-tailed)	.006**	.020*	.256	.637	.496	.432	.745	.247	.806	.634	.545	.978	.278	.715	.616	.285	.407	.376	.868	.078
TBpmol	Pearson Correlation	-.835	.633	-.338	.211	.192	.234	-.088	-.376	.110	.049	.222	.081	.198	-.069	-.134	.320	-.236	.236	.012	.453
	Sig. (2-tailed)	.001**	.036*	.309	.534	.572	.488	.796	.254	.748	.885	.512	.813	.559	.840	.694	.338	.484	.486	.971	.162

Table.4.64. Correlations between displacement and thickness values of the cortical bone at palatal and buccal molars areas for the five intrusive modalities

		6 U1+U2 M1	6 U3 M1	7 U1+U2 M1	7 U3 M1	6 U1+U2 M2	6 U3 M2	7 U1+U2 M2	7 U3 M2	6 U1+U2 M3	6 U3 M3	7 U1+U2 M3	7 U3 M3	6 U1+U2 M4	6 U3 M4	7 U1+U2 M4	7 U3 M4
TPmol	Pearson Correlation	-.039	.092	-.118	.373	.089	.165	-.252	.301	-.420	.020	-.078	.156	-.057	.331	-.517	.160
	Sig. (2-tailed)	.905	.776	.714	.233	.783	.609	.429	.342	.173	.951	.810	.628	.860	.294	.085	.620
TBmol	Pearson Correlation	-.556	.367	-.235	-.242	.480	.233	-.381	-.012	-.448	.283	.054	.401	.189	.192	-.466	.083
	Sig. (2-tailed)	.060	.241	.461	.449	.115	.465	.221	.971	.144	.373	.866	.196	.556	.549	.127	.798

		6 U1+U2 M4	6 U3 M4	7 U1+U2 M4	7 U3 M4
TPmol	Pearson Correlation	-.179	.378	-.324	.190
	Sig. (2-tailed)	.578	.226	.304	.555
TBmol	Pearson Correlation	.054	.322	-.472	.090
	Sig. (2-tailed)	.868	.307	.121	.782

3.6.3. Association between stress and displacement

3.6.3.1. Stiffness Variation

3.6.3.1.1. Canine

Except for the correlation of the added components of initial displacement including bucco-lingual (U1) and antero-posterior (U2) displacement and the stress on the canines of the first, the second and the third modalities (Stress 3 M1, M2, M3), all aspects of displacement correlated positively for the intrusive values with higher values for the Pearson correlation in model 4 (r=0.998), and for the secondary effects (r=-0.923) in model 5, (Table 3.65).

Table 3.65. Correlations between displacement and stress values of the cortical bone at palatal and buccal canines' areas for the five intrusive modalities.

		3 U1+U2	3 U3
Stress 3 M1	Pearson Correlation	.443	.726
	Sig. (2-tailed)	.200	.017*
Stress 3 M2	Pearson Correlation	-.177	.767
	Sig. (2-tailed)	.602	.006**
Stress 3 M3	Pearson Correlation	.493	.998
	Sig. (2-tailed)	.148	.000**
Stress 3 M4	Pearson Correlation	-.763	.994
	Sig. (2-tailed)	.010*	.000**
Stress 3 M5	Pearson Correlation	-.923	.994
	Sig. (2-tailed)	.000**	.000**

**. Correlation is significant at the 0.01 level (2-tailed).
*. Correlation is significant at the 0.05 level (2-tailed).

3.6.3.1.2. Premolars

In both first (4) and second (5) premolars, the undesirable effects of displacement (U1+U2), correlated negatively with their corresponding stresses in the third and the fourth modalities (r=-0.991 and r=-0.938 respectively). On the other hand, the correlation was positive and significant between intrusion in both premolars and their equivalent stresses, such as between intrusion of

the second premolar in the first modality (5 U3) and the stress (Stress 5 M1) with the highest

value (r=0.999), (Table 3.66).

Table 3.66. Correlations between displacement and stress values of the cortical bone at palatal and buccal premolars areas for the five intrusive modalities.

		4 U1+U2	4 U3			5 U1+U2	5 U3
Stress 4 M1	Pearson Correlation	-.038	.976	Stress 5 M1	Pearson Correlation	.474	.999
	Sig. (2-tailed)	.917	.000**		Sig. (2-tailed)	.167	.000**
Stress 4 M2	Pearson Correlation	.273	.528	Stress 5 M2	Pearson Correlation	-.246	.618
	Sig. (2-tailed)	.417	.095		Sig. (2-tailed)	.466	.043*
Stress 4 M3	Pearson Correlation	-.056	.666	Stress 5 M3	Pearson Correlation	-.216	.994
	Sig. (2-tailed)	.877	.029*		Sig. (2-tailed)	.549	.000**
Stress 4 M4	Pearson Correlation	-.662	.996	Stress 5 M4	Pearson Correlation	-.677	.993
	Sig. (2-tailed)	.037*	.000**		Sig. (2-tailed)	.031*	.000**
Stress 4 M5	Pearson Correlation	-.991	.960	Stress 5 M5	Pearson Correlation	-.938	.997
	Sig. (2-tailed)	.000**	.000**		Sig. (2-tailed)	.000**	.000**

**. Correlation is significant at the 0.01 level (2-tailed).
*. Correlation is significant at the 0.05 level (2-tailed).

3.6.3.1.3. Molars

The stress of the first molar (6) correlated positively with the displacement in the antero-posterior and the bucco-lingual directions (U1+U2) in the first modality (r=-0.917). As for the intrusion (U3) high positive correlation was found between the two variables, especially in the first modality (r=0.987).

The same pattern of correlations was found for the second molar's intrusion (7) (0.967 <r<0.997). The only correlation with the secondary effects was in the fourth modality (r=0.676), (Table 3.67).

Table 3.67. Correlations between displacement and stress values of the cortical bone at palatal and buccal molars areas for the five intrusive modalities.

		6 U1+U2	6 U3
Stress 6 M1	Pearson Correlation	-.917	.987
	Sig. (2-tailed)	.000**	.000**
Stress 6 M2	Pearson Correlation	.484	.436
	Sig. (2-tailed)	.131	.180
Stress 6 M3	Pearson Correlation	-.400	.812
	Sig. (2-tailed)	.252	.004**
Stress 6 M4	Pearson Correlation	.298	.942
	Sig. (2-tailed)	.402	.000**
Stress 6 M5	Pearson Correlation	-.626	.981
	Sig. (2-tailed)	.053	.000**

		7 U1+U2	7 U3
Stress 7 M1	Pearson Correlation	-.432	.985
	Sig. (2-tailed)	.212	.000**
Stress 6 M2	Pearson Correlation	-.187	.848
	Sig. (2-tailed)	.582	.001**
Stress 7 M3	Pearson Correlation	-.253	.957
	Sig. (2-tailed)	.481	.000**
Stress 7 M4	Pearson Correlation	.598	.997
	Sig. (2-tailed)	.068	.000**
Stress 7 M5	Pearson Correlation	.676	.971
	Sig. (2-tailed)	.032*	.000**

**. Correlation is significant at the 0.01 level (2-tailed).
*. Correlation is significant at the 0.05 level (2-tailed).

3.6.3.2. Thickness Variation

3.6.3.2.1. Canine

The only statistically significant correlation was found in the first intrusion modality between stress amounts at the level of the canine (3 Stress M1) and the initial intrusive displacement (3 U3) (r=0.814), (Table 3.68).

Table 3.68. Correlations between displacement and stress values of the cortical bone at palatal and buccal canines' areas for the five intrusive modalities.

		3 U1+U2	3 U3
3 Stress M1	Pearson Correlation	-.205	.814
	Sig. (2-tailed)	.524	.001**
3 Stress M2	Pearson Correlation	.029	.542
	Sig. (2-tailed)	.930	.069
3 Stress M3	Pearson Correlation	.360	.360
	Sig. (2-tailed)	.250	.251
3 Stress M4	Pearson Correlation	-.185	.201
	Sig. (2-tailed)	.564	.531
3 Stress M5	Pearson Correlation	-.557	.383
	Sig. (2-tailed)	.060	.219

**. Correlation is significant at the 0.01 level (2-tailed).
*. Correlation is significant at the 0.05 level (2-tailed).

3.6.3.2.2. Premolars

In modalities 2 and 5 and contrary to the rest of the modalities, a positive correlation was observed between the stress on the first premolar only (4) and the displacement on the x (U1) and y (U2) axes (r=0.734). The correlation was negative with the intrusion (U3) (r=-0.690), (Table 3.69).

The second model (M2), showed a positive correlation between stress at the level of the second premolar (5 Stress M2) and initial displacement in its two components (r=0.976).

Table 3.69. Correlations between displacement and stress values of the cortical bone at palatal and buccal premolars areas for the five intrusive modalities.

		4 U1+U2	4 U3			5 U1+U2	5 U3
4 Stress M1	**Pearson Correlation**	.290	.085	**5 Stress M1**	**Pearson Correlation**	.389	.134
	Sig. (2-tailed)	.361	.794		**Sig. (2-tailed)**	.211	.678
4 Stress M2	**Pearson Correlation**	.725	.507	**5 Stress M2**	**Pearson Correlation**	.665	.976
	Sig. (2-tailed)	.008**	.092		**Sig. (2-tailed)**	.018*	.000**
4 Stress M3	**Pearson Correlation**	.183	.067	**5 Stress M3**	**Pearson Correlation**	-.034	-.338
	Sig. (2-tailed)	.570	.837		**Sig. (2-tailed)**	.917	.283
4 Stress M4	**Pearson Correlation**	.160	-.297	**5 Stress M4**	**Pearson Correlation**	.286	-.407
	Sig. (2-tailed)	.619	.349		**Sig. (2-tailed)**	.368	.189
4 Stress M5	**Pearson Correlation**	.734**	-.690*	**5 Stress M5**	**Pearson Correlation**	-.058	.350
	Sig. (2-tailed)	.007	.013		**Sig. (2-tailed)**	.859	.264

**. Correlation is significant at the 0.01 level (2-tailed).
*. Correlation is significant at the 0.05 level (2-tailed).

3.6.3.2.3. Molars

Opposite to the stiffness-modified models, no significant correlations were found between the displacement at the molars in all modalities and the corresponding stresses, except for the second modality, where the stress on the molars (6 and 7 Stress M2) correlated with the

secondary effects (U1+U2) negatively for the first molar (r=-0.617) and positively with the

second molar(r=0.723) (Table 3.70).

Table 3.70. Correlations between displacement and stress values of the cortical bone at palatal and buccal molars areas for the five intrusive modalities.

		6 U1+U2 M1	6 U3 M1
6 Stress M1	Pearson Correlation	-.145	.158
	Sig. (2-tailed)	.653	.624
6 Stress M2	Pearson Correlation	-.617	.179
	Sig. (2-tailed)	.032*	.579
6 Stress M3	Pearson Correlation	-.250	.184
	Sig. (2-tailed)	.433	.568
6 Stress M4	Pearson Correlation	.097	.378
	Sig. (2-tailed)	.765	.225
6 Stress M5	Pearson Correlation	.162	.239
	Sig. (2-tailed)	.616	.454

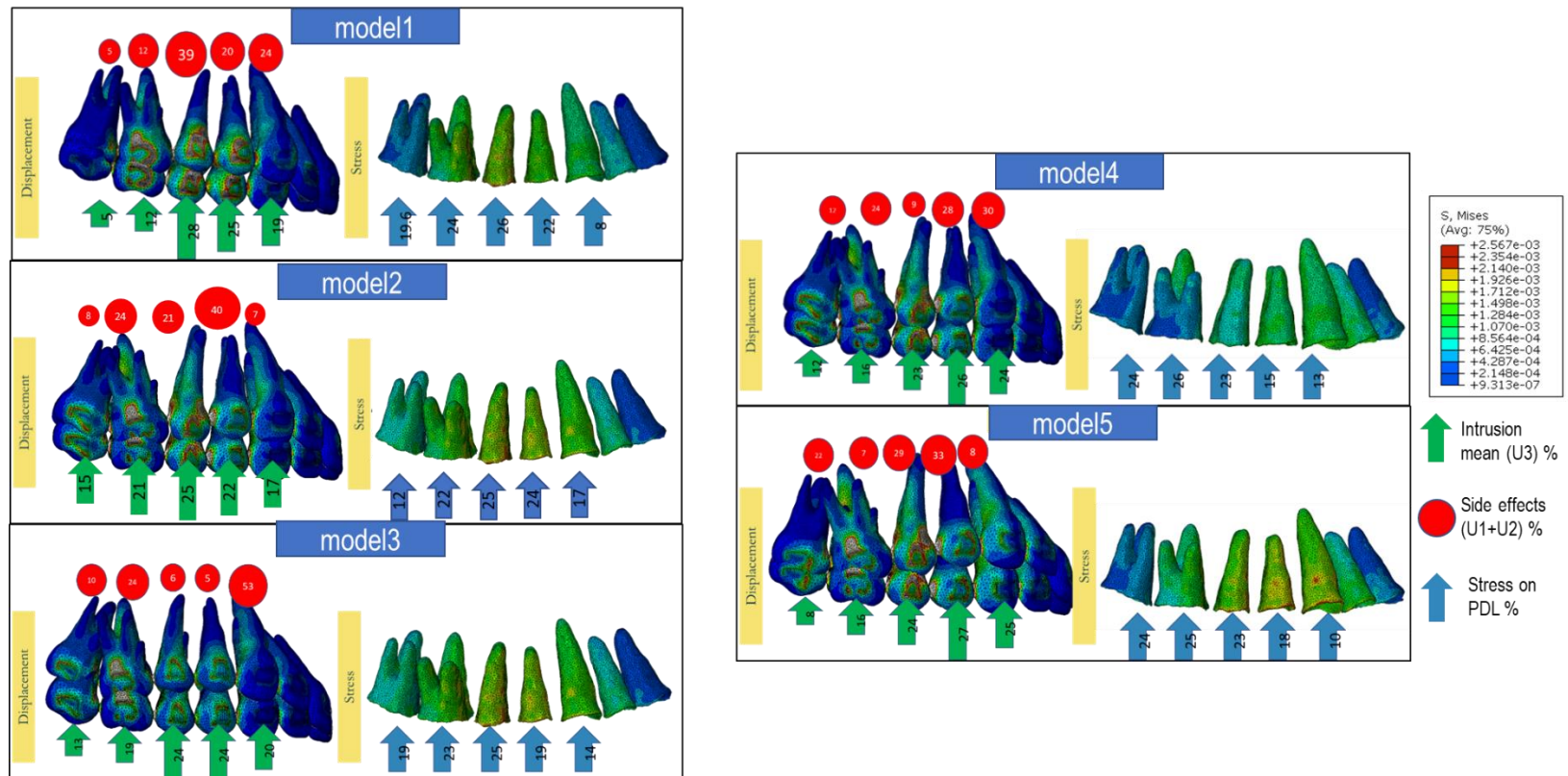|		7 U1+U2 M1	7 U3 M1
7 Stress M1	Pearson Correlation	-.132	.333
	Sig. (2-tailed)	.682	.291
6 Stress M2	Pearson Correlation	.723	-.162
	Sig. (2-tailed)	.008**	.615
7 Stress M3	Pearson Correlation	-.286	.376
	Sig. (2-tailed)	.367	.228
7 Stress M4	Pearson Correlation	-.526	.204
	Sig. (2-tailed)	.079	.525
7 Stress M5	Pearson Correlation	.196	-.198
	Sig. (2-tailed)	.541	.536

Figure.3.11. PDL Von mises stress distribution in the five intrusion modalities. Magnified displacements in the five modalities. Note: the proximity of results in stress between the first two modalities and between the last two modalities, stress is decreased on the extremity teeth (3 and 7) and more concentrated toward the premolars (4-5). The second modality displayed higher initial intrusion on the second molar with relatively reduced stress and secondary effects on that tooth. The last two modalities displayed higher intrusion values with different secondary effects.

CHAPTER 4

DISCUSSION

4.1. Study components

The orthodontic intrusion of posterior teeth is difficult because of the resistance to movement and anchorage requirements, TADs provide anchorage with minimal side effects. Accounting for bone variation in stiffness and thickness, this finite element study allowed the quantification of the primary intrusion and secondary displacement in five different maxillary posterior intrusion setups adopted from clinical situations. Several components of this study represent important contributions described in this section.

4.1.1. Model accuracy

Finite element analysis replicates accurately and predictably the clinical features and conditions (Hohmann et al., 2011) and has been utilized because any discrete anatomical approach is very invasive.

a. Although the CBCT provides less radiation than and is more commonly used in dental practice, our initial model was generated from a CT scan that captures more limited thickness slices than CBCT. Accordingly, for the purpose of this research, the used CT scan provided better contrast and resolution than studies relying on CBCT images.

The difference was best illustrated in a study by Loubele et al. (2007) who compared jaw dimensions and bone quality between images from a CBCT and multi-slice spiral CT scan (MSCT) (25 human mandibles). Apart from underrating the bone widths,

CBCT (on average 0.23 mm narrower) and MSCT (on average 0.49 mm narrower), the measurements were consistent. As for subjective image quality, the CBCT was superior in defining the lamina dura and PDL, but the MSCT provided improved visualization of the cortical bone and gingiva. These findings were confirmed by Scarfe et al. (2012) who concluded that MSCT offers better contrast (Fig. 2.21), implying more distinctions between different tissue types (i.e. bone, teeth, and soft tissue).
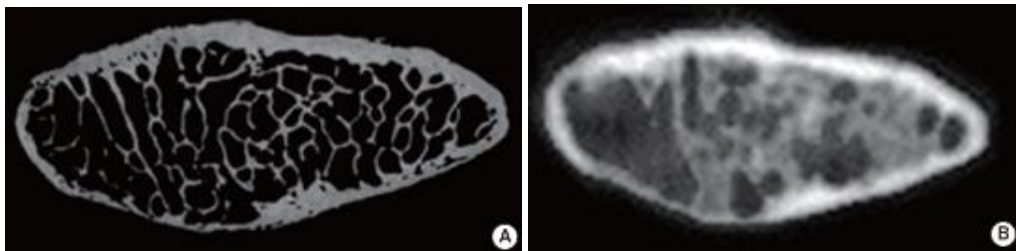
Fig.4.1 A. Micro-computed tomography (CT) image (27×27×27 µm3 voxel size); **B.** cone beam CT image (200×200×200 µm3 voxel size) of the same human condyle (D.-G. Kim, 2014).
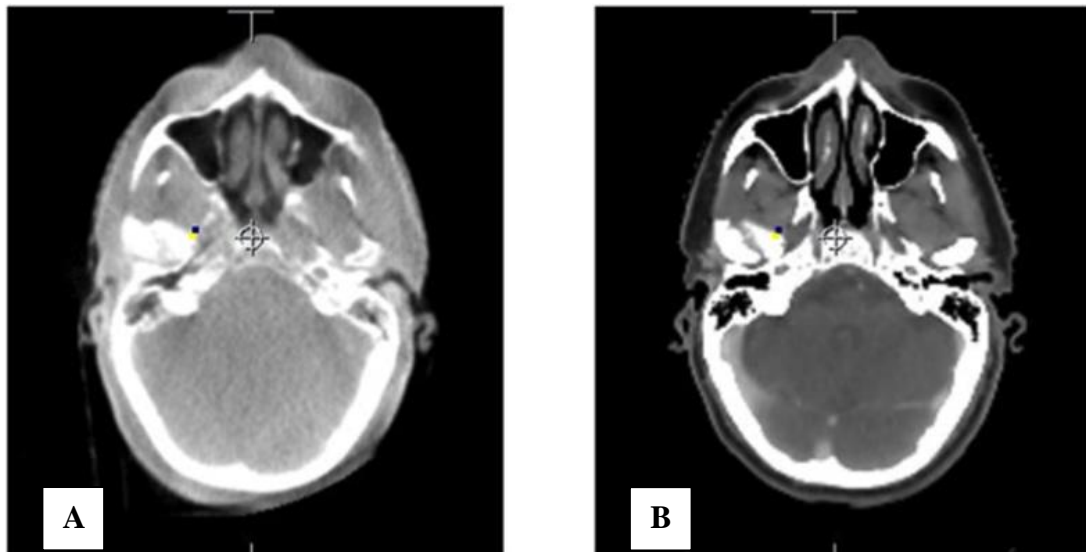

Fig.4.2. A. Cone beam CT vs. **B.** fan beam CT (right) of head and neck IGRT in axial and sagittal orientation (Lechuga et. al., 2016)

b.   In addition to the initial acquisition of the radiograph, the number of elements and nodes is a major parameter affecting the precision of the FEA study. We adopted a model with of 170798 nodes and 854698 linear tetrahedral elements including the gadgets added (brackets, Mini-implants, and archwire), providing for more accurate analysis.

c.   The construction of all the orthodontic items to precisely simulate the clinical situation, notably the brackets, the archwire and, the mini-implants also facilitated the selection of reproducible landmarks to achieve similar force simulation in all designed models for thickness and stiffness variation and acted as reference points for the initiation of movement and specificity of results.

d.   Previous FE studies in which only simplified segmented elements of anatomy were modeled, limiting the investigation to a narrowed field with theoretical outcomes that may not find clinical applications (Suggi et al. 2018, Yan et al., 2017, Saga et al., 2016, etc.). Some authors constructed the model based on a dentoform and not on radiographic images, thus displaying many structural shortcomings (Sung et al., 2015). In contrast, more elaborated model mirrored the adequate material properties and the actual components of the maxilla present in any clinical situation (alveolar bone fractioned at every dental-specific region [incisors, canines, premolars, and molars], compact bone, PDL, gingiva, teeth, etc.).

e.   The orthotropic behavior of bone was properly considered before model loading according to the theory of Schwartz-Dabney and Dechow (2003) who proved anisotropy of bone material along with an orthotropic behavior and defined the interdependence between material properties and direction in the 3 perpendicular directions X, Y, and Z. Applying regional variations reduces errors when measuring stress and strain as postulated by Cowin

et al. (1990) who showed that local anisotropy in skeletal material assets can have dire impacts on the correlation between stress and strain (Cowin and Hart, 1990). This setting is of major importance when running bone-dependent FEA studies especially in tooth movement which is considered a periodontally driven mechanism.

4.1.2. Individual variation

Hitherto, the latest in FE studies were used in situations where engineering settings such as stresses, energy storage, and displacement were often explored through a simplified model reflecting a fractioned clinical setup. However, in the medical and dental fields, individual variation induces diverse results for a similar clinical situation, hence the need to study greater samples to determine central tendencies and outliers. Variables significantly affecting clinical conditions and outcome include tissue thickness, density, stiffness, and other properties inherent to every component of a structure.

In the clinical setups that we investigated, included bone-related materials to examine the possible effect of bone properties on the loading force. Because of individual variations in bone quantity and stiffness, it was imperative to account for patient-specific responses to determine a central tendency of response, along with possible outliers outside this normal response.

Accordingly, instead of changing mechanical loads as in most previous FE, we introduced patient-related variations in the anatomical model. The associated statistical explorations allowed us to test hypotheses and determine variances of outcome measures.

Given the difficulty of computing differences in material properties in living persons the closest possibility was relying on data from human cadavers.

One way for modelling from radiographs of different patients, but such approach would also include other variables related to the reproducibility of the loading protocol, and the anatomical variation of teeth. Our method permitted the comparison between modalities within the same environment but differing in bone properties.

By integrating a valid connection between the simulated FE models and authentic clinical situations and statistically empowered conclusions related to new aims.

4.2. Comparison with FEA intrusion studies

Finite element analysis employed in orthodontic intrusion was most frequently used in movements of isolated over-erupted or extruded teeth (Dawer et. al., 2016), and not a complete section of teeth, specifically posterior intrusion of buccal teeth clinically applied to close an anterior open bite. Other studies had a complete model but did not to cover the details of developing the used model. The foremost explanations were the simpler analysis of the outcomes and avoiding complicating the model with interactions between the teeth.

Biomechanics is crucial in orthodontic treatments since stress fields occur in the supporting tissues when a force is applied. Finite element analysis can be used to simulate different orthodontic treatment approaches as an effective and non-invasive method, especially when more than one modality is tested, as in this study.

The intrusion of molars and premolars is a problematic movement with an indeterminate force system, in which moments and forces cannot be easily evaluated and assessed, thus the suitability for assessment through FEA. The studies by Uysal et. al. (2019), and Çifter et. al. (2011) are used for comparison with our results because they are the only two available that targeted maxillary segment intrusion against a miniscrew.

Our study differed from these investigations in many facets including the assessed intrusion modalities, aims, model construction and set up, data collection, and subsequently, findings observed. The procedural disparities and resemblances are summarized in this section, and outcomes contrasted when relevant. To this end, the intrusion modalities in those investigations are detailed for comparative purposes with our study.

4.2.1. Aims and intrusion modalities

1- Uysal et al. (2019) designed an acrylic appliance on the maxillary posterior teeth including premolars and molars, connected with two palatal arches. A round stainless steel archwire (0.9 mm) was used and intrusion was set along the axis of the first molar. The anchorage unit contained mini-plates, mounted on the zygomatic buttress area between the first and the second maxillary molar roots and three mini-screws to fix the plates according to setups:

    1- Intrusive force from the anchorage unit to the acrylic appliance without corticotomies.

2- Intrusion assisted by buccal subapical corticotomy.

3- Intrusion with buccal and palatal subapical corticotomies. The incisions were limited to the cortical bone and did not involve the cancellous bone.

Uysal et. al. (2019) aimed to assess the effect of corticotomy-assisted posterior maxillary intrusion anchorage by using finite element stress analysis. Von Mises stress distribution along the cortical and cancellous bone surfaces and dental structures were evaluated.
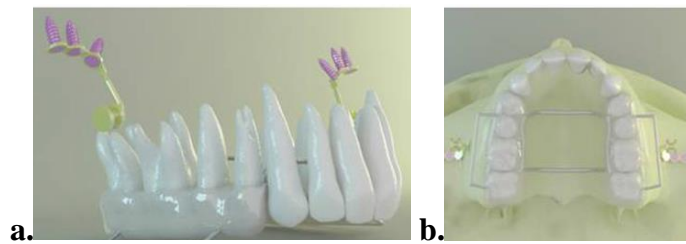

Fig.4.3. a. View of the acrylic appliance and the anchorage unit. **b.** Occlusal view of the appliance. (Uysal et al., 2019)

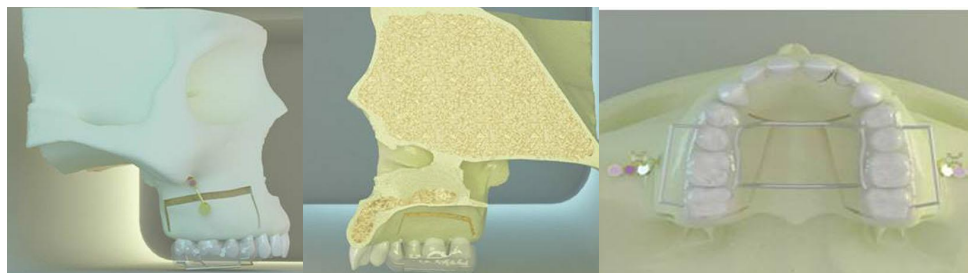**Fig.4.4.** Models presenting buccal and palatal subapical corticotomies (Uysal et al., 2019)

2- They applied 3 intrusion modalities: In the first model, the posterior teeth were connected by full-dimension segmental archwires from the vestibular and palatal sides. A total of four TADs were placed between the roots of the first and second premolars and the first and second molars on the buccal and palatal sides.

In the second model, the posterior teeth were connected from the vestibular side, and the mini-implants placed as in model 1 buccally and transpalatal arches connected the first premolars and the first molars palatally. The third model, varied from the second by placing the mini-implants between the roots of the first and second molars and the transpalatal arch connecting the first molars only.

Çifter et. al., they sought to compare and evaluate the stress and displacement effects of three maxillary posterior intrusion mechanics with mini-implant anchorage. The intrusive forces simulated by this study were allotted in proportion to the calculated root surface areas. To define tipping movements, vertical displacements, superimpositions have been used.

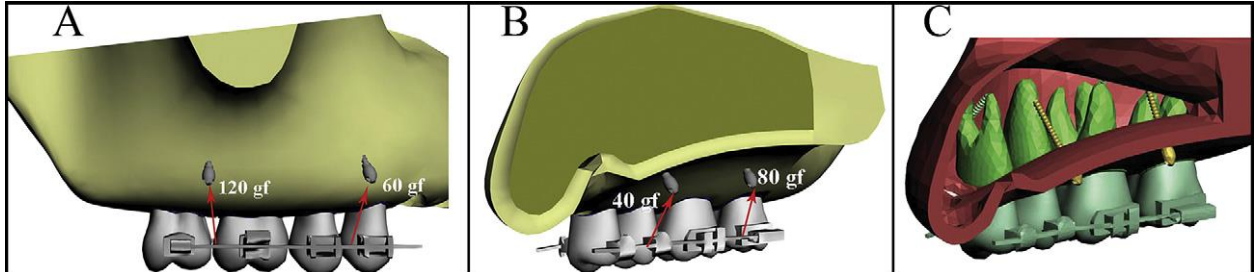**Fig.4.5**. Model 1: **A**, vestibular aspect with force distribution in proportion to the root surface area; **B**, palatal aspect; **C**, detailed view showing cortical bone thickness and the microimplants. (Çifter et. al., 2011)

4.2.2. Model construction

The final solid meshes were configured as a tetrahedron with eight nodes by Uysal et. al., whereas the configuration by Çifter et. al was a mix of hexahedral "brick" and

tetrahedral elements. For all the model researched by Uysal et.al, the number of elements ranged between 1, 567,870 and 3, 557,884 elements and between 120,074 and 124,800 for the nodes, compared with several elements ranging between 94,630 and 203,150 depending on each modality in the study of Çifter et al. (2011).

Mechanical properties of materials in the models were obtained from previous experimental data (Table 4.1) in both studies, and all structures were assumed to be isotropic, homogeneous, and linearly elastic.

Uysal et. al. applied boundary conditions at the superior and posterior skull regions, at zero displacements in the transverse, anteroposterior, and vertical axes (x, y, and z directions, respectively). They set the magnitude of the intrusive force for all models at 1.96 N (200 g). Çifter et al.'s boundary conditions were assigned to the nodes on the floor of the nasal cavity at zero displacements in all directions since not all the skull was included. The total loading force was 2.94 N (300 g) to each dental segment.

In the study of Çifter et. al., finite element models were generated by importing solid models into ALGOR software (Autodesk). Bracket-tooth, bracket-archwire, and bone-implant interfaces were defined as fully bonded surfaces. Distributions of the forces were calculated in proportion to the root surface areas determined by the 3ds Max software. The root surface area ratio of the molars to the premolars was calculated as 1.936 and rounded off to 2; the ratio of the vestibular roots along the segment to the palatinal roots was calculated as 1.36 and rounded to 1.5.

Table 4.1. Mechanical properties of the materials in the models of both studies contrasted to our study. *Converted from GPa to MPa for the sake of comparison

	Young's modulus (MPa) (Çifter et. al., 2011)	Young's modulus (MPa)* (Uysal et al., 2019)	Poisson's ratio (Çifter et. al., 2011)	Poisson's ratio (Uysal et al., 2019)	Young's modulus (MPa) (Current study)	Poisson's ratio (Current study)
Alveolar Bone	1370	1500	0.3	0.3	1500	0.33
Cortical bone	13700	15000	0.26	0.3	Variable	0.33
PDL	0.6668	Not defined	0.49	Not defined	0.68	0.45
Teeth	19613.3	1860	0.15	0.31	20000	0.3
Stainless Steel	200000	200000	0.3	0.29	200000	0.3

Table 4.2. Pertinent common points and differences between the 3 studies.

	Uysal et. al., 2019	Çifter et. al., 2011	Current study
Modalities designed	3 modalities including palatal bar, pterygoid implants and corticotomies	3 modalities including palatal Transpalatal bar and mini-implants	5 modalities including varied number and position of mini-implants with different force application
Number of elements/nodes	Between 567,870 and 3, 557,884 elements and between 120,074 and 124,800 nodes	between 94,630 and 203,150 elements	170798 nodes and 854698 elements
PDL	periodontal ligament thickness was uniformly set at 0.25 mm	thickness of 0.25 mm evenly: homogeneous, isotropic, and uniform in thickness	thickness of 0.25 mm evenly
Interactions	Not mentioned	No interactions created but, Bracket-tooth, bracket-archwire, and bone-implant interfaces were defined as fully bonded surfaces	"Surface to surface" interactions between the adjacent surfaces. Altered the tolerance of each surface to surface interaction to 0.4 to allow communication of nodes at a distance up to 0.4 mm
Boundary conditions	The superior and posterior skull regions formed the boundaries of the model, as zero displacement in all directions	Assigned to the nodes on the floor of the nasal cavity as zero displacement in all directions	Posterior and superior nodes of the maxilla considered zero in all directions
Load	1.96 N (200 g)	300 g to each dental segment. Distributions of the forces were calculated in proportion to the root surface areas	400 g (3.92 N), divided equally (200 g) palatally and buccally.
Individual variation	Not applied	Not applied	Through stiffness and thickness variation

4.2.4. Results

In dental FEA studies, it is irrelevant to speculate by comparing the absolute stress and displacement values to other studies, because many factors are involved and influence these quantitative data. Because of design differences, we limit the comparison of results to the qualitative finding, and only to setups of comparable design. Thus, only one model from each of the two studies in Çifter et. al. (2011) and Uysal et al. (2019), having in common the number of mini-implants used and the absence of transplatal-bars.

Considering the difference in the magnitude of load applied Çifter et. al. study (300g versus 400g), the color mapped representations of the stresses at the PDL distributed on all teeth had similarities with our results especially from our fourth and fifth modalities: lowest at the distal of the second molar and highest at the first premolar area. The notable difference is the presence of stresses on the second premolar in our modality was related to the force being divided equally on the involved teeth, which was not specified in their mechanics. The palatal stress distribution, were merely similar except for the second premolar (Fig. 4.6/8).
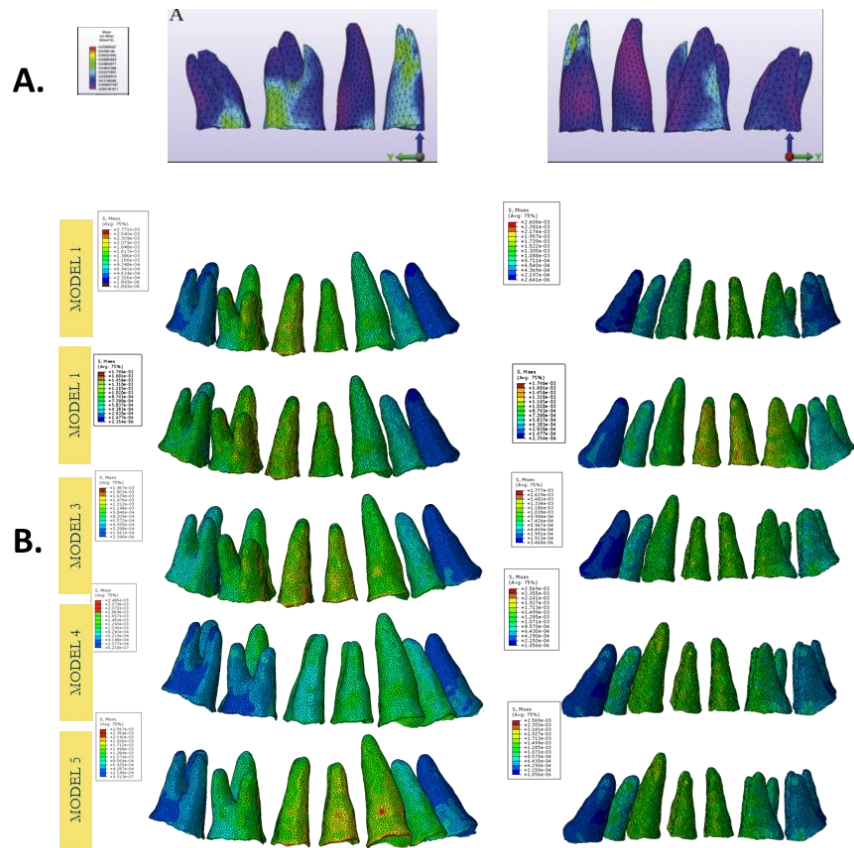
Fig.4.6. **A**, Model 1. Von Mises stress distribution (N/mm^2) (Çifter et. al., 2011). **B,** Von Mises Stress distribution (Average %) in the current study

In the study by Uysal et al. (2019), the stress was reported on teeth and not on the PDL. The equivalent scheme is extractable from our models, but all the numerical statistics were done on generated stress of the PDL. The color mapped representations of the stresses on the teeth show great resemblance between their modality and our modalities 4 and 5 at the furcation areas, the palatal aspect, and the buccal surface of the molars. The main difference was seen at the more coronal stress in our modalities versus more apical distribution, probably due to the difference in position between our MIs and their pterygoid plates (Fig 4.9).
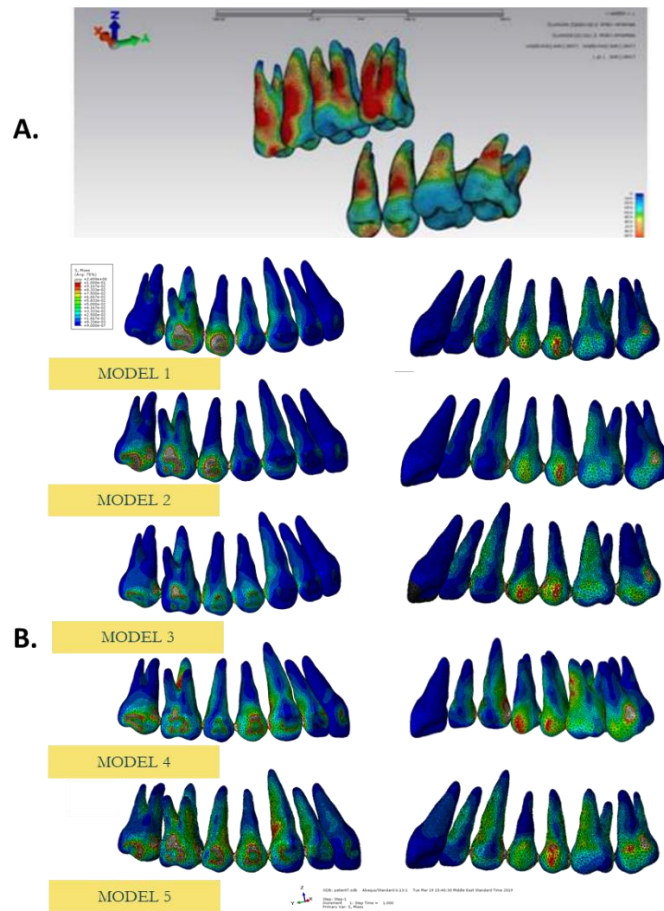
Fig.4.7. **A**, Stress distribution on dental structures, first setup (Uysal et. al., 2019). **B,** Von Mises Stress distribution (Average %) in the current study viewed from buccal (first column) and palatal (second column) aspects.

In that same study, the stress pattern evaluated on the alveolar bone in all modalities, was comparable to our results: highest at the alveolar crest between the first and the second molars specifically at the buccal aspect of the bone around the first molars alveola, and the alveola of the second premolar and the interdental septum.
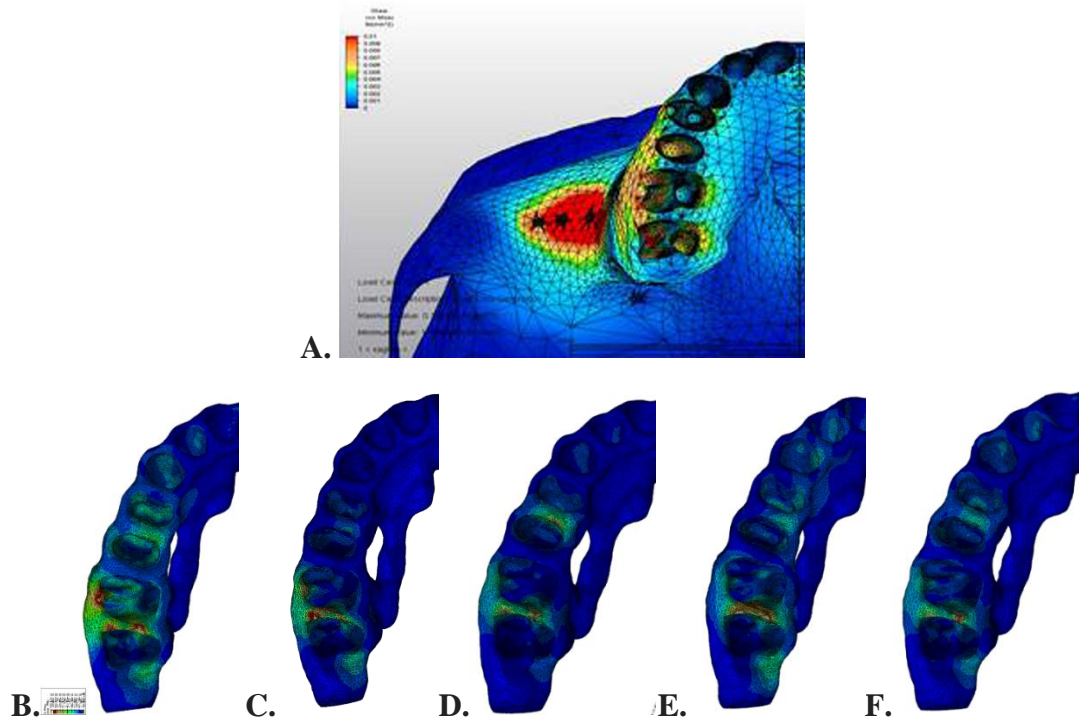
Fig.4.8. **A**, Stress distribution from occlusal view over cancellous bone, first setup (Uysal et. al., 2019). **B,** Von Mises Stress distribution (Average %) in the current study over the occlusal part of the alveolar bone: note the high stress at the level of the premolars and first molar in the first modality (B), less stress at the premolars in the second modality (C), septal stress even between molars and premolars in the third modality (D), similarity in stresses on the bone for the last two modalities (E and F)

Çifter et. al, reported secondary effects only in the second and third models which involved palatal control with transpalatal bars. In our study, secondary effects (bucco-lingual tipping and antero-posterior movement) were observed in different ranges in the five modalities. The total amount of intrusion in our protocols was greater on the first premolar (between 0.756(M4) and 1.167(M5) millimeters) compared to 0.552 millimeter in their study. The same pattern applies to the second premolar, the stress ranging between

0.727(M4) and 1.049 (M5) in our study and measured at 0.415 millimeter in theirs (Fig.4.11).

The displacement they reported in the first and second molars (0.95 and 0.952 millimeters respectively) exceeded our values (higher than the maximum value 0.794(M2) and 0.54 (M3) millimeters, respectively). The disparity, might be related to the concentration of force in their study more posteriorly compared to an even distribution in our study. Thus, more displacement occurred on teeth with smaller root areas (premolars) compared to molars.
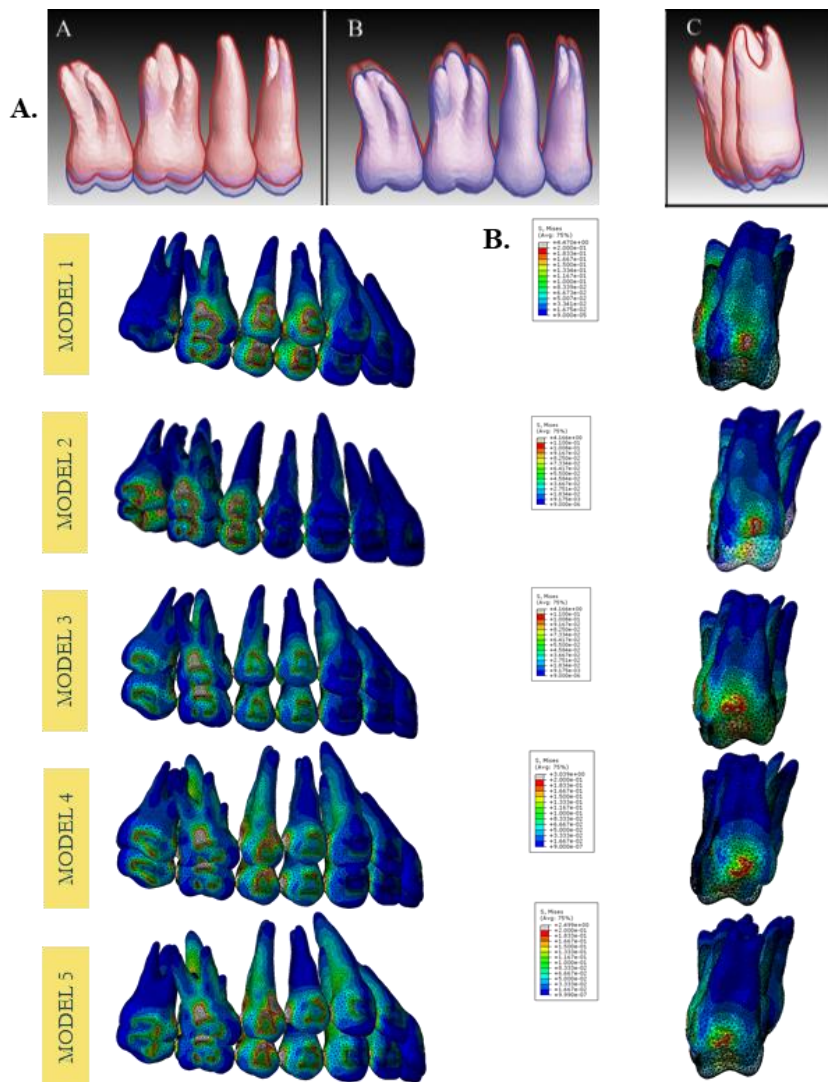
Fig.4.9. **A** Model 1: A, superimposition denoting the vertical displacement identified at the crowns (blue, before; pink, after); B, vertical displacement identified at the roots; C, displacement in the vestibulopalatinal direction. **B,** Displacement superimpositions in the antero-posterior direction and sagittal view of the current study.

4.3. Association between stress and displacement

From a clinical perspective, the correlations between stress and displacement

provide for the following observations:

1. In all the modalities (mostly 1 and 3), stresses on the canines and the premolars correlated with the displacements at the z axis, which corresponds to the vertical movement. Accordingly, modalities 1 and 3 would provide intrusion on the canines and first premolar with the least secondary effects. This conclusion applies to the molars in all five modalities, particularly, in modality 2 with the highest impact on the second molar.

2. On thickness variation, correlations were lower especially on modalities 3, 4 and 5, for the canine, premolars, and molars, suggesting that higher intrusive forces would be needed with thicker cortical bone.

3. At the molars, the correlation was low and not significant. Given that high correlations between stress and displacement indicate dental movement, a non-significant and low correlation may signal low movement compared to the premolars. Clinically, considering greater forces on the molars can increase stress on the premolars, leading to possible hyalinization and root resorption, a better alternative might be changing the force application by adopting for instance modality 2 for a posterior loading component.

4. In modality 1 the highest concentration of the secondary effects (39%) was on the second premolar which intruded the most [28%] and sustained the highest stress [26%]). The second molar sustained relatively high stress (19.6%) with the least amount of movement (5%).

Modality 2 displayed low stresses on the molars (12% on the second molar), despite of the high vertical percentage value on the second molar compared to the other modalities (15%) and low secondary effects on that same tooth (8%).

In modality 3, more than the half of the total in secondary effects was concentrated on the canine with a 53% but with a stress percentage (14%) more complemented with the intrusive movement (20%).

The clinical implication with this modality is that the system of forces should be well scrutinized to avoid round tripping on the maxillary canine.

5. The stress and corresponding displacement at the second molar in the modalities 4 and 5, were nearly half of that at the first and second premolars (12%, 26% and 23% respectively). These findings suggest that the initial displacement in the PDL occurred at the level of the premolars. Longer-term time dependent movement should be explored to determine the dynamic displacement beyond the initial response within the PDL and the force systems that should be planned on the multi-rooted teeth.

6. As would be expected, stress values were highest on the premolars and first molar during intrusion and least on the extremity teeth. Moreover, secondary effects (bucco-lingual and antero-posterior movements) were more prevalent on the extremity teeth, particularly, the canines, warranting better anchorage during clinical application.

7. All stresses were comparable among all modalities, but the amount of intrusion was more evident in modality 2. Thus, this modality should be considered with more severe openbites.

4.4. Association between stress and bone properties (stiffness and thickness)

Stiffness of bone, particularly at the palatal side, correlated significantly and negatively with stress values at different areas of the premolar. The same pattern was

observed on the molars but on the buccal side of the bone. Relatively, correlations were positive with all canines, premolars, and molars between stress and thickness indicating that thickness of the cortical bone does impact inversely initial movement compared to stiffness. Ammoury et. al (2017) advanced two possible theories that may explain the way stiffness might affect stresses:

Theory 1: Maxilla is a composite material

By definition, a composite material is made from two or more component materials with substantially different physical or chemical properties that, in combination, producing a material with characteristics different from its individual components (Fig. 4.5). Likewise, the maxilla can be considered a composite material with higher stiffness component on the outer surface than the components of the inner zones (trabecular bone versus PDL). Cortical bone is considered one of the components that we altered in our research, which might affect the whole maxilla changing its stiffness property. Moreover, stresses analyzed at one component of the composite material (here PDL) involves stiffness of the composite material:

$$\textbf{Stress } (\sigma) = \textbf{stiffness } (E) \times \textbf{strain } (\varepsilon).$$

Different stresses are expected at the PDL when cortical bone stiffness is altered.

Subsequently, representation of the cortical bone is mandatory in any FEA study even if only initial displacement is being studied.
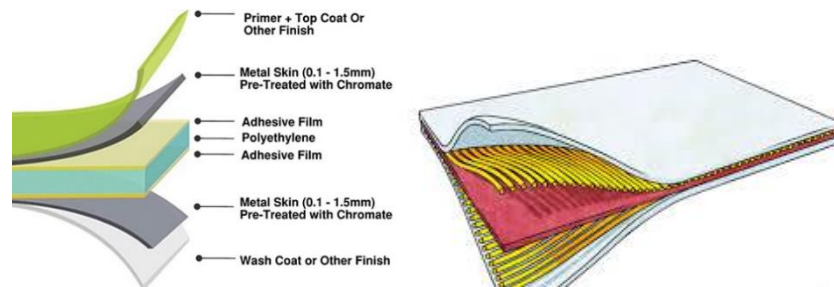
Fig.4.10. Composite material formed from multiple layers of materials with different physical and mechanical properties (http://www.twinkl.co.za- accessed December 27, 2019).

Theory 2: Presence of direct contact between PDL and cortical bone

Ten Hoeve et al. (1977) recommended the intrusion of the incisors in trabecular bone prior to palatal root torque application to avoid causing root resorption because retroclined maxillary incisors are close the palatal cortex. This bone would bend and remodel but not allow for a significant amount of palatal movement of the root. This observation is translatable in our findings:
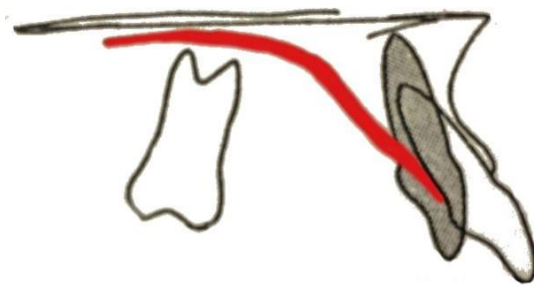
Fig.4.11: Proximity of the maxillary incisor root (in white) to the palatal cortex (in red) preventing palatal root torque movement. After intrusion (in gray), the tooth is bordered by trabecular bone facilitating the same movement. *(Adapted from Ten Hoeve et al. 1977)*

1. While stress at the PDL and stiffness at the molar exhibited high correlations, they were negative (-0.64<r<-0.91), indicating an inverse relationship: stress is higher at the PDL with a less hard cortical bone. This finding is in line with the equation

between stiffness, stress, and displacement: the higher the stiffness, the lower the

stress and displacement, and vice versa (Table 4.3).

Table 4.3: Cortical bone impact on PDL stress and crown displacement based on the correlation results

Cortical bone stiffness	PDL stress	Intrusion
↗	↘	↘
↘	↗	↗

A.

B.
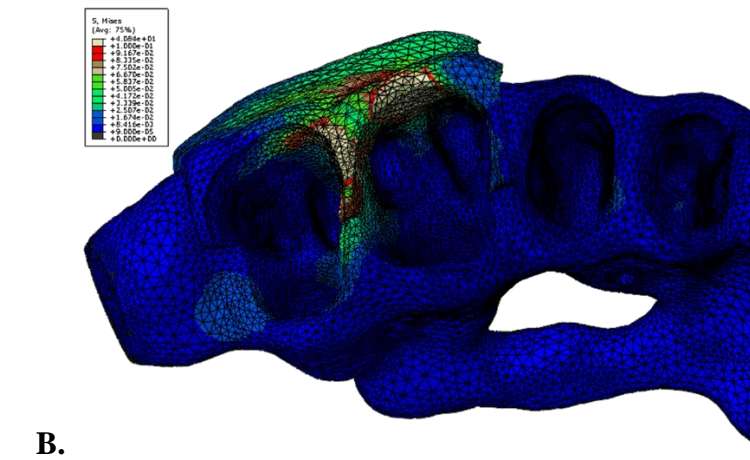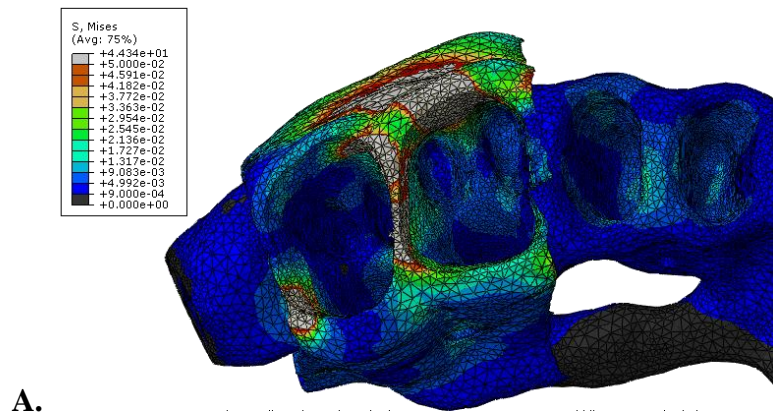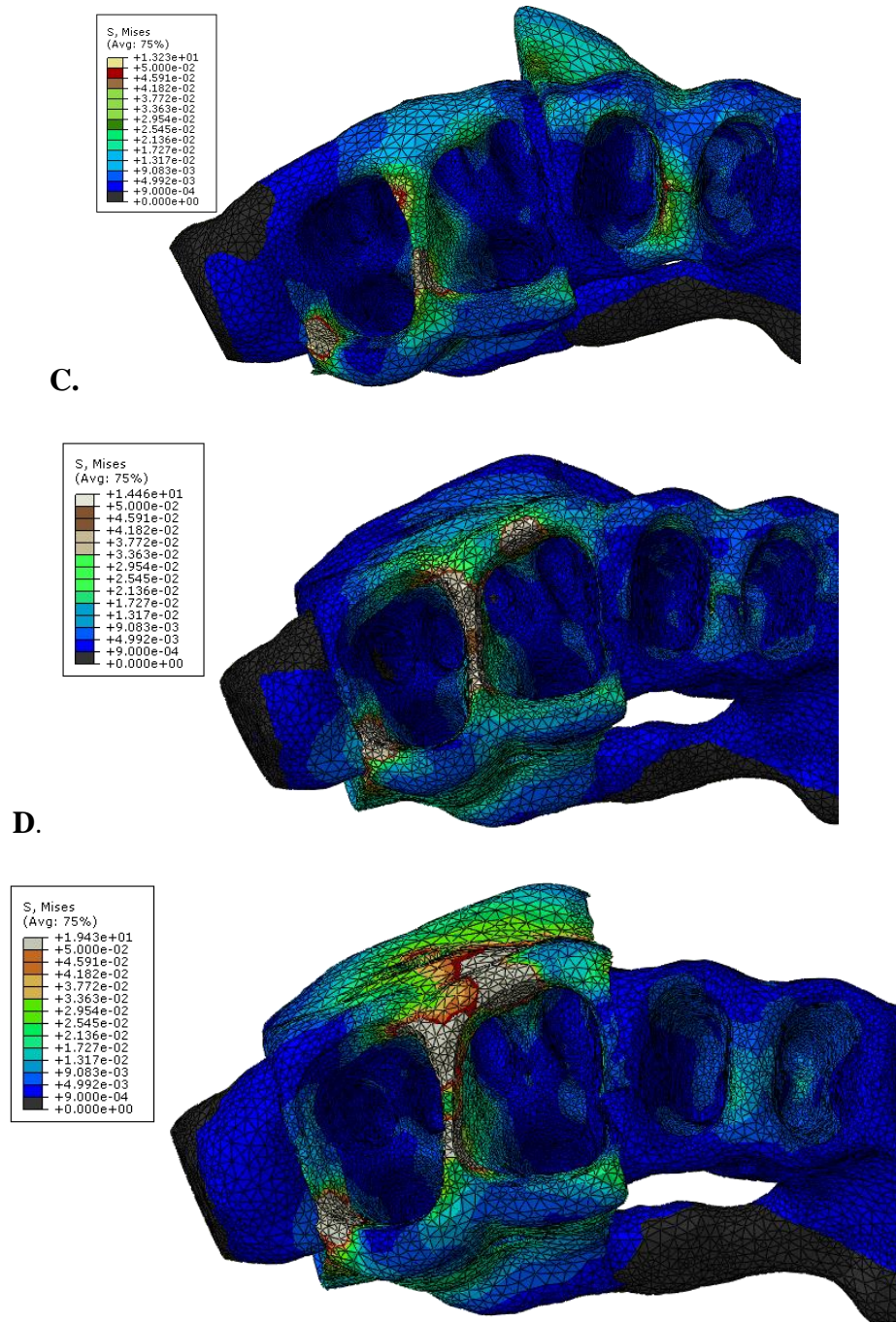
Fig.4.12: Occlusal view showing the trabecular bone and the buccal molar cortical part. Note the higher stresses at the occlusal and interdental cortical bone highlighting the direct transmission of stress from the PDL to the buccal cortex (Theory 2). Order of stresses from the highest to the lowest: fifth (E) fourth (D) first (A) second (buccal concentration on the molars) (B) third (C). Unlike at the PDL, higher stresses at the cortical bone level suggest resistance to movement because of the higher material property value.

2. Stress values increased at the cortical bone, indicating uptake of part of the stress by the PDL. In contrast to this reaction at the PDL, greater stress at cortical bone indicates resistance to movement because of the higher material properties (Young's modulus).

3. Given the above-mentioned negative correlations between stiffness and stress, one would question if higher stresses would be found at the less stiff (softer) trabecular bone. Consequently, greater displacement would be generated, as opposed to expectations of higher resistance from the cortical bone.

4. Only time-dependent FEA probing real clinical setting of teeth movement can permit adequate confirmation of these theories, because of the limitation of our experiment, giving only initial displacement.

Synthesis based on theories 1 and 2

Based on the previous theories, and on the significant stress/stiffness correlations we have observed, we recommend following clarifications:

1. The higher number of significant correlations observed at the buccal cortical bone area of the molar is probably related to the buccal tipping movement of the molar because of the thinner cortical bone buccally, and the anatomy variation of the roots. Moreover, more correlations were present in the third modality, suggesting more buccal tipping with this modality, mainly because the point of application of the force is closer to the first premolar and molar (Fig.3.9, table 3.39/40).

2. The highest stress values were observed at the bucco-cervical of surfaces of the PDL because these areas are in direct contact cortical bone especially when the buccal and palatal force goes to the cortex with less resistance.

3. The smaller bucco-lingual width and mesio-distal width of the canine's crown and the presence of only one thin and tapered root (vs 3 for the molar) helped guide its movement in the trabecular bone with minimal contact with the cortical bone.

This observation added to the fact that the forces were far from the canine, would explain the lack of any correlation of the PDL stresses with the cortical bone (Table 3.37).

4. Distribution of stresses between modalities and according to the colored map, highlights high bucco-cervical stress on the premolars especially the second premolar (close to the force application) and its narrow root anatomy and morphology compared to the molars makes it more susceptible to the posterior loading. This might explain the high stress on the second premolar. Which is more, high stresses were registered at the bone between the premolars and the canines and at the interdental bone (presence of the archwire and the interactions created transmitting the force along the arch). The third modality displayed uniformity of stress distribution between the teeth especially when comparing buccal to palatal.

4.5. Differential effects of cortical bone stiffness and thickness

Orthotropic models did not differ from the isotropic model in comparisons among intrusion modalities. The maximum difference found was between 12 and 27 Pa for the stiffness and thickness stresses respectively, and between 0.32 and 0.4 millimeters for the

displacement. These findings indicate that orthotropic material definition did not significantly influence the stresses at the PDL nor the displacements, and that isotropic representation of the cortical bone in FEA studies of initial tooth movement may be an acceptable assumption.

4.6. Clinical implications

The results suggest a number of clinical implications:

1- When planning intrusion of posterior teeth, all the components scrutinized in this research should be considered, such as cortical bone density (stiffness) and thickness, the number of teeth to be intruded, amount of intrusion (e.g. in relation to open bite and/or "gummy smile"), occlusal interferences, side effects, muscle activity, facial pattern (hyperdivergent versus hypodivergent), and as importantly the location of the mini-implants. Based on the literature, the amount of intrusion varies. And the variation is likely related to differences in the above-cited factors. In general, molar intrusion is considered complete when the tooth was leveled with adjacent teeth. Marzouk et al. found a mean amount of accomplished molar intrusion of 3.1mm (± 0.74mm), with a rate of 0.36mm (± 0.08mm) per month and a bite closure of 6.55mm (± 1.83mm). Carrillo et al. achieved 1.2 to 2.3 mm, Heravi et al. ranged from 1.5 to 4.5 mm whereas Al-Fraidi and Zawawi achieved 4 mm in their studies.

2- The findings that stress increases when stiffness decreases inducing more displacement, that the buccal cortex resists initial movement and that the palatal cortex is more resistant to initial movement at the level of the premolars suggest:

    a- The use of at least one mini-implant palatally to minimize the secondary effects (bucco-lingual tooth movement)

    b- The use of a heavy palatal archwire to connect all the teeth (usually by bonding or cementation)

    c- The use of heavy archwire connecting all teeth as one unit.

3- The choice between the five modalities investigated depends on the purpose of the intrusion. If the second molars do not interfere and do not require significant intrusion, modality 1 is recommended. If the "wedge" effect for anterior bite closure requires the intrusion of the second molar, modality 2 should be considered along with control of the anticipated secondary effects at the level of the premolars. If all teeth are to be intruded almost equally, the modalities 3 and 4 are better candidates, the choice between them depending on the state of the canine to avoid round-tripping. In such instance, modality 4 should be selected where the stresses are uniformly distributed, with secondary effects dissipated among the adjacent teeth.

4- Intrusion against the brackets is more effective with greater initial displacement and less secondary effects than pulling against the archwire.

4.7. Research consideration

4.7.1. Limitations

This research offers a "snap-shot" display of the initial stresses and displacement in the model and does not describe changes occurring over time on the biological aspect of the movement such as bone remodeling, healing, and friction. These findings represent the initial dental movement through the PDL space before the primary phases of bone resorption/apposition. Accordingly, the clinical results may not be generalized to total intrusion.

Additionally, several approaches have been used to design the PDL ranging from linear-elastic, viscoelastic, hyperelastic and multiphase methods (Fill et al., 2012). The absence of experimental research and were developed technologies to measure the properties of the oral tissues has kept investigators from determining the accurate simulation of the PDL properties. Our study was consistent with most dental FEA investigations designed to use an isotropic and homogeneous material property for the PDL, which can lead to simple and imprecise outcomes. Nevertheless, from this perspective, our results could be compared with other FEA investigations.

4.7.2. Future research

Time-dependent (continuous/dynamic) finite element analysis is needed to determine the dynamic process of intrusion, both in terms of sequential stress evaluation

132

and tooth displacement. Such research, linked to actual clinical data, should help develop schemes of simulation and prediction of tooth movement in the individual patient and under specific circumstances.

Our study suggests that tooth responses to a comparable load did not differ significantly between subjects. In another FEA study where individual variation was introduced to gauge the initial stress on palatally impacted canines to forces from different directions, the responses varied significantly between the different force directions (Zeno et al., 2016). Intrusion forces are mono-directional and are not expected to cause such variation. Nevertheless, longer-term differences between patients may be gauged in the time-dependent FEA model.

Future research should also focus on other factors affecting the intrusion, including anatomical and morphological variables such as the distance between teeth, furcations, the width of the alveolus, height of the coronal cortical bone in contact with the PDL, the bucco-lingual width of the molar, and the shape of the roots (thin elongated teeth are more prone to resorption necessitating proper planning of the loading).

Most of these anatomical factors are best evaluated using 3D radiographic imaging. Furthermore, experiments should be tested on the maxilla with the application of adjunct procedures such as micro-perforations (e.g. at the apical level of the bone) to determine their effectiveness in reducing resistance to tooth movement.

CHAPTER 5
CONCLUSION

1. **Study:**

The current study is the first FEA on tooth intrusion in which variation among human subjects was evaluated. The central tendencies and variations within the stress values and displacements were compared between five intrusion approaches of the maxillary buccal teeth.

2. **Stiffness versus thickness of cortical bone:**

a. Stiffness and to a lesser extent thickness of the cortical bone induced stress and the initial displacement among the buccal teeth.

Clinical implication:

If the tooth encounters even a thin but stiffer area of the cortical bone, stress is affected and consequently tooth movement

b. Upon thickness variation, correlations became less significant

Clinical implication:

Higher forces should be applied for intrusion when cortical bone is thick

3. **Force application:**

a. Stress and displacement were higher on the teeth anchoring the intrusive force.

b. The second molar displacement was higher when the miniscrew was placed between the molars (M2).

Clinical implication:

Place the MIs in a position adequate to apply direct forces to the teeth needing intrusion.

4. **Modalities:**

M3 was the closest to M2 in providing similar stresses and displacement of the posterior teeth.

Clinical implications:

If any anatomical limitation restricts the placement of 2 palatal mini-implants, the closest alternative is applying 2 buccal implants posteriorly and one palatal implant between PM2 and M1.

5. **Secondary effects:**

a. All the teeth engaged in the archwire were affected by the intrusion of the posterior teeth, including the canines (and by extension probably the incisors).

b. Secondary effects such as buccal movement of the teeth subjected to intrusion occurred more when force application was on the archwire rather than directly to the brackets.

c. Not only load magnitude and direction of force might cause secondary effects that reduce efficient intrusion, but also anatomical factors related to teeth shape and size and bone variation in the individual patient.

Clinical implications:

- If intrusion of the anterior teeth is to be avoided, consider using posterior sectional wires.

- The occlusal plane may be altered by the design of the intrusion location and direction.

- If additional anterior intrusion is needed, may consider anterior mini-implants

6. **Research considerations:**

a. The findings do not permit generalization on best intrusive modality, as anatomical and biologic individual traits may influence one or the other in individualized treatment.

b. Future research is needed with time dependent FEA

c. Clinical studies to test clinical implications are warranted

REFERENCES

Akan, S., Kocadereli, I., Aktas, A., & Taşar, F. (2013). Effects of maxillary molar intrusion with zygomatic anchorage on the stomatognathic system in anterior open bite patients. The European Journal of Orthodontics, 35(1), 93-102.

Alabdullah, M., Saltaji, H., Abou-Hamed, H., & Youssef, M. (2015). Association between facial growth pattern and facial muscle activity: A prospective cross-sectional study. International orthodontics, 13(2), 181-194.

Albogha, M. H., Takahashi, I., & Sawan, M. N. (2015). Early treatment of anterior open bite: Comparison of the vertical and horizontal morphological changes induced by magnetic bite-blocks and adjusted rapid molar intruders. The korean journal of orthodontics, 45(1), 38-46.

Al-Fraidi, A. A., & Zawawi, K. H. (2010). Selective Intrusion of Overerupted Upper First Molars Using a Temporary Anchorage Device: Case Report. Journal-Canadian Dental Association, 76(1), 25-30.

Alsafadi, A. S., Alabdullah, M. M., Saltaji, H., Abdo, A., & Youssef, M. (2016). Effect of molar intrusion with temporary anchorage devices in patients with anterior open bite: a systematic review. Progress in orthodontics, 17(1), 9.

Al-Zubair, Nabil. (2014). Orthodontic intrusion: a contemporary review." Journal of Orthodontic Research 2(3) 118-118.

Ammar, H. H., Ngan, P., Crout, R. J., Mucino, V. H., & Mukdadi, O. M. (2011). Three-dimensional modeling and finite element analysis in treatment planning for orthodontic tooth movement. American Journal of Orthodontics and Dentofacial Orthopedics, 139(1), e59-e71.

Ammoury, M. J., Mustapha, S., Dechow, P. C., & Ghafari, J. G. (2019). Two distalization methods compared in a novel patient-specific finite element analysis. American Journal of Orthodontics and Dentofacial Orthopedics, 156(3), 326-336.

Arisan, V., Karabuda, Z. C., Avsever, H., & Özdemir, T. (2013). Conventional multi-slice computed tomography (CT) and cone-beam CT (CBCT) for computer-assisted implant placement. Part I: Relationship of radiographic gray density and implant stability. Clinical implant dentistry and related research, 15(6), 893-906.

Ashman, R. B., Cowin, S. C., Van Buskirk, W. C., & Rice, J. C. (1984). A continuous wave technique for the measurement of the elastic properties of cortical bone. Journal of biomechanics, 17(5), 349-361.

Azevedo AFM. Método dos Elementos Finitos. (2003)
http://civil.fe.up.pt/pub/apoio/ano5/aae/pdf/Apontamentos/Livro_MEF_AA.pdf

Baek, M. S., Choi, Y. J., Yu, H. S., Lee, K. J., Kwak, J., & Park, Y. C. (2010). Long-term stability of anterior open-bite treatment by intrusion of maxillary posterior teeth. American Journal of Orthodontics and Dentofacial Orthopedics, 138(4), 396-e1.

Bayani, S., Heravi, F., Radvar, M., Anbiaee, N., & Madani, A. S. (2015). Periodontal changes following molar intrusion with miniscrews. Dental research journal, 12(4), 379.

Beane Jr, R. A. (1999, December). Nonsurgical management of the anterior open bite: a review of the options. In Seminars in orthodontics (Vol. 5, No. 4, pp. 275-283). WB Saunders.

Becker, W., Becker, B. E., Israelson, H., Lucchini, J. P., Handelsman, M., Ammons, W. & Lekholm, U. (1997). One-step surgical placement of Brånemark implants: a prospective multicenter clinical study. International Journal of Oral & Maxillofacial Implants, 12(4).

Black, J., & Hastings, G. (Eds.). (2013). Handbook of biomaterial properties. Springer Science & Business Media.

Bookstein, F. L. (1996). Combining the tools of geometric morphometrics. In Advances in morphometrics (pp. 131-151). Springer, Boston, MA.

Bourauel, C., Keilig, L., Rahimi, A., Reimann, S., Ziegler, A., & Jäger, A. (2007). Computer-aided analysis of the biomechanics of tooth movements. International journal of computerized dentistry, 10(1), 25-40.

Bouton, A., Simon, Y., Goussard, F., Teresi, L., & Sansalone, V. (2017). New finite element study protocol: Clinical simulation of orthodontic tooth movement. International orthodontics, 15(2), 165-179.

Burstone, C. R. (1977). Deep overbite correction by intrusion. American Journal of Orthodontics and Dentofacial Orthopedics, 72(1), 1-22.

Buschang, P. H., Jacob, H., & Carrillo, R. (2013, December). The morphological characteristics, growth, and etiology of the hyperdivergent phenotype. In Seminars in Orthodontics (Vol. 19, No. 4, pp. 212-226). WB Saunders.

Cambiano, A. O., Janson, G., Lorenzoni, D. C., Garib, D. G., & Dávalos, D. T. (2018). Nonsurgical treatment and stability of an adult with a severe anterior open-bite malocclusion. Journal of orthodontic science, 7.

Caputo, A. A., Chaconas, S. J., & Hayashi, R. K. (1974). Photoelastic visualization of orthodontic forces during canine retraction. American journal of orthodontics, 65(3), 250-259.

Carrillo, R., Rossouw, P. E., Franco, P. F., Opperman, L. A., & Buschang, P. H. (2007). Intrusion of multiradicular teeth and related root resorption with mini-screw implant anchorage: a radiographic evaluation. American Journal of Orthodontics and Dentofacial Orthopedics, 132(5), 647-655.

Cattaneo, P. M., Dalstra, M., and Melsen, B. (2005). The finite element method: a tool to study orthodontic tooth movement. Journal of dental research, 84(5), 428-433.

Chabanas, M., Luboz, V., & Payan, Y. (2003). Patient specific finite element model of the face soft tissues for computer-assisted maxillofacial surgery. Medical image analysis, 7(2), 131-151.

Chen, C. H., Chang, C. S., Hsieh, C. H., Tseng, Y. C., Shen, Y. S., Huang, I. Y., & Chen, C. M. (2006). The use of microimplants in orthodontic anchorage. Journal of Oral and Maxillofacial Surgery, 64(8), 1209-1213.

Cheol-ho, p. A. I. K., mccomb, r. Y. A. N., & hong, c. (2016). Differential molar intrusion with skeletal anchorage in open-bite treatment. Journal of clinical orthodontics: JCO, 50(5), 276.

Christensen, J. R., Fields, H., & Sheats, R. D. (2019). Treatment planning and management of orthodontic problems. In Pediatric Dentistry (pp. 512-553).

Christiansen, R. L., & Burstone, C. J. (1969). Centers of rotation within the periodontal space. American journal of orthodontics, 55(4), 353-369.

Çifter, M., & Saraç, M. (2011). Maxillary posterior intrusion mechanics with mini-implant anchorage evaluated with the finite element method. American Journal of Orthodontics and Dentofacial Orthopedics, 140(5), e233-e241.

Çinsar, A., Alagha, A. R., & Akyalçın, S. (2007). Skeletal open bite correction with rapid molar intruder appliance in growing individuals. The Angle Orthodontist, 77(4), 632-639.

Cook, R. D., Malkus, D. S., Plesha, M. E., and Witt, R. J. (1974). Concepts and applications of finite element analysis (Vol. 4). New York: Wiley.

Cope, J. B. (2005). Temporary anchorage devices in orthodontics: a paradigm shift. In Seminars in orthodontics (Vol. 11, No. 1, pp. 3-9). WB Saunders.

Costa, A., Raffainl, M., and Melsen, B. (1998). Miniscrews as orthodontic anchorage: a preliminary report. The International journal of adult orthodontics and orthognathic surgery, 13(3), 201-209.

Cowin, S. C., and Hart, R. T. (1990). Errors in the orientation of the principal stress axes if bone tissue is modeled as isotropic. Journal of Biomechanics, 23(4), 349-352.

DeBerardinis, M., Stretesky, T., Sinha, P., & Nanda, R. S. (2000). Evaluation of the vertical holding appliance in treatment of high-angle patients. American Journal of Orthodontics and Dentofacial Orthopedics, 117(6), 700-705.

Deguchi, T., Kurosaka, H., Oikawa, H., Kuroda, S., Takahashi, I., Yamashiro, T., and Takano-Yamamoto, T. (2011). Comparison of orthodontic treatment outcomes in adults with skeletal open bite between conventional edgewise treatment and implant-anchored orthodontics. American Journal of Orthodontics and Dentofacial Orthopedics, 139(4), S60-S68.

Deguchi, T., Nasu, M., Murakami, K., Yabuuchi, T., Kamioka, H., and Takano-Yamamoto, T. (2006). Quantitative evaluation of cortical bone thickness with computed tomographic scanning for orthodontic implants. American Journal of Orthodontics and Dentofacial Orthopedics, 129(6), 721. e727-721. e712.

DiBiase, A., & Sandler, P. J. (2017). Early treatment of class II malocclusion. In Orthodontic Management of the Developing Dentition (pp. 151-167). Springer, Cham.

Diewert, V. M., & Lozanoff, S. (1993). A morphometric analysis of human embryonic craniofacial growth in the median plane during primary palate formation. Journal of craniofacial genetics and developmental biology, 13, 147-147.

Ersahan, S., & Sabuncuoglu, F. A. (2015). Effects of magnitude of intrusive force on pulpal blood flow in maxillary molars. American Journal of Orthodontics and Dentofacial Orthopedics, 148(1), 83-89.

Field, C., Ichim, I., Swain, M. V., Chan, E., Darendeliler, M. A., Li, W., and Li, Q. (2009). Mechanical responses to orthodontic loading: a 3-dimensional finite element multi-tooth model. American Journal of Orthodontics and Dentofacial Orthopedics, 135(2), 174-181.

Fill, T. S., Toogood, R. W., Major, P. W., and Carey, J. P. (2012). Analytically determined mechanical properties of, and models for the periodontal ligament: critical review of literature. Journal of Biomechanics, 45(1), 9-16.

Gallas, M. M., Abeleira, M. T., Fernandez, J. R., & Burguera, M. (2005). Three-dimensional numerical simulation of dental implants as orthodontic anchorage. The European Journal of Orthodontics, 27(1), 12-16.

Gandedkar, N. H., Koo, C. S., Sharan, J., Chng, C. K., & Vaid, N. (2018, March). The temporary anchorage devices research terrain: Current perspectives and future forecasts! In Seminars in Orthodontics (Vol. 24, No. 1, pp. 191-206). WB Saunders.

Garfinkle, J. S., Cunningham Jr, L. L., Beeman, C. S., Kluemper, G. T., Hicks, E. P., & Kim, M. O. (2008). Evaluation of orthodontic mini-implant anchorage in premolar extraction therapy in adolescents. American Journal of Orthodontics and Dentofacial Orthopedics, 133(5), 642-653.

Geng, J. P., Ma, Q. S., Xu, W., Tan, K. B. C., & Liu, G. R. (2004). Finite element analysis of four thread-form configurations in a stepped screw implant. Journal of oral rehabilitation, 31(3), 233-239.

Geramy, A. (2002). Initial stress produced in the periodontal membrane by orthodontic loads in the presence of varying loss of alveolar bone: a three-dimensional finite element analysis. The European Journal of Orthodontics, 24(1), 21-33.

Ghafari, J. G., & Macari, A. T. (2013, December). Component analysis of predominantly vertical occlusal problems. In Seminars in Orthodontics (Vol. 19, No. 4, pp. 227-238). WB Saunders.

Ghosh, J., Nanda, R. S., Duncanson Jr, M. G., & Currier, G. F. (1995). Ceramic bracket design: an analysis using the finite element method. American Journal of Orthodontics and Dentofacial Orthopedics, 108(6), 575-582.

Greenlee, G. M., Huang, G. J., Chen, S. S. H., Chen, J., Koepsell, T., & Hujoel, P. (2011). Stability of treatment for anterior open-bite malocclusion: a meta-analysis. American journal of orthodontics and dentofacial orthopedics, 139(2), 154-169.

Grenga, V., & Bovi, M. A. U. R. O. (2013). Corticotomy-enhanced intrusion of an overerupted molar using skeletal anchorage and ultrasonic surgery. J Clin Orthod, 47(1), 50-55.

Gupta, A., Kohli, V. S., Hazarey, P. V., Kharbanda, O. P., & Gunjal, A. (2009). Stress distribution in the temporomandibular joint after mandibular protraction: a 3-dimensional finite element method study. Part 1. American journal of orthodontics and dentofacial orthopedics, 135(6), 737-748.

Gurton, A. U., Akın, E., & Karacay, S. (2004). Initial intrusion of the molars in the treatment of anterior open bite malocclusions in growing patients. The Angle Orthodontist, 74(4), 454-464.

Haddad, R., & Saadeh, M. (2019). Distance to alveolar crestal bone: a critical factor in the success of orthodontic mini-implants. Progress in orthodontics, 20(1), 19.

Hakami, Z. (2016). Molar intrusion techniques in orthodontics: A review. Journal of International Oral Health, 8(2), 302.

Harris, E. F., & Butler, M. L. (1992). Patterns of incisor root resorption before and after orthodontic correction in cases with anterior open bites. American Journal of Orthodontics and Dentofacial Orthopedics, 101(2), 112-119.

Heravi, F., Bayani, S., Madani, A. S., Radvar, M., and Anbiaee, N. (2011). Intrusion of supra-erupted molars using miniscrews: clinical success and root resorption. American Journal of Orthodontics and Dentofacial Orthopedics, 139(4), S170-S175.

Hohmann, A., Kober, C., Young, P., Dorow, C., Geiger, M., Boryor, A. & Sander, F. G. (2011). Influence of different modeling strategies for the periodontal ligament on finite element simulation results. American Journal of Orthodontics and Dentofacial Orthopedics, 139(6), 775-783.

Huang, H. L., Chang, C. H., Hsu, J. T., Faligatter, A. M., & Ko, C. C. (2007). Comparison of implant body designs and threaded designs of dental implants: a 3-dimensional finite element analysis. International Journal of Oral & Maxillofacial Implants, 22(4).

Huang, Y., Keilig, L., Rahimi, A., Reimann, S., & Bourauel, C. (2012). Torque capabilities of self-ligating and conventional brackets under the effect of bracket width and free wire length. Orthodontics & craniofacial research, 15(4), 255-262.

Hussein, Mohammed Ali. A. (2012) "Mechanical analysis of orthodontic wires." diyala journal of engineering sciences 5(1). 172-180.

Jafari, A., Shetty, K. S., & Kumar, M. (2003). Study of stress distribution and displacement of various craniofacial structures following application of transverse orthopedic forces—a three-dimensional FEM study. The Angle Orthodontist, 73(1), 12-20.

Jane Yao, C. C., Wu, C. B., Wu, H. Y., Kok, S. H., Frank Chang, H. F., & Chen, Y. J. (2004). Intrusion of the overerupted upper left first and second molars by mini-implants with partial-fixed orthodontic appliances: a case report. The Angle Orthodontist, 74(4), 550-557.

Janson, G., Crepaldi, M. V., de Freitas, K. M. S., de Freitas, M. R., & Janson, W. (2008). Evaluation of anterior open-bite treatment with occlusal adjustment. American Journal of Orthodontics and Dentofacial Orthopedics, 134(1), 10-e1.

Jiang, L., Kong, L., Li, T., Gu, Z., Hou, R., & Duan, Y. (2009). Optimal selections of orthodontic mini-implant diameter and length by biomechanical consideration: a three-dimensional finite element analysis. Advances in Engineering Software, 40(11), 1124-1130.

Jing, Y., Han, X., Cheng, B., & Bai, D. (2013). Three-dimensional FEM analysis of stress distribution in dynamic maxillary canine movement. Chinese Science Bulletin, 58(20), 2454-2459.

Jones, M. L., Hickman, J., Middleton, J., Knox, J., & Volp, C. (2001). A validated finite element method study of orthodontic tooth movement in the human subject. Journal of orthodontics, 28(1), 29-38.

Kamble RH, Lohkare S, Hararey Kamble, R. H., Lohkare, S., Hararey, P. V., and Mundada, R. D. (2012). Stress distribution pattern in a root of maxillary central incisor having various root morphologies: a finite element study. The Angle Orthodontist, 82(5), 799-805.

Kanomi, R. (1997). Mini-implant for orthodontic anchorage. J clin Orthod, 31, 763-767.

Katada, H., Arakawa, T., Ichimura, K., Sueishi, K., & Sameshima, G. T. (2009). Stress distribution in mandible and temporomandibular joint by mandibular distraction: a 3-dimensional finite-element analysis. The Bulletin of Tokyo Dental College, 50(4), 161-168.

Kato, S., & Kato, M. (2006). Intrusion of molars with implants as anchorage: a report of two cases. Clinical implant dentistry and related research, 8(2), 100-106.

Kiliaridis, S., Egermark, I., & Thilander, B. (1990). Anterior open bite treatment with magnets. The European Journal of Orthodontics, 12(4), 447-457.

Kim, Y. H., Han, U. K., Lim, D. D., & Serraon, M. L. P. (2000). Stability of anterior openbite correction with multiloop edgewise archwire therapy: a cephalometric follow-up study. American Journal of Orthodontics and Dentofacial Orthopedics, 118(1), 43-54.

Kojima, Y., & Fukui, H. (2014). A finite element simulation of initial movement, orthodontic movement, and the centre of resistance of the maxillary teeth connected with an archwire. The European Journal of Orthodontics, 36(3), 255-261.

Kojima, Y., Kawamura, J., and Fukui, H. (2012). Finite element analysis of the effect of force directions on tooth movement in extraction space closure with miniscrew sliding mechanics. American Journal of Orthodontics and Dentofacial Orthopedics, 142(4), 501-508.

Kravitz, N. D., Kusnoto, B., Tsay, T. P., and Hohlt, W. F. (2007). The use of temporary anchorage devices for molar intrusion. The Journal of the American Dental Association, 138(1), 56-64.

Kucera, J., Marek, I., Tycova, H., & Baccetti, T. (2011). Molar height and dentoalveolar compensation in adult subjects with skeletal open bite. The Angle Orthodontist, 81(4), 564-569.

Küçükkeles, N., Acar, A., Demirkaya, A. A., Evrenol, B., & Enacar, A. (1999). Cephalometric evaluation of open bite treatment with NiTi arch wires and anterior elastics. American journal of orthodontics and dentofacial orthopedics, 116(5), 555-562.

Kupietzky, A., and Tal, E. (2007). The transpalatal arch: an alternative to the Nance appliance for space maintenance. Pediatric dentistry, 29(3), 235-238.

Kuroda, S., Katayama, A., and Takano-Yamamoto, T. (2004). Severe anterior open-bite case treated using titanium screw anchorage. The Angle Orthodontist, 74(4), 558-567.

Lechuga, L., & Weidlich, G. A. (2016). Cone beam CT vs. fan beam CT: a comparison of image quality and dose delivered between two differing CT imaging modalities. Cureus, 8(9).

Lee, J. S., Hyung Kim, D., Park, Y. C., Kyung, S. H., and Kim, T. K. (2004). The efficient use of midpalatal miniscrew implants. The Angle orthodontist, 74(5), 711-714.

Lee, S. J., Jang, S. Y., Chun, Y. S., & Lim, W. H. (2013). Three-dimensional analysis of tooth movement after intrusion of a supraerupted molar using a mini-implant with partial-fixed orthodontic appliances. The Angle Orthodontist, 83(2), 274-279.

Lei, Z., Feng, D., Yi, Z., Yubo, F. (2007). Three-dimensional finite element analysis of the initial tooth displacement in different micro implant-bone interfaces using micro-implant anchorage system. Proceedings of the IEEE/ICME International Conference on Complex Medical Engineering,1901-4.

Li, W., Chen, F., Zhang, F., Ding, W., Ye, Q., Shi, J., & Fu, B. (2013). Volumetric measurement of root resorption following molar mini-screw implant intrusion using cone beam computed tomography. PloS one, 8(4).

Lim, J. W., Kim, W. S., Kim, I. K., Son, C. Y., and Byun, H. I. (2003). Three-dimensional finite element method for stress distribution on the length and diameter of orthodontic miniscrew and cortical bone thickness. Korean Journal of Orthodontics, 33(1), 11-20.

Lin, L. H., Huang, G. W., & Chen, C. S. (2013). Etiology and treatment modalities of anterior open bite malocclusion. Journal of Experimental & Clinical Medicine, 5(1), 1-4.

Lotti, R. S., Machado, A. W., Mazzieiro, Ê. T., and Landre Júnior, J. (2006). Aplicabilidade científica do método dos elementos finitos. R Dental Press Ortodon Ortop Facial, 11(2), 35-43.

Loubele, M., Guerrero, M. E., Jacobs, R., Suetens, P., & Van Steenberghe, D. (2007). A comparison of jaw dimensional and quality assessments of bone characteristics with cone-beam CT, spiral tomography, and multi-slice spiral CT. International Journal of Oral & Maxillofacial Implants, 22(3).

Maia, F. A., Janson, G., Barros, S. E., Maia, N. G., Chiqueto, K., & Nakamura, A. Y. (2010). Long-term stability of surgical-orthodontic open-bite correction. American Journal of Orthodontics and Dentofacial Orthopedics, 138(3), 254-e1.

Marcotte, M. R. (1976). The use of the occlusogram in planning orthodontic treatment. American journal of orthodontics, 69(6), 655-667.

Marzouk, E. S., Abdallah, E. M., & El-Kenany, W. A. (2015). Molar Intrusion in Open-bite Adults Using Zygomatic Miniplates. International journal of orthodontics (Milwaukee, Wis.), 26(2), 47-54.

McIntyre, G. T., & Mossey, P. A. (2003). Size and shape measurement in contemporary cephalometrics. The European Journal of Orthodontics, 25(3), 231-242.

Melsen, B., & Fiorelli, G. (1996). Upper molar intrusion. Journal of clinical orthodontics: JCO, 30(2), 91-96.

Meštrović, S., Šlaj, M., & Rajić, P. (2003). Finite element method analysis of the tooth movement induced by orthodontic forces. Collegium antropologicum, 27(2), 17-21.

Middleton, J., Jones, M., and Wilson, A. (1996). The role of the periodontal ligament in bone modeling: the initial development of a time-dependent finite element model. American Journal of Orthodontics and Dentofacial Orthopedics, 109(2), 155-162.

Mohammed, S. D., & Desai, H. (2014). Basic concepts of finite element analysis and its applications in dentistry: An overview. Oral Hyg Health, 2(156), 2332-0702.

Moon, C. H., Wee, J. U., and Lee, H. S. (2007). Intrusion of overerupted molars by corticotomy and orthodontic skeletal anchorage. The Angle Orthodontist, 77(6), 1119-1125

Moss, M. L., Skalak, R., Patel, H., Sen, K., Moss-Salentijn, L., Shinozuka, M., & Vilmann, H. (1985). Finite element method modeling of craniofacial growth. American Journal of Orthodontics, 87(6), 453-472.

Motegi, N., Tsutsumi, S., & Wakatsuki, E. (1996). A facial growth analysis based on FEM employing three-dimensional surface measurement by a rapid laser device. Okajimas folia anatomica Japonica, 72(6), 323-328.

Moutaftchiev, V., & Moutaftchiev, A. (2009). The individually prepared transpalatal arch. Oral Hlth J, 8, 13-16.

Ng, J., Major, P. W., and Flores-Mir, C. (2006). True molar intrusion attained during orthodontic treatment: a systematic review. American journal of orthodontics and dentofacial orthopedics, 130(6), 709-714.

Ngan, P., & Fields, H. W. (1997). Open bite: a review of etiology and management. Pediatric dentistry, 19(2), 91-98.

Nikolai, R. J. (1985). Bioengineering: analysis of orthodontic mechanics. Lea & Febiger.

Obaidellah, U., Radzi, Z., Yahya, N. A., Osman, N. A., & Merican, A. F. (2008). The facial soft tissue simulation of orthognathic surgery using biomechanical model. In 4th Kuala Lumpur International Conference on Biomedical Engineering 2008 (pp. 751-757). Springer, Berlin, Heidelberg.

Oliveira, D. D., Oliveira, B. F. D., & Soares, R. V. (2010). Alveolar corticotomies in orthodontics: Indications and effects on tooth movement. Dental Press Journal of Orthodontics, 15(4), 144-157.

Paccini, J. V. C., Cotrim-Ferreira, F. A., Ferreira, F. V., Freitas, K. M. S. D., Cançado, R. H., & Valarelli, F. P. (2016). Efficiency of two protocols for maxillary molar intrusion with mini-implants. Dental press journal of orthodontics, 21(3), 56-66.

Park, H. S. (1999). The skeletal cortical anchorage using titanium microscrew implants. KOREA J (ORT-OD 1999, 29 (6), 699, 706

Park, H. S., Jang, B. K., & Kyung, H. M. (2005). Maxillary molar intrusion with micro-implant anchorage (MIA). Australian Orthodontic Journal, 21(2), 129.

Peterson, J., Wang, Q., and Dechow, P. C. (2006). Material properties of the dentate maxilla. The Anatomical Record Part A: Discoveries in Molecular, Cellular, and Evolutionary Biology, 288(9), 962-972.

Pilla, A. A. (2002). Low-intensity electromagnetic and mechanical modulation of bone growth and repair: are they equivalent? Journal of Orthopaedic Science, 7(3), 420-428.

Poggio, P. M., Incorvati, C., Velo, S., & Carano, A. (2006). "Safe zones": a guide for miniscrew positioning in the maxillary and mandibular arch. The Angle Orthodontist, 76(2), 191-197.

Pollei, J. K. (2009). Finite element analysis of miniscrew placement in maxillary alveolar bone with varied angulation and material type.

Pritam, M., Sah, M. P. S. N. S., & Debapreeti, M. (2015). Finite Element Method: A Research Tool in Orthodontics. J. Res. Adv. Dent, 4(3), 58-63.

Proffit, W. R., Fields Jr, H. W., and Sarver, D. M. (2012). Contemporary Orthodontics (5th Ed.). St. Louis: Mosby.

Prosterman, B., Prosterman, L., Fisher, R., & Gornitsky, M. (1995). The use of implants for orthodontic correction of an open bite. American Journal of Orthodontics and Dentofacial Orthopedics, 107(3), 245-250.

Reitan, K. (1960). Tissue behavior during orthodontic tooth movement. American Journal of Orthodontics, 46(12), 881-900.

Reitan, K. (1964). Effects of force magnitude and direction of tooth movement on different alveolar bone types. The Angle Orthodontist, 34(4), 244-255.

Rubin, C., Krishnamurthy, N., Capilouto, E., & Yi, H. (1983). Stress analysis of the human tooth using a three-dimensional finite element model. Journal of Dental Research, 62(2), 82-86.

Rudolph, D. J., Willes, M. G., & Sameshima, G. T. (2001). A finite element model of apical force distribution from orthodontic tooth movement. The Angle Orthodontist, 71(2), 127-131.

Saga, A. Y., Maruo, H., Argenta, M. A., Maruo, I. T., & Tanaka, O. M. (2016). Orthodontic intrusion of maxillary incisors: a 3D finite element method study. Dental press journal of orthodontics, 21(1), 75-82.

Salmon, J. R., Liggett, J. A., & Gallagher, R. H. (1980). Dispersion analysis in homogeneous lakes. International Journal for Numerical Methods in Engineering, 15(11), 1627-1642.

Sarver, D. M. (2001). The importance of incisor positioning in the esthetic smile: the smile arc. American Journal of Orthodontics and Dentofacial Orthopedics, 120(2), 98-111.

Sasaki, A., Takeshita, S., Publico, A. S., Moss, M. L., Tanaka, E., Ishino, Y., ... & Tanne, K. (2004). Finite element growth analysis for the craniofacial skeleton in patients with cleft lip and palate. Medical engineering & physics, 26(2), 109-118.

Scarfe, W. C. (2012). A comparison of maxillofacial CBCT and medical CT. Atlas of the Oral and Maxillofacial Surgery Clinics of North America: Digital Technologies in Oral and Maxillofacial Surgery, 20(1), 1.

Schwartz-Dabney, C. A., & Dechow, P. C. (2003). Variations in cortical material properties throughout the human dentate mandible. American Journal of Physical Anthropology: The Official Publication of the American Association of Physical Anthropologists, 120(3), 252-277.

Seo, Y. J., Kim, S. J., Munkhshur, J., Chung, K. R., Ngan, P., & Kim, S. H. (2014). Treatment and retention of relapsed anterior open-bite with low tongue posture and tongue-tie: A 10-year follow-up. The korean journal of orthodontics, 44(4), 203-216.

Shaw, A. M., Sameshima, G. T., and Vu, H. V. (2004). Mechanical stress generated by orthodontic forces on apical root cementum: a finite element model. Orthodontics and craniofacial research, 7(2), 98-107.

Sherwood, K. H., Burch, J. G., & Thompson, W. J. (2002). Closing anterior open bites by intruding molars with titanium miniplate anchorage. American Journal of Orthodontics and Dentofacial Orthopedics, 122(6), 593-600.

Shetty, P., Hegde, A., and Rai, K. (2010). Finite element method–an effective research tool for dentistry. Journal of Clinical Pediatric Dentistry, 34(3), 281-285.

Shigeeda, T. (2014). Root proximity and stability of orthodontic anchor screws. Journal of oral science, 56(1), 59-65.

Soares, C. J., Versluis, A., Valdivia, A. D. C. M., Bicalho, A. A., Veríssimo, C., Barreto, B. D. C. F., & Roscoe, M. G. (2012). Finite element analysis in dentistry-Improving the quality of oral health care. Moratal D. Finite element analysis-from biomedical applications to industrial developments. Rijeka: In Tech Croatia, 25-56.

Stein, G., & Weinmann, J. (1925). Die physiologische Wanderung der Zähne. Z. Stomatol, 23, 733-744.

Strait, D. S., Wang, Q., Dechow, P. C., Ross, C. F., Richmond, B. G., Spencer, M. A., & Patel, B. A. (2005). Modeling elastic properties in finite-element analysis: how much precision is needed to produce an accurate model? The Anatomical Record Part A: Discoveries in Molecular, Cellular, and Evolutionary Biology: An Official Publication of the American Association of Anatomists, 283(2), 275-287.

Sugii, M. M., Barreto, B. D. C. F., Francisco Vieira-Júnior, W., Simone, K. R. I., Bacchi, A., & Caldas, R. A. (2018). Extruded upper first molar intrusion: Comparison between unilateral and bilateral miniscrew anchorage. Dental press journal of orthodontics, 23(1), 63-70.

Tanaka, E., Tanne, K., & Sakuda, M. (1994). A three-dimensional finite element model of the mandible including the TMJ and its application to stress analysis in the TMJ during clenching. Medical engineering & physics, 16(4), 316-322.

Tanaka, O., Oliveira, W., Galarza, M., Aoki, V., & Bertaiolli, B. (2016). Breaking the thumb sucking habit: When compliance is essential. Case reports in dentistry, 2016.

Tanne, K., Sakuda, M., and Burstone, C. J. (1987). Three-dimensional finite element analysis for stress in the periodontal tissue by orthodontic forces. American Journal of Orthodontics and Dentofacial Orthopedics, 92(6), 499-505.

Tanne, K., Tanaka, E., & Sakuda, M. (1996). Stress distribution in the temporomandibular joint produced by orthopedic chincup forces applied in varying directions: a three-dimensional analytic approach with the finite element method. American Journal of Orthodontics and Dentofacial Orthopedics, 110(5), 502-507.

Tasanapanont, J., Wattanachai, T., Apisariyakul, J., Pothacharoen, P., Ongchai, S., Kongtawelert, P. & Jotikasthira, D. (2017). Biochemical and clinical assessments of segmental maxillary posterior tooth intrusion. International journal of dentistry, 2017.

Ten Hoeve, A., Mulie, R. M., and Brandt, S. (1977). Technique modifications to achieve intrusion of the maxillary anterior segment. Journal of clinical orthodontics: JCO, 11(3), 174.

Thilander, B., Rygh, P., & Reitan, K. (2011). Tissue reactions in orthodontics. Orthodontics: Current Principles and Techniques. Elsevier, Philadelphia, PA, 247-286.

Timoshenko, S., & Goodier 2nd, J. N. Theory of Elasticity 2nd ed., (1951).

Topkara, A., Karaman, A. I., and Kau, C. H. (2012). Apical root resorption caused by orthodontic forces: A brief review and a long-term observation. European Journal of Dentistry, 6(4), 445–453.

Umemori, M., Sugawara, J., Mitani, H., Nagasaka, H., and Kawamura, H. (1999). Skeletal anchorage system for open-bite correction. American Journal of Orthodontics and Dentofacial Orthopedics, 115(2), 166-174.

Uribe, F. A., & Nanda, R. (2010). Efficient mechanics and appliances to correct vertical excess and open bite. In Current Therapy in Orthodontics (pp. 171-185). Mosby.

Van Steenbergen, E., Burstone, C. J., Prahl-Andersen, B., & Aartman, I. H. A. (2004). The role of a high pull headgear in counteracting side effects from intrusion of the maxillary anterior segment. The Angle Orthodontist, 74(4), 480-486.

Vela-Hernández, A., López-García, R., García-Sanz, V., Paredes-Gallardo, V., & Lasagabaster-Latorre, F. (2017). Nonsurgical treatment of skeletal anterior open bite in adult patients: Posterior build-ups. The Angle Orthodontist, 87(1), 33-40.

Viecilli, R. F. (2006). Self-corrective T-loop design for differential space closure. American journal of orthodontics and dentofacial orthopedics, 129(1), 48-53.

Wajid, M. A., Chandra, P., Kulshrestha, R., Singh, K., Rastogi, R., & Umale, V. (2018). Open bite malocclusion: An overview. J Oral Health Craniofac Sci, 3, 11-20.

Wise G.E. and King G.J., (2008), "Mechanisms of Tooth Eruption and Orthodontic Tooth Movement", 87(5), 414-34.

Xun, C., Zeng, X., & Wang, X. (2007). Microscrew anchorage in skeletal anterior open-bite treatment. The Angle Orthodontist, 77(1), 47-56.

Yan, W., & Shao, P. (2017). Three-dimensional finite element stress analysis of micro-implant anchorage-assisted intrusion of orthodontic teeth molar. Int J Clin Exp Med, 10(10), 14695-14698.

Yao, C. C. J., Lee, J. J., Chen, H. Y., Chang, Z. C. J., Chang, H. F., & Chen, Y. J. (2005). Maxillary molar intrusion with fixed appliances and mini-implant anchorage studied in three dimensions. The Angle Orthodontist, 75(5), 754-760.

Zeno, K. G., El-Mohtar, S. J., Mustapha, S., & Ghafari, J. G. (2019). Finite element analysis of stresses on adjacent teeth during the traction of palatally impacted canines. The Angle Orthodontist, 89(3), 418-425.

Zuroff, J. P., Chen, S. H., Shapiro, P. A., Little, R. M., Joondeph, D. R., & Huang, G. J. (2010). Orthodontic treatment of anterior open-bite malocclusion: stability 10 years postretention. American journal of orthodontics and dentofacial orthopedics, 137(3), 302-e1.